

The impact of membrane technology to human life

Edited by:
Marek Bryjak
Katarzyna Majewska-Nowak
Małgorzata Kabsch-Korbutowicz



The impact of membrane technology to human life

Edited by:

Marek Bryjak

Katarzyna Majewska-Nowak

Małgorzata Kabsch-Korbutowicz



Oficyna Wydawnicza Politechniki Wrocławskiej
Wrocław 2006

Reviewers

Wojciech ADAMSKI

Piotr WIECZOREK

The book has been published in the camera-ready form

All rights reserved.

No part of this book may be reproduced, stored in a retrieval system,
or transmitted in any form or by any means, electronic, mechanical, photocopying,
recording or otherwise, without the prior permission in writing of the Publisher.

© Copyright by Oficyna Wydawnicza Politechniki Wrocławskiej, Wrocław 2006

ISBN 83-7085-922-4

OFICyna WYDAWNICZA POLITECHNIKI WROCLAWSKIEJ

Wybrzeże Wyspiańskiego 27, 50-370 Wrocław, Poland

<http://www.oficyna.pwr.wroc.pl>

oficwyd@pwr.wroc.pl

CONTENTS

Foreword	5
A. CHWOJNOWSKI, K. DUDZIŃSKI, E. ŁUKOWSKA, Z. CHWOJNOWSKA, C. WOJCIECHOWSKI, Application of polysulfone and polyeteresulfone membranes in dry tests	7
W. KOCHKODAN, N. HILAL, V. GONCHARUK, Composite imprinted membranes like synthetic receptor systems for biologically active compounds	17
A. TIMOSZYK, L. LATANOWICZ, Physical stability of temperature-sensitive liposomes	27
O. B. BORISEVICH, D.A. SYRISOVA, V.V. TEPLYAKOV, V.S. KHOTIMSKII, D.A. ROIZARD, The influence of film thickness on permeability of gases and organic vapours through poly(1-trimethylsilyl-propyne)	35
K. FRIESS, J. MACHKOVÁ, M. SIPEK, V. HYNEK, Y.P. KUZNETSOV, Sorption of VOCs and water vapors in myristate cellulose membrane	43
A. STACHECKA, W. KAMIŃSKI, Empirical approach to dewatering of isopropanol-water system by pervaporation	53
K. LAPIŠOVÁ, Exploitation of ceramic membrane bioreactor for thermophilic bacteria cultivation	65
J. MARCQ, Q.T. NGUYEN, K. GLINEL, G. LADAM, Dialysis membranes with immobilized heparin and their anti-blood clotting properties	73
V. KOCHKODAN, N. HILAL, R. NIGMATULLIN, V. GONCHARUK, Lipase-immobilized biocatalytic membranes in enzymatic esterification	85
A. CAR, G. FERK, C. STROPNIK, Effect of surface modification with friedel-crafts reaction with (1,3)-propane sultone on the physical properties of polysulfone membranes	97
J. CERMAKOVA, K. FIALOVA, R. PETRYCHKOVYCH, V. KUDRNA, P. UCHYTI, Effect of input non-perfect step concentration function on diffusion coefficient evaluation	109
Z. A. FEKETE, E. WILUSZ, F.E. KARASZ, C. VISY, Ion beam irradiation of fluoropolymers for preparing new membrane materials – a theoretical study	115
Z. A. FEKETE, E. WILUSZ, F.E. KARASZ, Integrally skinned barrier layer preparation by ion beam irradiation of ionomers	123
M. KABSCH-KORBUTOWICZ, A. BIŁEK, M. MOŁCZAN, Impact of water pretreatment on the performance of ultrafiltration membranes	131
I. KOWALSKA, K. MAJEWSKA-NOWAK, M. KABSCH-KORBUTOWICZ, The influence of complexing agents on anionic surfactant removal from water solutions by ultrafiltration	145

FOREWORD

To illustrate the reconstruction in our way of thinking, Arup SenGupta – the editor-in-chief of the Reactive and Functional Polymers Journal – has used the old Kashmiri proverb “*We have not inherited the world from our forefathers, we have borrowed it from our children*” [A. SenGupta, Two continents of our environment, Trans IChemE, 80, Part B, 2002, 175]. Hence today, nobody should be surprised with a growing challenge to balance same efforts connected with protection of environment to improve human life. To better understand how these efforts are difficult to manage, one recalls plenty of idiomatic phrases to be introduced to name this challenge. It is possible to enumerate here such terms as: Pollutant Preservation, Green Chemistry, Clean Technologies, Industrial Ecology or more phrasal descriptions: Environment Friendly Techniques and Sustainable Development. In his consideration, SenGupta suggested to split of our world onto two categories: developed countries that should play a role of the knowledge donors and developing countries that attract the achievements of the first group. Finally, he admitted that exchange of knowledge has still positive function. It “*generates new ideas and creates partnership toward meaningful solutions*”. Is anyone against such point of view?

Similar impressions come after careful reading the materials connected to the seven thematic areas of the European 6 Frame Program. They are as follows: 1. Genomics and biotechnology for health, 2. Information Society technologies, 3. Nanotechnologies and new production processes, 4. Aeronautic and space, 5. Food safety and health risks, 6. Sustainable development and global change, 7. Citizens and governance in the knowledge-based society. As the membrane engineers we can point at five of the seven European Research Area priorities that are related to membranes and membrane based processes. The use of membranes in biotechnology is well documented for the last years. Moreover, the application of membrane devices for medical purposes is not only connected to hemodialysis now. Development of such artificial organs as liver, lung, pancreas or devices that release medicines in the controlled way are now being on the top of interest for many companies. Production of chiral medicines is also depended on new membranes. Membranes play the essential role in the development of new analytical assays. In the third priority, directly connected to nanoscale architecture and machinery, membranes are also the versatile bodies. They act as some separating elements, contactors, nanoreactors, stress-sensitive bodies or catalyst carriers. At the first glance, the forth priority should not be

related to membrane. However, the development of new technologies that allow to survive in the space (water regeneration, oxygen recycle and energy saving) is based on the membrane techniques. The fifth priority is also related to the use of membrane processes. Desalination of water or wastewater treatments are the two branches of modern membranology that have to be developed intensively in the nearest future. Shortage of potable water, desertification of land, contamination of surface water are the reasons of growing death rate. Today, it is estimated that more than 10 thousands people die everyday due to the water problems. It is also told that water will be the strategic material in this century. The sixth priority concerns on sustainable development. Here membranes can be used to prepare fuel-cells, in recycling of gases and in separation of valuable gaseous components, in removal of carbon dioxide from the exhausted gases (reduction of greenhouse effect), in production of organic species by means of bioreactors, and so on.

Some membrane authorities state that membrane technologies are still in its infancy stage and they will be developed. Enrico Drioli, fonder and former President of the European Membrane Society, concludes each one presentation with the following two sentences “*Membrane science and engineering have made huge progresses in the last years. They are expected to play an increasingly important role in the furor for various industrial sectors*”, “*Despite its success and undoubtedly great potential, membrane technology is still quite far from fulfilling all expectations of its role in the intensification of a large variety of processes*”.

Taking in mind these conclusions one can merge them with the SenGupta’s idea of two categories of countries. When membranes are still in its infancy stage, it seems impossible to specify the developed and the developing countries. Finally, the exchange of the knowledge takes place on the equal opportunity mode and the position of teachers and students is fully interchangeable.

Taking the above into account we have prepared the book “**Impact of membrane technology to human life**” that illustrates versatility of membrane application to our daily activity. To keep the book more concise we have selected the authors’ contributions to the following thematic groups: medical application (chapter 1, 2, 3), treatment of gases and vapors (chapter 4, 5, 6), membrane bioreactors (chapter 7, 8, 9), membrane modification and properties (chapter 10, 11, 12, 13) and wastewater treatment (chapter 14, 15). We hope our selection allows better recognize potentialities of some membrane applications.

Marek Bryjak
Małgorzata Kabsch-Korbutowicz,
Katarzyna Majewska-Nowak

Keywords: semipermeable membranes, dry tests

ANDRZEJ CHWOJNOWSKI*, KONRAD DUDZIŃSKI*, EWA ŁUKOWSKA*,
ZOFIA CHWOJNOWSKA**, CEZARY WOJCIECHOWSKI*

APPLICATION OF POLYSULFONE AND POLYETERESULFONE MEMBRANES IN DRY TESTS

The results of the studies on the reproducibility of dry tests containing semi-permeable polysulfone and polyeteresulfone membranes are presented. It was found that the semi-permeable membrane deposited on a test field enables to carry out of analysis of samples containing suspensions of various origin. The application of chromatographic type tests permits also the analysis in the presence of dyes. It was found that it is more favorable to use membranes made from polyeteresulfones, due to the shorter permeation time of solutions through the membrane and test field.

1. INTRODUCTION

Fast analytical methods are the field of analytics being constantly developed. This concerns both kit type tests, ion-selective electrodes, as well as dry tests. The development of dry tests even caused the formation of a separate name, dry chemistry, for this field of analytical chemistry. Fast analytical methods have some common features: low unit costs of analysis, short time of carrying out the analysis and possibility of carrying out the analysis outside the laboratory. Fast analytical methods had until now considerable limitations: they could not separate dyes giving intensive colors and suspensions masking the reactions. Tests for the analysis of whole blood were the only exemption here, for which a number of solutions is known enabling the separation of erythrocytes on the surface of the tests [1]–[5]. In our to date researches we dealt with the development of membranes on a cellulose support enabling the separation of various suspensions, especially of suspensions in fruit and vegetable juices [6] and erythrocytes in tests for whole blood [7]. Polysulfones and polyeteresulfones were used for the preparation of

* Institute of Biocybernetics and Biomedical Engineering PAS, ul. Trojdena 4, 02-109 Warszawa, Poland. E-mail: achwoj@ibib.waw.pl

** National Institute of Food and Nutrition, ul. Powsińska 61/63, 02-903 Warszawa, Poland.

these semi-permeable membranes. These polymers are successfully used for the obtaining of semi-permeable capillary membranes [8], [9]. Due to the easiness in casting of membranes by the phase inversion method and high chemical resistance, polysulfones and polyethersulfones are a very good starting material for the obtaining of semi-permeable membranes for the dry tests preparation. With these semi-permeable membranes obtained by us, we developed tests for the determination of vitamin C and for the determination of selected anions and cations in aqueous solutions containing suspensions and dyes giving intensive colors. The purpose of this work was the estimation of the action of dry tests under real conditions and comparison of the action of polysulfonic and polyethersulfonic membranes in dry tests.

2. EXPERIMENTAL

2.1. MATERIALS

Polymeric membranes on a cellulose support were obtained as described earlier [8]. Blotting papers saturated by non solvent (ethanol) were covered by 18-25 μm membrane forming layer containing polymer solution and pore forming additives in polymer solvent. For membrane coagulation water was used. All dry tests were obtained in our laboratory as described previously [9]. The test fields of dry test were saturated by reagent mixtures in room temperature and dried suitably in temperature between 60 °C to 110, fix on carrier and cut on test strips. All the reactants used in the work were from one of the three companies: POCh, Fluka or Aldrich. Fruit juices and pulps used for analysis were from fruit juices and preserves factories and were obtained directly after their production. Wastewaters for analysis were collected from three wastewater purification plants directly from the drain supplying the wastewaters and transferred to the laboratory. Immediately before analysis the samples were exactly mixed, and after mixing dosed onto the test field.

2.2. DETERMINATION OF PERMEATION TIMES

The determination of permeation time was carried out by means of a specially designed device that operated on an electric conductance basis. Penetration of the aqueous solution through the membrane caused the appearance of a contact between the two separated parallel electrodes, thus sound and light signals are initiated. This corresponds to the time after which the amount of the aqueous solution with the analyte permeating through a semi-permeable membrane is sufficient for a correct coloring of the test. The method was described previously in detail [10].

2.3. PERFORMING OF INSTRUMENTAL ANALYSIS

Ascorbic acid was determined by means of HPLC [11]. The metals were determined as follows. A well mixed sample containing precipitates was dried at 100 °C,

then burned and the remaining ash was mineralized in a standard way. The nickel content was determined gravimetrically by the dithizone method, and the other metals were determined colorimetrically by typical methods. A Hitachi U3010 spectrophotometer was used for the measurements.

2.4. PERFORMING OF ANALYSIS BY MEANS OF DRY TESTS

The determinations by means of a test with a semi-permeable membrane were carried out as follows. Two drops of the studied solution were deposited onto the test field by means of a disposable polyethylene Pasteur-type pipette and after 60 seconds the result of measurement was read by comparison with a color scale. The read-out was carried out through the transparent support from the opposite side than the deposited sample (Fig. 1).

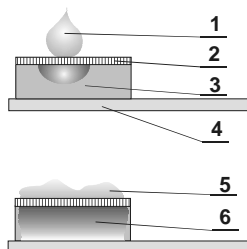


Fig. 1. Idea of performing a test with a deposited semi-permeable membrane. The test is shown when the sample is deposited (top image) and ready for reading (bottom image).

- 1) solution with suspension; 2) semi-permeable membrane, 3) test field, 4) transparent support,
- 5) deposited suspension, 6) dyed test field

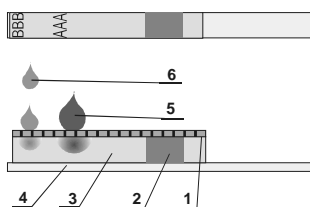


Fig. 2. Chromatographic type of test: top view and end view (below).

- 1) semi-permeable membrane, 2) reagent region, 3) test field, 4) support,
- 5) colored sample studied, 6) water or developing solution

The determination by means of a chromatographic type test was carried out as follows. Two drops of the studied solution containing a suspension and dyes were deposited where mark "A" is placed (Fig. 2). After 60 seconds one drop of the developing solution was deposited exactly onto the mark "B", and after the next 60 seconds still one more drop of the solution was deposited onto the same place, after the next 30

seconds still one more drop of the solution was deposited onto the same place. After 4.5 minutes the result was read by comparison of the coloring of the reagent region with a color scale.

2.4. MICROSCOPIC PICTURES OF THE MEMBRANES

Microphotographs of the membranes were taken on a Hitachi S-3500N scanning electron microscope at the Faculty of Material Engineering of Warsaw University of Technology. Magnifications were performed at pressures of 25, 40 and 60 Pa at a voltage of 20 kV. This is a so-called biological microscope, not requiring the depositing of samples with a conductor, e.g., graphite or gold. This convenience, however, results in a poorer sharpness of the images.

3. RESULTS AND DISCUSSION

During the studies on the usefulness of polysulfone and polyethersulfone membranes we found a very interesting regularity. The membranes made of polyethersulfones in comparison with those of polysulfones showed shorter filtration times. These differences were very essential. The observed tendency did not depend on the mode of membrane preparation or on their composition. The pictures taken on a scanning electron microscope did not show differences in the structure of membranes (Figs. 3 and 4).

When comparing by pairs the membranes made from solutions of the same concentration of the membrane-forming polymer, in the same solvent of the same composition of the pore precursors, and obtained under the same deposition conditions (temperature, transport rate, the same degree of support saturation) onto a cellulose support, always the same tendency was obtained. The polyethersulfonic membranes showed permeation times shorter by 15-30% than that of polysulfonic ones. This concerned both aqueous solutions of salts, fruit juices as well as juices containing suspensions.

This regularity has not been confirmed only for permeation times of plasma from whole blood. However, no effect of the polymer on the analytical properties of the tests was found. The observed effect is most probably connected with the lower hydrophobicity (based on moisture angle polymer-water) of polyethersulfones in comparison with that of polysulfones. The results obtained suggest that at identical separation parameters, when the separation time is the only difference, it is more favorable to use membranes made of polyethersulfones on a cellulose support as a material for test fields.

As was found earlier, both types of tests enable a sufficient accuracy in concentration determination in the studied suspensions and solutions. In this work we checked the reproducibility of the performance of tests in the analysis of real solutions, i.e. in analysis for which these tests are to be used. These tests are intended for rapid estimation of concentrations with the use of a color scale for read-out. For reproducibility estimation, 50 determinations with each test were carried out. The result of analysis for a given

analyte in a respective matrix carried out by classical methods was assumed as a comparative value. An experienced experimenter can distinguish without any problems the concentrations corresponding to the half of concentrations between subsequent points. Therefore, we undertook the following qualification of the read-out. A correct read-out is such a one for which the discoloring of the test field differs less than half the distance between the subsequent points of the scale. A lowered or increased result is such a one in which the discoloring of the test field differs by more than half interval of the scale, but less than one interval of the scale. A decisively wrong result was when the read-out differed by one or more intervals on the scale. The accepted mode of read-out results from the greatest possible accuracy of reading dry tests by means of a color scale.

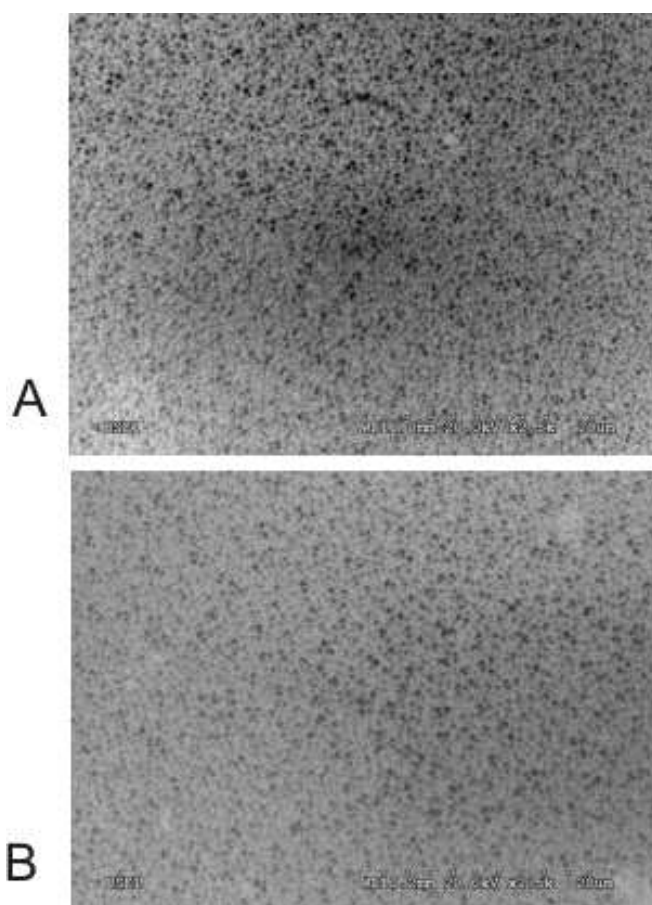


Fig. 3. Microphotograph of the external layer of the membrane (skin).
A) a polysulfonic membrane, B) a polyethersulfonic membrane. Magnification $\times 2.5$ k

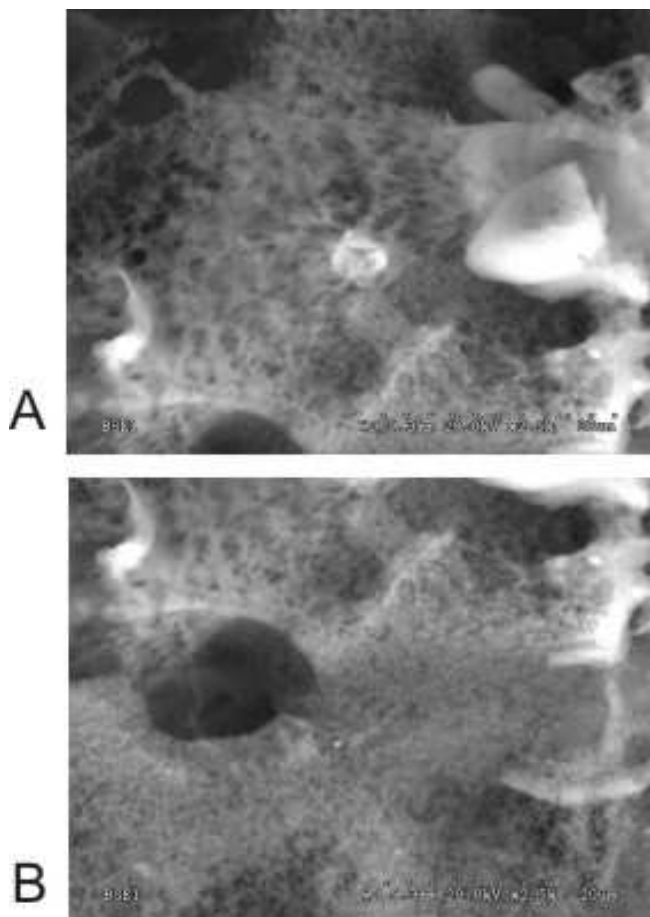


Fig. 4. Microphotograph of the internal layer of the membrane from the chromatographic paper side, after dissolution of cellulose. Visible traces of cellulose fibers. A) a polysulfonic membrane, B) a polyethersulfonic membrane. Magnification $\times 2.5$ k

The results of determinations performed for fruit pulps without intensive dyes, which are not separated by the membranes applied, are presented in Table 1. In total, 350 determinations of 7 different fruit pulps were carried out. The differentiation in the determinations of apple pulps (entries 6 and 7) consisted in studies of two different kinds of apples. A very good correlation of the results was found from the studies carried out. In the worst case (white grapes), only 6% of answers were different than expected. In this entire series of studies, for all the pulps there were at an average 97.1% of results in agreement with those expected. Considerable errors constitute only 0.6%.

Table 1. Results of reproducibility studies of tests with a semi-permeable polysulfone membrane for the determination of ascorbic acid in fruit pulps of fresh fruits

No.	Fruit pulp	Ascorbic acid content, mg/100 cm ³	Correct read-out	Decreased read-out	Increased read-out	Definitely erroneous read-out
1	Tomatoes	16.73	50	–	–	–
2	Raspberries	30.87	48	–	2	–
3	Strawberries	65.14	49	1	–	–
4	White currant	39.63	49	–	–	1
5	White grapes	5.12	47	1	2	–
6	Apples I	4.98	49	–	1	–
7	Apples II	5.06	48	1	–	1
Total			340	3	5	2

Slightly worse results were obtained for determinations carried out by means of chromatographic type tests. This was as expected, since this is technically more difficult and the way of development must generate greater errors (Table 2). In this case most of the errors, right up to 10%, were achieved when determining pulps from black currents. However, 8% were decreased results. For the whole series of determinations in four pulps 92% of answers were as expected. This should be accepted as a surprisingly good result, especially since there was only 1% of large errors.

The third series of measurements consisted in the determination of five ions of various metals in wastewaters containing suspensions (Table 3). The choice of the determined ions was resulted only by what is present in the wastewaters or sewages. Certainly, contrary to determinations in fruit pulps, to the same measurement, series of 5 different tests predicted for the determination of respective ions were used. The best correlation was obtained for cobalt and copper ions (98% concordance). The results were slightly worse for the other ions. For all the determinations 96% of responses were achieved as expected.

Table 2. Results of reproducibility studies of chromatographic tests with a semi-permeable polyethersulfone membrane for the determination of ascorbic acid in fruit pulps from fresh fruits containing an intensive dye

No.	Fruit pulp	Ascorbic acid content, mg/100 cm ³	Correct read-out	Decreased read-out	Increased read-out	Definitely erroneous read-out
1	Black current	44.96	45	4	1	–
2	Bilberry	14.28	47	1	1	1
3	Chokeberry	8.11	46	2	2	–
4	Sour cherry	11.54	46	0	3	1
Total			184	7	7	2

Table 3. Results of reproducibility studies of tests with a semi-permeable polyethersulfone membrane for the determination of ions in wastewaters containing suspensions

No.	Ion	Concentration, mg/dm ³	Correct read-out	Decreased read-out	Increased read-out	Definitely erroneous read-out
1	Nickel	11.7	48	1	1	–
2	Copper	25.8	49	1	–	–
3	Cobalt	17.8	49	–	1	–
4	Chromates	30.6	47	1	1	1
5	Iron II	54.9	47	–	2	1
Total			240	3	5	2

The fourth series of measurements consisted in the determination of 5 ions of different metals (Table 4) in sewages containing dyes and suspensions by means of chromatographic type tests. The choice of ion determination was resulting, as before, only by the wastewater content and therefore involved only the same 5 ions, but at different concentrations than previously. The general results, as expected, are slightly worse than in the case of the third series. However, the agreement with the expected value reached 93.6%. The determination of copper ions was the best (98% of concordance), and that of iron II the worst (90.5% of concordance). What is very important, in this measurement series no considerable errors were found.

The results obtained permitted to state that the reproducibility of tests in which semi-permeable membranes were used is very good. These results were the equivalent to those obtained for tests commercially available and developed earlier by us classical tests for the determination of anions and cations in clear aqueous solutions. The results of analysis obtained with dry tests are of course not as exact as those of classical analysis. When the matrix contains only suspensions, then the separation on the semi-permeable membrane is absolutely sufficient for their removal and the result of analysis is very quick.

Table 4. Results of reproducibility studies of chromatographic tests with a semi-permeable polysulfone membrane for ions in sewages containing suspensions and intensive dyes

No.	Ion	Concentration, mg/dm ³	Correct read-out	Decreased read-out	Increased read-out	Definitely erroneous read-out
1	Nickel	27.4	47	1	2	–
2	Copper	15.7	49	–	1	–
3	Cobalt	19.9	47	1	2	–
4	Chromates	16.8	46	3	1	–
5	Iron II	42.2	45	2	3	–
Total			234	7	9	–

The detection threshold in tests with a semi-permeable membrane is the same as in classical tests – usually 5 mg/dm^3 , and in several cases (e.g., Ni II, Fe II) – 2 mg/dm^3 . In the case of chromatographic type tests which are intended for matrices containing dyes or matrices and suspensions it is also possible to carry out analysis directly of the sample studied. However, the detection threshold for these tests is somewhat worse than that for classical tests and is usually $8\div 12 \text{ mg/dm}^3$, and in the case of several ions (Ni II, Fe II) and ascorbic acid – $5\div 7 \text{ mg/dm}^3$. The read-out time is also longer, which is connected with the development of the chromatogram on the test. However, the most essential feature of both tests is that they permit to carry out the analysis without any preliminary processing of the sample studied. The analysis can be performed in the place of sample collection, without the necessity of transporting to a laboratory.

The application of a semi-permeable membrane permitted to separate suspensions in such different matrices like wastewaters or fruit pulps. This proves the high versatility of this solution. The membranes do not decrease the basic parameters of the test, such as detectability threshold or distinguishability between the points of the color scale. They only prolong the analysis time from 30–45 seconds for classical tests to 60 seconds for tests with a membrane and to 4.5 minutes for chromatographic type tests. This is caused by the mode of action of the tests, and not by applying a semi-permeable membrane. However, this time prolongation is of no importance in comparison with the saving of time and costs due to the possibility of abandoning the preliminary processing of the samples analyzed.

4. CONCLUSIONS

The test field material formed due to the deposition of a semi-permeable membrane made of polysulfone or polyethersulfones may be applied for the obtaining of test fields of dry tests. The presence of the membrane on the surface has no essential effect on the reproducibility of tests. Such tests can find application anywhere, where there is a necessity of carrying out fast, approximate analysis in matrices comprising masking suspensions or suspensions and dyes. Due to the character of the tests, even persons without professional qualifications can use them.

The shorter permeation time through the polyethersulfone membranes in comparison with that of polysulfonic ones causes that at identical separation conditions, when the separation time is the only difference, it is more favorable to use membranes on a cellulose surface made of polyethersulfones as a material for test fields.

REFERENCES

- [1] ADAMS E.C., SMEBY R.R., *Diagnostic test device for blood sugar*, US Patent nr. 3, 092, 465 Jun. 4, 1963.
- [2] KOYAMA M., KIGUGAWA S., OKANIWA K., TAMAKI K., *Analytical element and method of use*, US Patent nr. 4, 430, 436 Feb. 7, 1984.

-
- [3] COLUMBUS R.L., PALMER H.J., "Architextured" fluid Management of biological Liquids, Clin. Chem., 33, 1987, pp. 1531–1537.
- [4] CASS A.E.G., DAVIS G., ASTON W.J., HIGGINS I.J. et al., Ferrocene-mediated enzyme electrode for amperometric determination of glucose, Anal. Chem., 56, 1984, pp. 667–671.
- [5] VOGEL P., RITTERSDORF W., THYM D., BARTL K., Development of a potassium assay on the Reflotron, Clin. Chem., 36, 1990, pp. 1070.
- [6] CHWOJNOWSKI A., ŁUKOWSKA E., DUDZIŃSKI K., Applications of semipermeable membranes in dry chemistry/dry tests technology. "Using Membranes to assist in Cleaner Processes" Wrocław 2001, ARGİ, pp. 227–232.
- [7] ŁUKOWSKA E., DUDZIŃSKI K., CHWOJNOWSKI A., WOJCIECHOWSKI C., Dry test for determination of salicylates in whole blood – preliminary tests, J. Art. Organs., 27(7), 2004, p. 604.
- [8] CHWOJNOWSKI A., ŁUKOWSKA E., DUDZIŃSKI K., WOJCIECHOWSKI C., ŚWIĄTEK P., SZCZEPANIAK M., BUKOWSKI J., KOZUCHOWSKI M., Semipermeable polysulfonic membranes for the obtaining of dry tests, Desalination, 163, 2004, pp. 93–101.
- [9] CHWOJNOWSKI A., Dry chemistry (in polish), Exit, Warszawa 2003.
- [10] CHWOJNOWSKI A., DUDZIŃSKI K., WOJCIECHOWSKI C., ŁUKOWSKA E., Dry tests in environmental study. Selected problems and their solutions, Analytical Forum 2004, Warszawa 8–10 July 2004.
- [11] BEHRENS W.A., MADERE R., A high sensitive high performance liquid chromatography method for the estimation of ascorbic acid in tissue, biological fluids and foods, Anal. Biochem., 165, 1987, pp. 102–107.

Keywords: molecularly imprinted membranes, cAMP, selective binding, atomic force microscopy

VICTOR KOCHKODAN*, NIDAL HILAL**,
VLADISLAV GONCHARUK*

COMPOSITE IMPRINTED MEMBRANES LIKE SYNTHETIC RECEPTOR SYSTEMS FOR BIOLOGICALLY ACTIVE COMPOUNDS

Molecularly imprinted membranes for selective recognizing of adenosine 3:5-cyclic monophosphate (cAMP) were prepared through photoinitiated copolymerization of dimethylaminoethyl metacrylate as a functional monomer and trimethylpropane thrimethacrylate as a crosslinker in the presence of cAMP as template using polyvinidendiftoride microfiltration membranes as porous support. The separation and recognizing properties of membranes obtained were studied. It was concluded that the ability of imprinted membranes to selectively binding of cAMP is a result of both specific shape and dimension of recognizing site as well as specific interactions between functional groups responsible for selective template binding inside receptor site. Atomic force microscopy and scanning electron microscopy were used to visualise surfaces and cross-sections of imprinted membranes and to determine their main structural and morphological parameters such as pore size, thickness of selective imprinted layer and surface roughness.

1. INTRODUCTION

Molecular recognition is crucial for living systems, where biological receptors, such as antibodies and enzymes play decisive roles in biological activities. Due to the limitations of biological receptors, i.e. poor stability in harsh environments, the lack of suitable receptors for many practically important compounds, their low stability and/or

* Institute of Colloid and Water Chemistry of National Academy of Science of Ukraine, Vernadskii Pr. 42, 03142 Kyiv, Ukraine. Tel.: 38 044 424 7521; fax: 38 044 423 82 24;

e-mail: vkochkodan@hotmail.com

** Centre for Clean Water Technologies, School of Chemical, Environmental and Mining Engineering, University of Nottingham, University Park, Nottingham NG7 2RD, UK. Tel.: + 44 (0)115 9514168; fax: +44 (0)115 9514115; e-mail: nidal.hilal@nottingham.ac.uk

a high cost, the development of synthetic molecular recognition systems able to mimic the biological molecular recognition has drawn a special attention [1]. Recently it has been shown that molecularly imprinted polymers (MIPs) having a specific synthetic receptor structure are an attractive option for this purpose [2], [3]. The preparation of MIPs usually includes copolymerisation of functional and cross-linker monomer in the presence of a template molecule. Subsequent removal of the template molecules leaves behind receptor sites, which are complementary to the template because of shape and the position of the functional groups. In this way a molecular memory is introduced into the polymer, which becomes capable of selectively rebinding the template molecule.

The polymeric nature of MIPs results in several advantages over natural biological receptors. For instance, the physical and chemical resistances of MIPs permit their sterilization and use in harsh environments.

It has been shown in the last decade that membranes prepared by means of phase inversion technique in the presence of a template molecule possess molecular recognition properties [4]–[6]. Surface modification by grafting in the presence of a template can be also used for synthesis of MIP membranes [7], [8].

Recently, it has been reported that composite thin layer MIP membranes can be prepared using a α -cleavage photoinitiator for initiation of copolymerisation reaction in monomer mixture [9]. In the present work this approach has been used to prepare composite imprinted membranes capable of selective recognizing of adenosine 3':5'-cyclic monophosphate (cAMP).

cAMP is one of the most important “second messengers”, acting as an intracellular regulator, which is also involved in regulating neuronal, glandular, cardiovascular, immune and other functions [10]. Biological recognition elements, such as antibodies, are typically used to specifically bind cAMP. This is an expensive procedure, which requires special handling. Therefore artificial synthetic systems for cAMP recognition are highly desirable.

To gain better understanding in the analysis of MIP layer deposited on membranes, atomic force microscopy (AFM) and scanning force microscopy (SEM) were used in this work to visualise surfaces and cross sections of MIP membranes.

2. MATERIALS AND METHODS

Polyvinylidene fluoride (PVDF) microfiltration membranes of thickness 125 μm (Durapore, Millipore) were used in this study as porous support for deposition of polymer layer imprinted with cAMP.

Benzoin ethyl ether (BEE), trimethylpropane trimethacrylate (TRIM), dimethylaminoethylmethacrylate (DMAEM) and adenosine 3':5'-cyclic monophosphate (cAMP) were obtained from Sigma-Aldrich. The inhibitor was removed from the monomers by passing them through a column of aluminium oxide (activated basic, Brockmann, Sigma-Aldrich) immediately before use.

To produce the imprinted polymer layer on the surface of PVDF membranes, the samples were coated with photoinitiator by soaking in 0.25 M BEE in methanol and the membranes were dried at 40 °C. Thereafter they were immersed in solution containing 6 mM of cAMP, 50 mM or varied concentrations of DMAEM as a functional monomer and 200 mM or varied concentrations of TRIM as a crosslinker in ethanol/water mixture (70:30 vol. %). Samples were ultraviolet (UV) irradiated with a B-100 lamp (Ultra-Violet Products Ltd) of relative radiation intensity of 21.7 mW/cm² at a wavelength of 355 nm. MIP membranes with different degrees of modification (DM) were obtained by varying the time of UV exposure (polymerisation time).

After polymerisation, membranes were extracted with an ethanol/water solution for at least 4 hours and washed with distilled water to remove non-grafted polymer, monomer, residual initiator and the template. The efficiency of this procedure was checked by filtration of distilled water through selected samples and recording the UV absorbance of the filtrate. The absorbance was less than 0.005 at 258 nm.

Degree of modification (DM) was calculated from the difference in weight between the modified membrane with deposited MIP layer and the initial membrane sample. The variation in DM was less than 10%. For comparison blank membranes, without using the template, were prepared using the same procedure.

Binding of cAMP with MIP membranes was evaluated by measuring the adsorption of cAMP from aqueous solution during filtration tests. 5·10⁻⁵ M solution of cAMP in water was filtered through the membranes at a rate of 3 cm³/min using a syringe connected to a 25-mm filter-holder (Swinnex, Millipore). A UV spectrophotometer DMS 80/90 (Varian Techtron, Australia) was used for quantitative determination of cAMP ($\lambda = 258$ nm).

The AFM used was an Explorer (TMX 2000), a commercial device from Veeco Instruments (USA). Silicon cantilevers (Ultralevers, Park Scientific Instruments) with a high aspect ratio tip of typical radius of curvature 50–100 Å were used to produce the images. Profile imaging mode was selected to study the polymeric membranes with the AFM [11]. Images were taken at room temperature of 25 °C.

Scanning electron microscope (SEM) was used to produce cross-sectional images of initial PVDF and MIP membranes. An ISI-SX-30 scanning electron microscope (operating at 30 kV electron accelerating voltage) was employed to view the samples. All photomicrographs were obtained using secondary electron detection mode.

3. RESULTS AND DISCUSSION

The degree of modification (DM) of PVDF membranes depends on the loading concentration of photoinitiator during pre-soaking as well as on the time of polymerisation. Modification of PVDF membranes is a very fast process at these conditions with only short UV exposure times were required to obtain even the highest DM values as shown in

Table 1. Usually lower DM values were obtained for the MIP than for the blank membranes. Obviously this is due to the formation of pre-polymerisation complex between the monomer and the template that influence the kinetics of the copolymerisation reaction [9].

Preliminary arrangement of functional monomer molecules around a template is assumed as an important factor for successful imprinting procedure [12]. The fixation of the structure of this complex during the polymerisation in the growing polymer network generates recognition sites able to bind template. Therefore, the choice of the functional monomers is very important for the creation of recognition sites in MIPs. Because of the acidic nature of cAMP, a functional monomer of a base type such as DMAEM was used for MIP preparation. TRIM, a rigid trifunctional monomer was chosen as a crosslinker due to its efficiency in imprinting procedure [13].

Table 1. Effect of UV exposure time on DM of MIP and blank PVDF membranes

UV exposure time, min	DM, $\pm 20 \mu\text{g}/\text{cm}^2$	
	MIP	Blank
0.5	250	420
1	470	620
2	700	810
3	820	880
4	920	940
5	1100	1140

Concentrations of the crosslinker and the functional monomer in the reaction mixture were varied to optimise the composition for modification of PVDF membranes with imprinted polymer layers. An increase of TRIM concentration in reaction mixture, up to 200 mM leads to enhanced cAMP binding as shown in Fig. 1. Thus the MIP polymer matrix should be rather rigid to preserve the selective cavity structure after the removal of the template [2], [12]. An increase of crosslinking density reduces polymer chain flexibility and in that way provides improved stabilisation of the structure of selective cavity. This improves the contribution of specific binding to receptor sites and leads to an increase of cAMP sorption. High TRIM concentration in the reaction mixture ($> 200 \text{ mM}$) leads to a decrease of cAMP sorption. Obviously this is a result of formation an increasing fraction of excessively cross-linked domains in MIP matrix, which possess a reduced number of MIP receptor sites and a poor access of the template to them.

As can be seen in Fig. 2, an increase of DMEAM concentration in reaction mixture results in an increase of cAMP sorption with MIP membranes, apparently due to the creation of an increasing number of specific template bonding sites in the imprinted polymer. At the same time the non-specific sorption of cAMP also tends to increase with DMEAM concentration, though much less pronounced. This indi-

cates that the number of non-specific binding sites in MIP rise as the functional monomer content increases. The excessive concentration of the functional monomer was five times more than that of the template. This may result in the formation of a variety of binding sites with different affinities.

Aqueous solution of $5 \cdot 10^{-5}$ M cAMP used for filtration experiments has pH 4.2. Dimethylamino groups are positively charged at this pH [14]. It can be assumed that the ionic interactions between the phosphorous residue in the cAMP molecule and the protonated dimethylamino groups of MIP network contribute to the affinity of MIP membranes. This was proved by a decline of cAMP sorption when the ionic strength of the solution is increased as shown in Table 2. The ionic interaction becomes weaker with increasing of NaCl concentration due to more effective shielding of charged groups. It also shows that the sorption of cAMP is sensitive to pH of filtered solution. This is probably due to change of degree of protonation of dimethylamino groups [15].

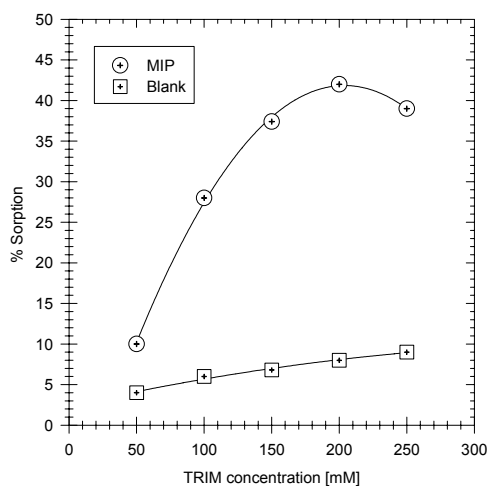


Fig. 1. Effect of cross-linker concentration in the reaction mixture on cAMP sorption on MIP and blank PVDF membranes (DM of $540 \pm 20 \mu\text{g}/\text{cm}^2$)

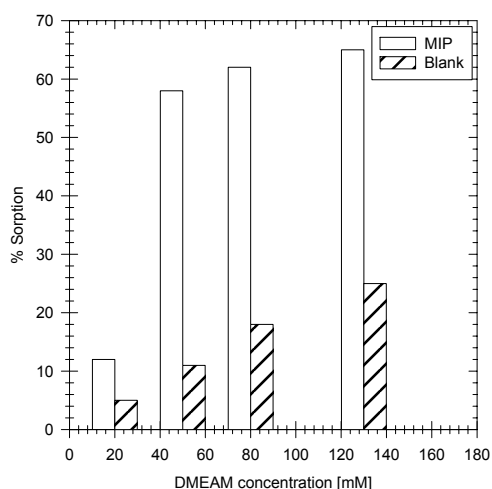


Fig. 2. Effect of DAEAM concentration on sorption of cAMP on MIP and blank PVDF membranes (DM of $820 \pm 20 \mu\text{g}/\text{cm}^2$)

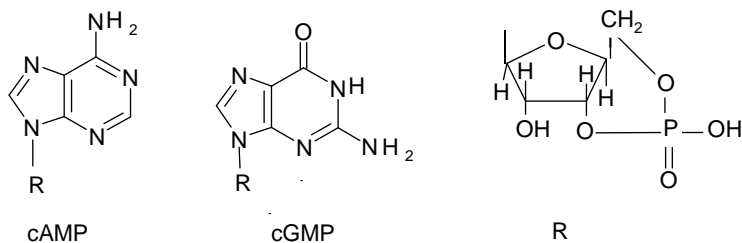
Table 2. Influence of pH and NaCl concentration on the cAMP sorption on MIP and blank PVDF membranes at DM of $1100 \pm 40 \mu\text{g}/\text{cm}^2$

Membrane	NaCl concentration, M			PH	
	10^{-4}	10^{-3}	10^{-1}	4.2	11.2
MIP	70	42	32	72	22
Blank	24	10	8	24	6

Table 3. Sorption of cAMP and cGMP and binding capacity of MIP PVDF membranes

Degree of modification, $\pm 20 \mu\text{g}/\text{cm}^2$	Sorption, %		Binding capacity to cAMP, $\mu\text{g}/\text{cm}^2$
	cAMP	cGMP	
0	4	3	
540	44	22	4.2
920	67	30	10.5
1100	72	41	12.6

Table 3 shows sorption of adenosine 3:5-cyclic monophosphate (cAMP) and guanosine 3:5-guanidine cyclic monophosphate (cGMP) on MIP membranes with different degree of modification. It may be seen from this table that essentially less sorption of structurally similar cGMP is obtained for MIP membranes compared to cAMP. Both cAMP and cGMP molecules include a phosphorous group and they only differ in the substituents on their purine base moiety. The adenine base of cAMP contains an NH_2 group at the C6 position, whereas in the guanine base of cGMP the same position is replaced with a carboxyl group, the C2 position is substituted with an NH_2 group as shown in the formula below.



The ability of the cAMP imprinted membranes to distinguish between cAMP and the structurally similar cGMP suggests that the binding of cAMP to the recognising sites is not only based on ionic interactions. Other interactions may also contribute to affinity of MIP membranes, possibly hydrogen bonding between amino and hydroxyl groups of template molecule and carbonyl groups of MIP. The size and the shape of binding cavity along with the correct spatial orientation of the functional groups in the MIP binding sites also play an important role [2], [3].

The schematic representation for the formation of the recognition sites specific to cAMP is presented in Fig. 3. At the first stage (non shown) the molecules of DMEAM are arranged around the cAMP, this results in formation of the so-called pre-polymerisation complex. This complex is fixed in a rigid polymer matrix created during the polymerisation of the functional monomer with crosslinker (Fig. 3a). Following template extraction leaves in the polymer matrix the specific recognition sites complementary to the cAMP in shape and in the positioning of the functional groups (Fig. 3b). Due to these specific sites, the MIP is capable to rebind cAMP molecules. Thus, it can be concluded that binding of cAMP with MIP membranes is a result of both ionic inter-

actions between functional groups of polymer matrix and the template and the specific shape of recognizing sites which are complementary to cAMP molecule.

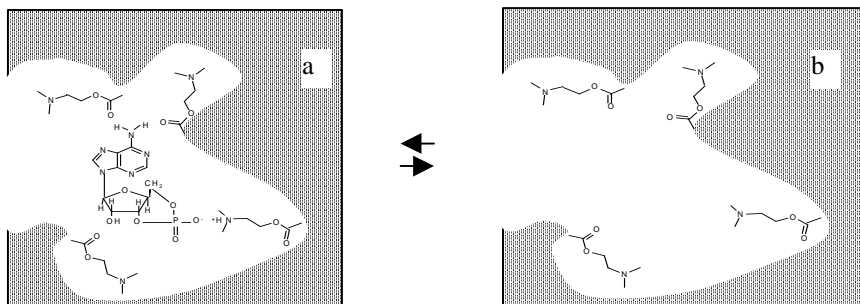


Fig. 3. Scheme for formation of special recognizing sites in MIP matrix

It is important to note that the binding capability of MIP membranes can be adjusted by varying the degrees of modification (DM). cAMP sorption on MIP membranes increases with an increase of DM (Table 3). Two factors, obviously, contribute to this effect. Firstly, increasing DM values leads to a decrease in pore size of MIP membranes, secondary higher DM values results in increasing the thickness of deposited imprinted polymer layer. The thicker the deposited imprinted layer the larger number of recognition sites can “meet” the template molecules while passing through the membrane thus enhancing the cAMP binding. It should be noted that changes in the non-specific sorption of cAMP are negligible with increasing of DM values. Sorption of cAMP on blank membranes proceeds mainly via non-specific binding with the dimethylamino groups of polymer matrix.

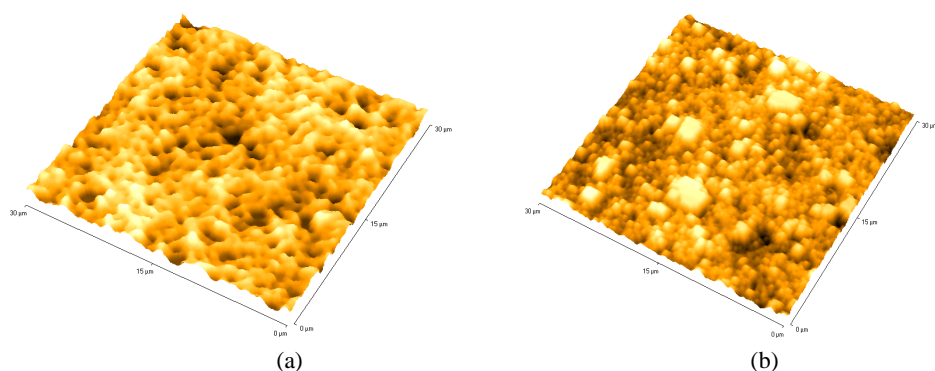


Fig. 4. 3D AFM images of: (a) initial PVDF membrane; (b) MIP membrane with DM of $1100 \mu\text{g}/\text{cm}^2$

Fig. 4 shows high-resolution AFM images of initial and modified PVDF membrane with DM of $1100 \mu\text{g}/\text{cm}^2$ in three-dimensional form over an area of $35 \times 35 \mu\text{m}$. SEM cross-sectional images for these membranes are presented in Fig. 5.

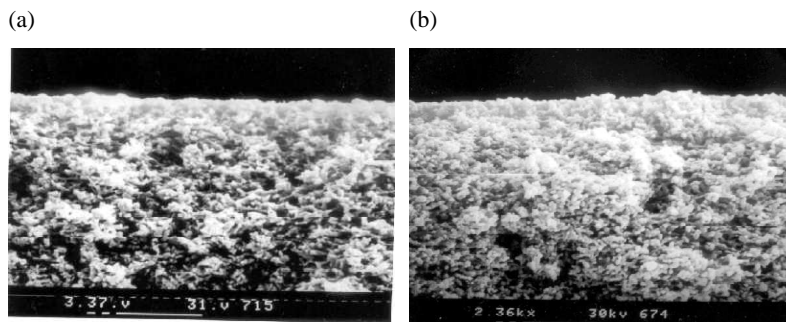


Fig. 5. SEM cross-section images of: (a) initial PVDF membrane;
(b) MIP membrane with DM of 1100 $\mu\text{g}/\text{cm}^2$

The colour density in Fig. 4 shows the vertical profile of the sample with the light regions being the highest points and the darkest regions being the pores. The pores are clearly visible as well-defined dark areas. The AFM software allows quantitative determination of the diameter of pores as well as surface roughness and total surface area of membrane samples.

As can be seen from Table 4, deposition of imprinted layer results in a decrease of surface pore size of MIP membranes when compared with the pore size for initial PVDF membrane. Additionally, modification of porous support with imprinted layer leads to increasing surface roughness and therefore total contact surface area of MIP membrane. These effects can also contribute to the increase of cAMP sorption on MIP membranes.

The modification method described results in the formation of a very thin imprinted polymer layer. As was found from SEM images, even at high DM of 1000–1100 $\mu\text{g}/\text{cm}^2$ the thickness of deposited MIP does not exceed 10–11 nm. This preserves the high permeability properties of the composite MIP membranes.

Table 4. AFM characteristics of porous structure of initial PVDF membrane and MIP membrane at DM of 1100 $\mu\text{g}/\text{cm}^2$

Membrane	DM, $\mu\text{g}/\text{cm}^2$	Roughness, nm	Total contact area, μm^2	Mean pore diameter, μm
PVDF initial	0	192.3	1020	1.08 ± 0.10
MIP	1100	296.4	1167	0.56 ± 0.17

Due to the small area of membrane samples cAMP binding capacity was saturated at relatively low permeate volumes (15–25 cm^3). However, the high MIP membrane water fluxes allow the application of membrane stacks for membrane solid-phase separation [16]. Re-use of the MIP membranes is possible after release of sorbed cAMP by treatment with 0.1 M NaOH and subsequent washing membrane with water.

4. CONCLUSIONS

Thin layer molecularly imprinted composite membranes capable to specifically recognize of 3':5'-cyclic monophosphate (cAMP) were developed using photoinitiated copolymerisation of dimethylaminoethylmetacrylate (DMAEM) with trimethylpropanethrimethacrylate (TRIM) in the presence of cAMP. As a result, PVDF membranes covered with a thin layer of imprinted polymer selective to cAMP were obtained. It was found the sorption of cAMP on MIP membranes varies with pH and ionic strength of a feed solution. It was concluded that the ability of MIP membranes to bind cAMP is a result of both ionic interactions between charged dimethylamino groups of polymer matrix and the phosphorous group of the cAMP molecule as well as the correct position of functional groups involved in binding imprinted polymer and the specific shape/size of recognizing sites which are complementary to cAMP molecule. The binding capability of MIP membranes can be adjusted by varying of DM values. Surface pore size, surface roughness of MIP membranes and thickness of deposited imprinted layer were determined using AFM and SEM techniques. It was shown that the synthesis of MIP results in the deposition of a very thin imprinted polymer layer (10–11 nm) on the surface of PVDF membranes that retains the high flux for MIP membranes.

REFERENCES

- [1] KLEIN E., *Affinity membranes: a 10-year review*, Journal of Membrane Science, 179, 2000, pp. 1–27.
- [2] WULFF G., *Molecular imprinting in cross-linked materials with the aid of molecular templates – A way towards artificial antibodies*, Angew. Chem., Int. Ed. Engl. 34, 1995, pp. 1812–1826.
- [3] MOSBACH K., RAMSTROM O., *The emerging technique of molecular imprinting and its future impact on biotechnology*, Bio/Technology, 14, 1996, pp. 163–166.
- [4] MATHEW-KROTZ J., SHEA K.J., *Imprinted polymer membranes for the selective transport of target neutral molecules*, Journal of American Chemical Society, 118, 1996, pp. 8154–8158.
- [5] WANG H.Y., KOBAYASHI T., FUJI N., *Molecular imprint membranes prepared by the phase inversion precipitation technique*, Langmuir, 12, 1996, pp. 4850–4856.
- [6] PILETSKY S.A., PANASYUK T.L., PILETSKAYA E.V. et al., *Receptor and transport properties of imprinted polymer membranes*, Journal of Membrane Science, 157, 1999, pp. 263–272.
- [7] PILETSKY S.A., MATUSCHEWSKI H., SCHEDLER U. et al., *Surface functionalization of porous polypeptide membranes with molecularly imprinted polymers by photograft copolymerization in water*, Macromolecules, 33, 2000, pp. 3092–3098.
- [8] SERGEEVA T.A., MATUSCHEWSKI H., PILETSKY S.A. et al., *Molecularly imprinted polymer membranes for substance selective solid-phase extraction from water by surface photo-grafting polymerization*, Journal of Chromatography A, 907, 2001, pp. 89–96.
- [9] KOCHKODAN V., WEIGEL W., ULBRICHT M., *Thin layer molecularly imprinted microfiltration membranes by photofunctionalization using a coated α -cleavage photoinitiator*, Analyst, 126, 2001, pp. 803–809.
- [10] ROBINSON G.A., BUTCHER R.A., SUTHERLAND E.W., *Cyclic AMP*, Academic Press, NY, 1971.
- [11] BOWEN W.R., HILAL N., LOVITT R.W., WRIGHT C.J., *Atomic force microscope studies of membrane surfaces*, in: Surface Chemistry and Electrochemistry of Membrane Surfaces (ed. Sorensen T.S.), Surfactant Science Series, Marcel Dekker Inc, USA, 79, 1999, pp. 1–37.

- [12] SELEGREN B., *Important consideration in the design of receptor sites using noncovalent imprinting*, in: *Molecular and ionic recognition with imprinted polymers*, (eds. Bartsch, R.A., Maeda, M.), ACS Symposium, Ser.703, American Chemical Society, Washington, 1998, pp. 49–80.
- [13] KEMPE M., MOSBACH K., *Separation of amino acids, peptides and proteins on molecularly imprinted stationary phases*, *Journal of Chromatography A.*, 691, 1995, pp. 317–325.
- [14] YAMADA K., SATO T., TATEKAWA S., HIRATA M., *Membrane properties of polyethylene films photografted with hydrophilic monomers*, *Polymer Gels Networks*, 2, 1994, pp. 323–328.
- [15] YAMADA K., SATO T., HIRATA M., *Uphill transport of organic electrolytes using polyethylene films photografted with 2-(dimethylamino)ethyl methacrylate*, *Journal of Material Science*, 34, 1999, pp. 1081–1086.
- [16] ROPER D.K., LIGHTFOOT E.N., *Separation of biomolecules using adsorptive membranes*, *Journal of Chromatography A.*, 702, 1995, pp. 3–21.

Keywords: model lipid membrane, temperature-sensitive liposome, membrane fluidity, ¹H-NMR spectroscopy, drug delivery

ANNA TIMOSZYK*, LIDIA LATANOWICZ*

PHYSICAL STABILITY OF TEMPERATURE-SENSITIVE LIPOSOMES

Physical stability of liposome depends on the vesicle size and other factor such as electric charge density of lipid membrane, pH and osmotic pressure difference across the membrane and fluidity of the membrane. The membrane fluidity, pH and vesicle size were investigated for two types of model membranes. The first model membrane is formed from 1,2-Diacyl-*sn*-glycero-3-phosphocholine (PC) and the second model membrane is formed from mixture of 1,2-Diacyl-*sn*-glycero-3-phosphocholine and octadecylamine (PC/ODA). The membrane fluidity was studied by ¹H – NMR Spectroscopy. The paper reports the temperature dependence of the chemical shift (σ , ppm), half-width of spectral lines ($\nu_{1/2}$, Hz) and splitting of signal assigned to $-N^+$ (CH₃)₃ choline groups (δ , Hz). Studies were carried out in the temperature range of 5–50 °C. Increasing the temperature level caused an increase in a chemical shift. The half-width of ¹H – NMR spectral lines decreases with temperature. Increasing of temperature caused increasing fluidity of model membranes. The PC membrane fluidity changes more rapidly than fluidity of PC/ODA membrane. PC/ODA liposomes grow slowly with temperature, whilst, PC liposomes are growing to damage liposome structure between temperatures 35–40 °C. *In vivo* temperature-sensitive PC/ODA large unilamellar vesicles may preferentially release encapsulated in locally heated target area (42–44 °C).

1. INTRODUCTION

Potential uses of liposomes for drug delivery to cells or organs are attractive mode of therapy to increase the therapeutic effects and to reduce drug toxicity. The concept of utility of temperature-sensitive liposomes is based on the dramatic increase in permeability of a liposome at a temperature where its molecules are rearranging from one stable state to a second stable state [1], [2]. The properties of liposomes depend on the

* Laboratory of Biophysics, Department of Biotechnology, Institute of Biotechnology and Environmental Sciences, University of Zielona Góra, 65-561 Zielona Góra, Poland. Tel. /fax: +48(68)3287323, e-mail: A.Timoszyk@ibos.uz.zgora.pl

composition and concentration of constituent's lipids and the ionic strength of the aqueous medium, as well as the method of lipid suspension and the time of hydration.

The liposome size is the key to the *in vivo* behaviour of liposomes since their clearance from circulation is a function of the particle diameter and surface composition [3], [4]. Changes in the liposome size can have dramatic effects on *in vivo* behaviour of liposome. Small liposomes (SUV) are better than large liposomes for a specific *in vitro* drug delivery [5]. Large unilamellar vesicles (LUV) appear more favourable than SUV, as they can be made induced to release their contents rapidly in the presence of serum. Their much larger ratio of internal volume to lipid, temperature-sensitive LUVs may be especially useful *in vivo* [1].

One of the critical characteristics of liposome systems is their physical stability. Temperature-sensitive liposomes with local hyperthermia are generally used for the treatment of cancer via chemotherapy. *In vivo*, temperature-sensitive liposomes preferentially release encapsulated in locally heated area [6], [7]. The rate of release is dependent on the rate of change of temperature and is markedly enhanced by serum components, particularly lipoproteins [8]. There are a number of ways in which local hyperthermia might increase the effectiveness of drugs containing liposome: (a) by promoting selective drug release at phase transition temperature; (b) by increasing local blood flow; (c) by increasing endothelial permeability to particles, thereby enhancing accumulation of liposome in the target tissues; (d) by increasing the permeability or susceptibility of target cells to drug released from the liposome; (e) by increasing direct transfer of drug from liposome to cells by fusion or endocytosis. Local hyperthermia is currently receiving increased attention as a therapeutic tool, for use either alone or in conjunction with radiation. Local hyperthermia methods have been applied to animal and human tumors [9], [10]. Mild local hyperthermia (37–41 °C) has been found to be ineffective in treating tumors and may stimulate metastasis [10], [11]. Moderate hyperthermia (42–44 °C) is currently under intensive study due to the difference in temperature sensitivity between cancer cells and normal cells [12], [13]. The local hyperthermia treatments reduced the size and the growth of the treated tumors compared with control values for eight different solid mouse tumors (Lewis carcinoma, ovarian carcinoma, colon carcinoma 38, colon carcinoma 26, mammary adeno carcinoma C3 HBA, mammary adeno carcinoma 16 C, glioma and melanoma) [1]. Since many normal mammalian cells begin to show damage at about 40 °C the aim of research has been to achieve therapeutic results in just a few degrees above physiological temperature [14].

2. MATERIALS AND METHODS

1,2-Diacyl-*sn*-glycero-3-phosphocholine as lyophilized powder and octadecylamine ($\text{CH}_3(\text{CH}_2)_{17}\text{NH}_2$) were purchased from Sigma. Heavy water (D_2O) was obtained from the Institute of Nuclear Research, Świerk, Poland.

The stock solution of 1,2-Diacyl-*sn*-glycero-3-phosphocholine (PC) and stock solution of 1,2-Diacyl-*sn*-glycero-3-phosphocholine (PC) mixed with octadecylamine (ODA) in chloroform were dried under nitrogen and dispersed in D₂O. The final concentration of PC was 25 mg/cm³. The constant concentration of ODA was 0.435 mg/cm³. The PC and PC/ODA liposome suspensions had pH 4.7. The suspensions were then sonicated under nitrogen for 45 min with a 20 kHz sonicator with a titanium probe. During the sonication the samples were thermo stated at 0–2 °C.

NMR data were collected for samples of 0.5 cm³ vesicle suspension in 5 mm NMR tubes. ¹H – NMR spectra were recorded on BRUCER DRX-500 spectrometer in temperature range 5–50 °C. The measurement of temperature was conducted with exact to 0.01 °C.

3. RESULTS AND DISCUSSION

The fluidity of model membranes was monitored in the temperature range of 5–50 °C in pH 4.7. Table 1 and Table 2 show changes in the chemical shift (σ , ppm) of ¹H – NMR spectral lines of PC and PC/ODA liposomes.

Table 1. Changes of chemical shift (σ , ppm) of ¹H – NMR spectral lines PC liposomes in the temperature range of 5–50 °C

temperature (°C)	5	10	15	20	25	30	35	40	45	50
–CH ₃	0.49	0.58	0.67	0.75	0.82	0.90	0.98	0.58	1.12	1.17
–(CH ₂) _n	0.88	0.96	1.05	1.13	1.20	1.28	1.37	1.44	1.52	1.57
–CH ₂ –C–CO–	1.18	1.26	1.37	1.45	1.53	1.61	1.70	1.78	1.84	1.89
–CH ₂ –C=	1.64	1.73	1.82	1.90	1.98	2.06	2.14	2.21	2.27	2.32
–CH ₂ –CO–	1.99	2.07	2.19	2.25	2.33	2.37	2.46	2.52	2.59	2.64
=C–CH ₂ –C=	2.39	2.48	2.57	2.64	2.74	2.81	2.89	2.96	3.00	3.05
–N ⁺ (CH ₃) ₃	2.83	2.93	3.01	3.09	3.17	3.25	3.34	3.42	3.48	3.53
	2.86	2.95	3.03	3.11	3.19	3.27	3.35			
–CH ₂ –N ⁺	3.31	3.40	3.48	3.56	3.63	3.71	3.79	3.85	3.91	3.97
–CH ₂ –OP–	–	3.72	3.80	3.88	3.96	4.03	4.12	4.18	4.25	4.29
–O ₃ POCH ₂ –	3.91	4.00	4.09	4.17	4.24	4.32	4.41	4.47	4.54	4.59
–CH=CH–	4.92	5.02	5.10	5.17	5.24	5.32	5.40	5.47	5.54	5.62

For both model membranes the chemical shift increased with the increase of temperature. It means that all ¹H – NMR spectral lines shift in the direction of lower field. This is a typical effect of increasing temperature. The changes in the chemical shift of signals assigned to all chemical groups are proportional to the level of temperature (Table 1 and Table 2).

Table 2. Changes of chemical shift (σ ppm) of ^1H – NMR spectral lines PC/ODA liposomes in the temperature range of 5–50 °C

temperature (°C)	5	10	15	20	25	30	35	40	45	50
$-\text{CH}_3$	0.52	0.60	0.68	0.74	0.81	0.87	0.93	0.99	1.04	1.11
$-(\text{CH}_2)_n$	0.92	0.98	1.05	1.12	1.22	1.25	1.33	1.40	1.45	1.50
$-\text{CH}_2-\text{C}-\text{CO}-$	-	1.29	1.37	1.45	1.52	1.58	1.65	1.71	1.77	1.83
$-\text{CH}_2-\text{C}=\text{}$	1.67	1.76	1.83	1.90	1.96	2.03	2.08	2.15	2.20	2.26
$-\text{CH}_2-\text{CO}-$	2.02	2.10	2.18	2.24	2.31	2.37	2.40	2.49	2.49	2.57
$=\text{C}-\text{CH}_2-\text{C}=\text{}$	2.43	2.50	2.57	2.64	2.70	2.76	2.82	2.88	2.93	2.99
$-\text{N}^+(\text{CH}_3)_3$	2.85	2.94	3.01	3.08	3.14	3.21	3.27	3.32	3.38	3.44
	2.88	2.96	3.04	3.11	3.17	3.23	3.29	3.35	3.41	4.79
$-\text{CH}_2-\text{N}^+$	3.33	3.41	3.49	3.55	3.61	3.67	3.73	3.79	3.84	3.90
$-\text{CH}_2-\text{OP}-$	-	-	-	-	-	4.01	4.07	4.12	4.18	4.23
$-\text{O}_3\text{POCH}_2-$	3.93	4.02	4.09	4.16	4.22	4.29	4.35	4.41	4.46	4.52
$-\text{CH}=\text{CH}-$	4.97	5.03	5.10	5.17	5.23	5.29	5.34	5.40	5.46	5.52

The NMR parameter used in this work is the spin–spin relaxation time, T_2 . The half-width of spectral line $\nu_{1/2}$ for a Lorentzian lineshape:

$$\nu_{1/2} = (\pi T_2)^{-1}. \quad (1)$$

The relaxation time T_2 , measures how long neighbouring nuclei take to exchange magnetic energy. T_2 is approximately proportional to the rate of motion [15]. It follows that rapid motions lead to narrow spectral lines, while slow motions lead to lines broad. Decreasing half-width signals gives information about increasing freedom of motion. Fig. 1 show decrease of half-width of ^1H – NMR spectral lines assigned to $-(\text{CH}_2)_n$, $-\text{CH}_3$ and $-\text{N}^+(\text{CH}_3)_3$ groups of PC and PC/ODA liposomes as a function of temperature. The half-width of spectral lines decreased with increasing of temperature.

The temperature of a typical liposome structure we can to qualify measure splitting (δ , Hz) between choline groups of outer and inner layer of membrane ($-\text{N}^+(\text{CH}_3)_3$) [16]–[20]. Fig. 2 show changes of splitting (δ , Hz) PC and PC/ODA choline groups as a function of temperature. The structural organization and the dynamics of lipid bilayer can be modulated in different ways. To obtain good approximation of a model membrane it is very important to obtain small unilamellar vesicles (SUV). The impact of temperature on mechanical properties of lipid liposome is strongly pronounced during the formation of small unilamellar vesicles by a sonication procedure. The effect of increasing temperature on model membranes has been found to perturb the fluidity of the lipid bilayer. The effect of the increase in a chemical shift (σ , ppm) of ^1H – NMR spectral lines for both model membranes was also observed (Table 1 and Table 2). The increase in a chemical shift provides insights about decreasing of Van der Waals interchain interactions.

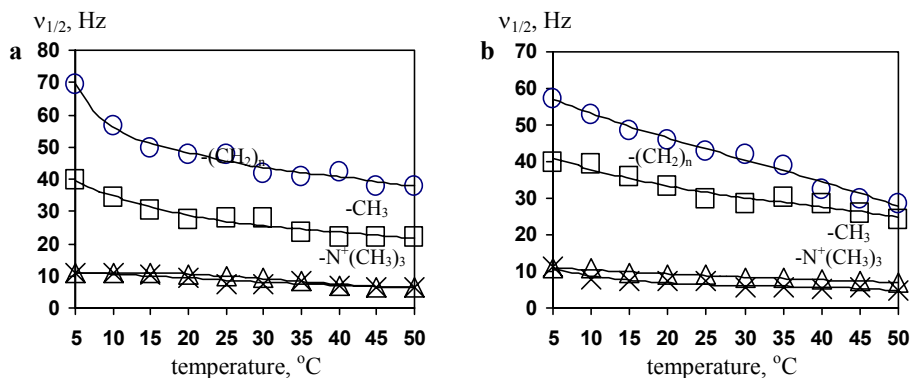


Fig. 1. The half-width ($\nu_{1/2}$, Hz) of ^1H -NMR spectral lines assigned to $-(\text{CH}_2)_n$, $-\text{CH}_3$ groups of lipid alkyl chains and $-\text{N}^+(\text{CH}_3)_3$ choline groups PC liposomes (a) and PC/ODA liposomes (b) as a function of temperature. The half-width of spectral lines assigned to choline groups from outer layer of membrane is designated as a triangle and half-width of spectral lines assigned to choline groups from inner layer of membrane is designated as a cross

The effect of narrowing of the spectral lines is directly related to the unlimitation of segmental movement of lipid molecules [15]. This effect was observed in narrowing of ^1H -NMR spectral lines assigned to $-(\text{CH}_2)_n$, $-\text{CH}_3$ groups of lipid alkyl chain and $-\text{N}^+(\text{CH}_3)_3$ choline groups (Fig. 1a and Fig. 1b). The half-width ($\nu_{1/2}$, Hz) of NMR lines assigned to $-(\text{CH}_2)_n$ groups changes the most. This is characteristic for the chain-melting phase transition effect. The increase in temperature has been found ineffective in changing fluidity in hydrophilic core of lipid bilayer. The fluidity of PC liposomes changes more rapidly than the fluidity of PC/ODA liposomes. The fluidity of PC/ODA liposome changes progressively. The effect of narrowing spectral lines of PC/ODA liposome is dependent on the physical properties of ODA. Adding the 0.435 mg/cm^3 of ODA has modified the ionic strength and the value of positive membrane charge [21], [22].

Splitting the signals assigned to $-\text{N}^+(\text{CH}_3)_3$ is typical for small unilamellar liposomes (SUV: $0.02\text{--}0.03 \mu\text{m}$) [23]. With an increase in temperature, a diameter of liposomes increases (LUV: $0.05\text{--}1 \mu\text{m}$) and therefore the splitting decreases [1]. In the temperature range of $5\text{--}50 \text{ }^\circ\text{C}$ the size of PC/ODA liposomes changes a little (Fig. 2b). With an increase in temperature, PC liposomes systematically grow and between temperatures $35\text{--}40 \text{ }^\circ\text{C}$ a stable state of liposome structure is damaged (Fig. 2a). In fact, local hyperthermia ($37\text{--}41 \text{ }^\circ\text{C}$) has been found to be ineffective in treating tumors so temperature-sensitive PC liposomes are ineffective as drug delivery vehicles in the hyperthermia therapy.

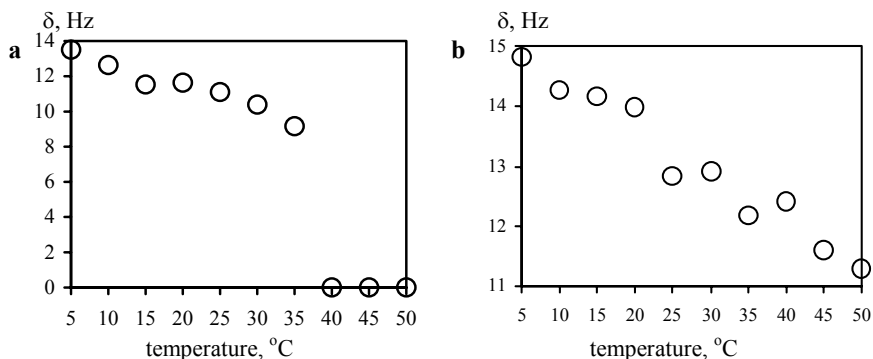


Fig. 2. The splitting (δ , Hz) of ^1H – NMR spectral line assigned to choline group ($-\text{N}^+(\text{CH}_3)_3$) PC liposomes (a) and PC/ODA liposomes (b) as a function of temperature

The PC/ODA liposomes are growing slowly with an increase in temperature from SUVs (0.02–0.03 μm) to LUVs (0.05–1 μm) (Fig. 2b). *In vivo* temperature-sensitive PC/ODA LUVs may preferentially release encapsulated in locally heated target area (42–44 $^\circ\text{C}$). Consequently, changes in the vesicle size cause an increase of permeability of lipid bilayer [1], [3]. Temperature-sensitive LUVs in hyperthermia can aggregate or fuse [1]. Perhaps, temperature-sensitive PC/ODA liposomes may transfer drug from liposomes to cells by fusion or endocytosis in hyperthermia. The temperature-sensitive PC/ODA liposomes seem to be stable even in high temperatures (45–50 $^\circ\text{C}$) but stability of liposomes in the presence of serum is smaller than predicted by theory [3]. LUVs in moderate local hyperthermia (42–44 $^\circ\text{C}$) can be made to release their contents rapidly in the presence of serum [1].

4. CONCLUSIONS

The results of ^1H – NMR investigations indicate that temperature-sensitive liposomes with local hyperthermia seem to be a promising approach to targeting of drug. The physical characteristic of liposomes to target release has been successful with temperature-sensitive PC/ODA liposomes in moderate temperature range (42–44 $^\circ\text{C}$) of local hyperthermia. The temperature-sensitive positively charged PC/ODA liposomes may be useful for drug entrapment and their controlled release.

ACKNOWLEDGEMENTS

This work was supported by the State Committee for Scientific Research, grant no. 2 P03B 08625

REFERENCES

- [1] ÖZER A.Y., FARIVAR M., HINCAL A.A., *Temperature- and pH-Sensitive Liposomes*, Eur. J. Pharm. Biopharm., 39, 1993, pp. 97–101.
- [2] BENDAS G., KRAUSE A., BAKOWSKY U., VOGEL J., ROTHE U., *Targetability of novel immunoliposomes prepared by a new antibody conjugation technique*, Int. J. Pharmaceutics, 181, 1999, pp. 79–93.
- [3] ARMENGOL X., ESTELRICH J., *Physical stability of different liposome compositions obtained by extrusion method*, J. Microencapsulation, 12, 1995, pp. 525–535.
- [4] CULLIS P.R., HOPE M.J., BALLY M.B., MADDEN T.D., MEYER L.D., JANOFF A.S., *Liposomes, From Biophysics to Therapeutics*, Wiley & Sons, New York, 1987.
- [5] MACHY P., LESERMAN L.D., *Small liposomes are better than large liposomes for specific drug delivery in vitro*, Biochim. Biophys. Acta, 730, 1983, pp. 313–320.
- [6] WEINSTEIN J.N., MARGIN R.L., YATVIN M.B., ZAHARKO D.S., *Liposomes and local hyperthermia: selective delivery of methotrexate to heated tumors*; Science, 204, 1979, pp. 188–191.
- [7] YATVIN M.B., MUHLENSIEPEN H., PORSCHEN W., WEINSTEIN J.N., FEINENDEGEN L.E., *Selective delivery of liposomes – associated cis-dichlorodiamineplatinum (II) by heat and its influence on tumor drug uptake and growth*, Cancer Res., 41, 1981, pp. 1602–1607.
- [8] ZBOROWSKI J., ROERDINK F., SCHERPHOF G., *Leakage of sucrose from phosphatidylcholine liposomes induced by interaction with serum albumin*, Biochim. Biophys. Acta, 497, 1977, pp. 183–186.
- [9] HAR-KEDAR I., BLEEHAN N.M., *Experimental and clinical aspects of hyperthermia applied to the treatment of cancer with special reference to the role of ultrasonic and microwave heating*, Adv. Radiat. Biol., 6, 1976, pp. 229–234.
- [10] DICKSON A.J., *The effects of hyperthermia in animal tumor systems*, Resent Results Cancer Res., 59, 1977, pp. 43–51.
- [11] DICSON J.A., ELLIS H.A., *The influence of tumor volume and the degree of heating on the response of the solid yoshida sarcoma to hyperthermia*, Cancer Res., 36, 1976, pp. 1188–1195.
- [12] MARGIN R.L., WEINSTEIN J.N., *Delivery of drug in temperature sensitive liposomes, in targeting of drugs*, Plenum Press, New York, 1982.
- [13] YATVIN M.B., CREE T.C., GIPP J.J., *Targeting of drugs*, Plenum Press, New York, 1981.
- [14] YATVIN M.B., WEINSTEIN J.N., DENNIS W.H., BLUMENTHAL R., *Design of liposomes for enhanced local release of drugs by hyperthermia*, Science, 202, 1978, pp. 1290–1293.
- [15] DARKE A., FINER E.G., MOORHOUSE R., REES D.A., *Studies of Hyaluronate Solutions by Nuclear Magnetic Relaxation Measurements: Detection of Covalently-defined, Stiff Segments within the Flexible Chains*, J. Mol. Biol., 99, 1975, pp. 477–486.
- [16] GABRIELSKA J., SARAPUK J., PRZESTALSKI S., *Role of Hydrophobic and Hydrophilic Interactions of Organotin and Organolead Compounds with Model Lipid Membranes*, Verlag der Zeitschrift für Naturforschung, 52, 1997, pp. 209–216.
- [17] KASZUBA M., HUNT G.R. A., ^{31}P - and ^1H – NMR investigations of the effect of n-alcohols on the hydrolysis by phospholipase A_2 of phospholipid vesicular membranes, Biochim. Biophys. Acta, 1030, 1990, pp. 88–93.
- [18] JANAS T., KRAJINSKI H., TIMOSZYK A., *Translocation of polysialic acid across model membranes: kinetic analysis and dynamic studies*, Acta Biochim. Pol., 48, 2001, pp. 163–173.
- [19] TIMOSZYK A., JANAS T., *Effect of sialic acid polymers on dynamic properties of lecithin liposomes modified with cationic octadecylamine*, Molecular Phys. Rep., 37, 2003, pp. 67–70.
- [20] HUNT G.R.A., JONES I.C., *Application of ^1H – NMR to the design of liposomes for oral use: Synergistic activity of bile salts and pancreatic phospholipase A_2 in the induced permeability of small unilamellar phospholipid vesicles*, J. Microencapsulation, 1, 1985, pp. 113–122.

- [21] WEBB M.S., WHEELER J.J., BALLY M.B., MAYER L.D., *The cationic lipid stearylamine reduces the permeability of the cationic drugs verapamil and prochlorperazine to lipid bilayers: implications for drug delivery*, *Biochim. Biophys. Acta*, 1238, 1995, pp. 147–155.
- [22] KOZUBEK A., *Positively and negatively charged submicron emulsions for enhanced topical delivery of antifungal drugs*, *J. Control. Release*, 58, 1999, pp. 177–187.
- [23] GUBERNATOR J., STASIUK M., KOZUBEK A., *Dual effect of alkylresorcinols, natural amphiphilic compounds, upon liposomal permeability*, *Biochim. Biophys. Acta*, 1418, 1999, pp. 253–260.

*Keywords: gas separation, poly(1-trimethylsilylpropyne),
organic vapors*

O.B. BORISEVICH*, D.A. SYRTSOVA*, V.V. TEPLYAKOV*,
V.S. KHOTIMSKII*, D.A. ROIZARD**

THE INFLUENCE OF FILM THICKNESS ON PERMEABILITY OF GASES AND ORGANIC VAPORS THROUGH POLY(1-TRIMETHYLSILYLPROPYNE)

Permeability properties of the most permeable polymer poly(1-trimethylsilylpropyne) depend on different factors, particularly catalytic system used for synthesis and conditions of film preparation. Permeability of gases and organic vapors through PTMSP films synthesized with different catalytic systems (Nb and Ta-based) in wide range of thickness (5–60 μm) was investigated. It was shown that permeability coefficients of all studied penetrants decrease with decreasing of film thickness. It is known that permeability properties of PTMSP films can change during storage. The influence of aging on separation parameters of PTMSP films with different thickness was studied. It was determined that Nb-based PTMSP thin films (5 μm) demonstrate the best selective properties and the highest stability.

1. INTRODUCTION

One of the base purposes of membrane gas separation is development of composite membrane with thin polymeric selective layers. Preparation of such membranes allows to obtain high productivity for desired products, to save mechanical properties of polymeric films because of using supports and to decrease a cost of membranes. Poly(1-trimethylsilylpropyne) (PTMSP), the glassy polymer having preferential permeability for lower hydrocarbons and vapor of organic substances, is the most perspective polymer for preparation of such composite membranes for practical application, for example, in petrochemical industries and for recovery of organic vapors from gaseous streams.

* Topchiev Institute of Petrochemical Synthesis RAS Leninskii pr., 29, Moscow, Russia.

** Centre National de la Recherche Scientifique Laboratoire des Sciences du Genie Chimique, UPR 6811 – Groupe ENSIC-Nancy, France.

As it is known, permeability parameters of PTMSP may depend on different factors such as catalytic system used for synthesis, solvents for polymer dilution, and conditions of film preparations [1], [2]. It was shown that separation properties of PTMSP are not stable during storage [3]–[5]. Some researchers have noted that permeability parameters of some polymers including PTMSP can depend on film thickness [6]. This work presents results of investigation of transport properties of Nb- and Ta-based PTMSP films with different thickness for gases and organic vapors. The influence of aging on different modifications of PTMSP was studied.

2. EXPERIMENTAL

PTMSP was obtained by polymerization of monomer 1-trimethylsilylpropyne in the presence of catalysts NbCl_5 and $\text{TaCl}_5/\text{TIBA}$ (triisobutylaluminium) [7]. It was determined that PTMSP obtained with NbCl_5 contains 60% of cis-units in contrast with PTMSP synthesized with $\text{TaCl}_5/\text{TIBA}$ (40% of cis-units) by NMR-spectroscopy. Homogeneous polymeric films for measurement of gas and vapor transport parameters were prepared by casting onto glass plate. Thickness of samples was $5\div 60\ \mu\text{m}$. The samples were removed from glass plates by distilled water after drying under ambient conditions and then they were dried under vacuum until constant weight. Measurements of permeability parameters of gases were carried out by differential methods with gas chromatograph analysis at ambient temperature and drop pressure 1 atm (Fig. 1). After

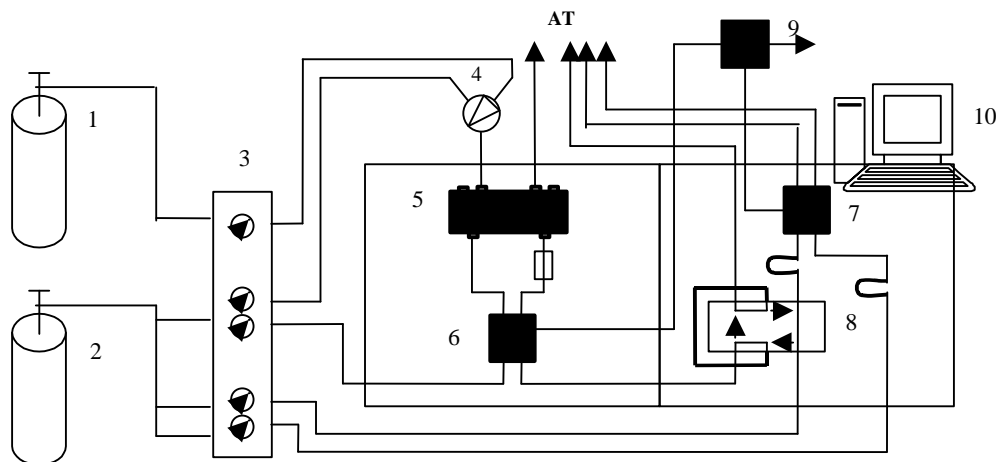


Fig. 1. Scheme of experimental gas chromatograph setup

- 1, 2 – penetrants, 3 – microadjust valves, 4 – valve for penetrant supply into the membrane sell,
 5 – membrane cell, 6, 7 – thermal conductivity detectors, 8 – gas chromatograph,
 9 – analog-digital converter, 10 – computer

preliminary measurements of permeability coefficients the films were annealed during 6 hours at 100 °C and then their transport parameters were tested again. Measurements of permeability coefficients of organic vapors were carried out by integral method using gravimetric setup (Fig. 2). The films for vapor permeation were aged during storage in air atmosphere under room conditions. Activity of vapors were 0.1, temperature of membrane cell was 40 °C and down pressure was $\sim 10^{-3}$ MPa. Permeability coefficients were measured for O₂, N₂, dichloromethane, hexane and heptane.

3. RESULTS AND DISCUSSION

Permeability parameters of light gases (O₂, N₂) through the Nb- and Ta- based PTMSP films with different thickness were studied before and after aging (Figs. 3–6). It was shown that permeability coefficients decrease with decreasing of film thickness as for Ta-based PTMSP as for Nb-based, both for just cast and aged films. For Ta-based PTMSP films permeability parameters decrease in about two orders of magnitude after aging for all investigated samples. But for thin aged Nb-based films (~ 5 μm) decreasing of permeability is not so significant both for oxygen and nitrogen as for other films.

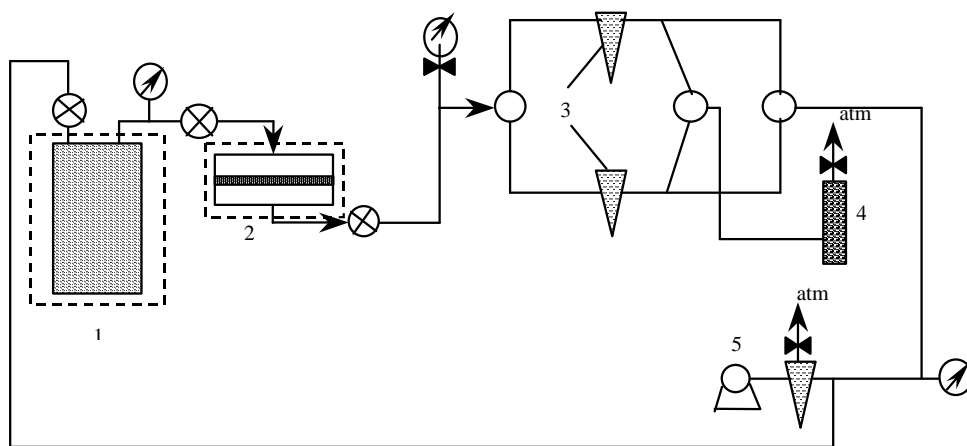


Fig. 2. Scheme of gravimetric experimental setup

1 – tank with vapors, 2 – membrane cell, 3 – traps, 4 – dehumidification block, 5 – vacuum pump

It has been shown in literature that permeability parameters can depend on film thickness for another classes of polymers such as polyvinyltrimethylsilane and polynorbornens [8]. Authors [8] have noted that thin films have a higher density in comparison with thick films. But for investigated polymers permeability coefficients depend on thickness weakly because diffusivity coefficient decrease compensates solubility coefficient increasing for thin films. Probably in the case of PTMSP thin films the decreasing

of diffusivity coefficients predominates over solubility coefficients increasing for light gases and thus permeability coefficients decrease with decreasing of film thickness.

It is known that Nb-modification of PTMSP has higher density than Ta-based (0.82 g/cm^3 for Nb-based and 0.79 g/cm^3 for Ta-based) [9]. This phenomenon can be connected with their differences in cis-trans relation in polymer structure. Such difference is one of the possible reasons that Nb-based PTMSP thin films have got the same level of permeability after aging in contrast with Ta-based, which permeability coefficients decrease drastically.

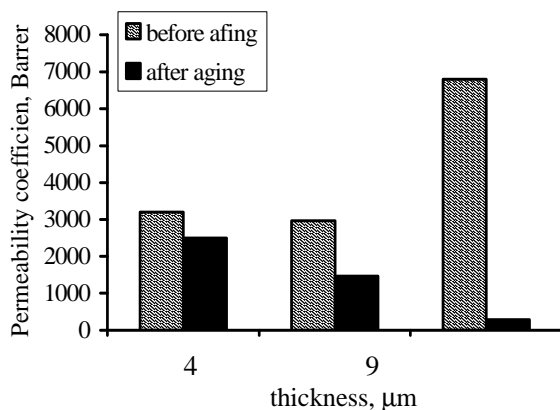


Fig. 3. Influence of aging on oxygen permeability of Nb-based PTMSP films with different thickness

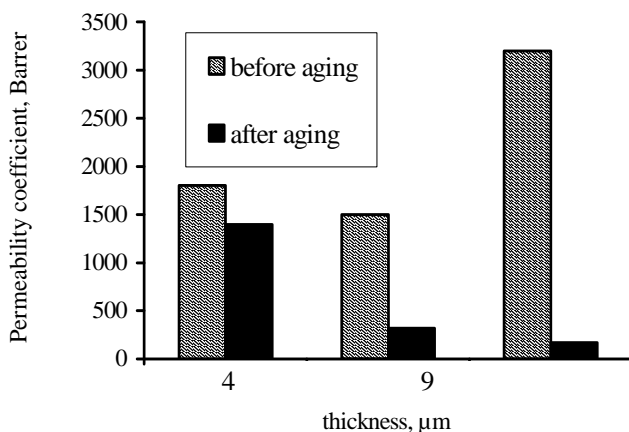


Fig. 4. Influence of aging on nitrogen permeability of Nb-based PTMSP films with different thickness

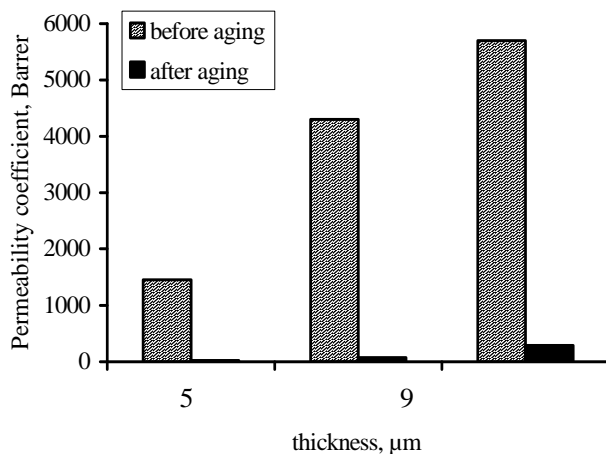


Fig. 5. Influence of aging on oxygen permeability of Ta-based PTMSP films with different thickness

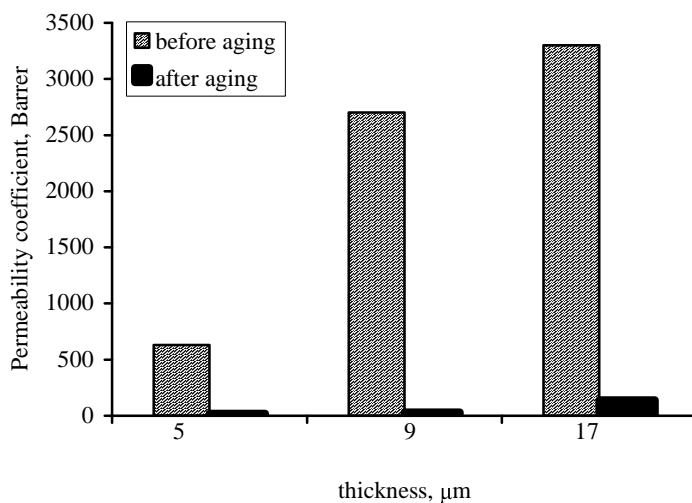


Fig. 6. Influence of aging on nitrogen permeability of Ta-based PTMSP films with different thickness

It was observed that thin films ($\sim 5 \mu\text{m}$) are more selective than thicker ones and Nb-based modification of PTMSP resulted in a higher selectivity in comparison with Ta-based. These facts are in a good agreement with literature data [3]. It was also found mentioned that further changes of selectivity of pair O_2/N_2 do not occur at film thickness $\geq 10 \mu\text{m}$ both for Nb- and Ta-based PTMSP (Table 1).

Table 1. Selectivity of PTMSP films with different thickness

Thickness, μm	Selectivity O_2/N_2			
	NbCl_5		$\text{TaCl}_5/\text{TIBA}$	
	before aging	after aging	before aging	after aging
5	2.3	2.8	1.8	1.8
9	1.6	2.0	2.0	1.5
14	1.7	2.1	2.0	1.6

Recently, dependence of permeability on film thickness has been noted also for hexane for PTMSP synthesized with $\text{TaCl}_5/\text{TIBA}$ [10]. In the present work it was shown that the tendency is the same for other organic vapors such as dichloromethane and heptane as for Nb-based as Ta-based (Fig. 7). It was found that permeability coefficients of thin films are lower than for thick films for all studied vapors. These results are in agreement with data obtained for light gases. Probably the reasons of such behavior relate with particularity of PTMSP structure like in the case of light gases μ .

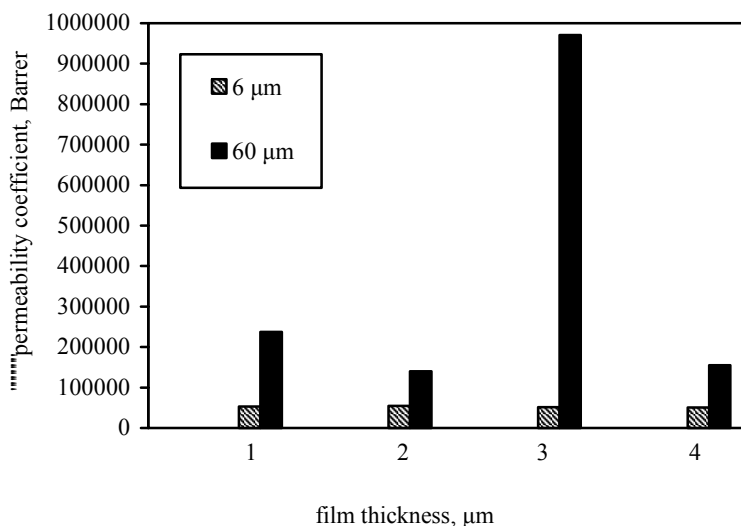


Fig.7. Influence of thickness on vapour permeability of PTMSP.
 1 – CH_2Cl_2 , Ta-based PTMSP; 2 – CH_2Cl_2 , Nb-based PTMSP,
 3 – hexane, Nb-based PTMSP, 4 – heptane, Nb-based PTMSP

4. CONCLUSIONS

In the present work permeability parameters of oxygen and nitrogen of just cast and aged films for Nb- and Ta-modifications of PTMSP (poly(1-trimethylsilyl-

propyne) with different thickness were studied. It was shown that permeability coefficients of light gases decrease with decreasing of film thickness for both of PTMSP modifications but Nb-based PTMSP much more stable.

It was noted that data obtained for permeability of organic vapors through PTMSP films with different thickness are in a good agreement with results for light gases. The results obtained for thin films are very important for development of preparation of composite membranes with thin selective layers based on PTMSP and using such membranes in industry separation processes.

ACKNOWLEDGEMENT

Authors are thankful to the INTAS Grant № 2000-0230 and Grant NATO SFP 973991 for support of this study.

REFERENCES

- [1] MASUDA T., ISOBE E., HIGASHIMURA T., *Polymerization of 1-(trimethylsilyl)-1-propyne by halides of niobium (V) and tantalum (V) and polymer properties*, *Macromolecules*, 18, 1985, pp. 841–845.
- [2] NAGAI K., MASUDA T., NAKAGAWA T., FREEMAN B.D., PINNAU I., *Poly[1-(trimethylsilyl)propyne] and related polymers: synthesis, properties and functions*, *Prog. Polym Sci.*, 26, 2000, pp. 721–798.
- [3] NAGAI K., NAKAGAWA T., *Effects of aging on the gas permeability and solubility in poly(1-trimethylsilyl-1-propyne) membranes synthesized with various catalysts*, *J. Memb. Sci.*, 105, 1995, pp. 261–272.
- [4] YAMPOLSKII Yu.P., SHISHATSKII S.M., SHANTOROVICH V.P., ANTIPOV E.M., KUZMIN N.N., RYKOV S.V., KHODJAEVA V.L., PLATE N.A., *Transport characteristics and other physicochemical properties of aged poly(1-trimethylsilyl-1-propyne)*, *J. Appl. Polym. Sci.*, 48, 1993, pp. 1935–1944.
- [5] DOGHIERI F., BIAVATI D., SARTI G.C., *Solubility and diffusivity of ethanol in PTMSP: effect of activity and polymer aging*, *Ind. Eng. Chem. Res.*, 35, 1996, pp. 2420–2430.
- [6] DORKENOO K.D., PFROMM P.H., *Accelerated physical aging of thin poly(1-trimethylsilylpropyne)*, *Macromolecules*, 33, 2000, pp. 3747–3751.
- [7] TEPLYAKOV V.V., ROIZARD D., FAVRE E., KHOTIMSKII V.S., *Investigations on the peculiar permeation properties of volatile organic compounds and permanent gases through PTMSP*, *J. Memb. Sci.*, 220, 2003, pp. 165–175.
- [8] SHISHATSKII A.M., YAMPOLSKII Yu.P., PEINEMANN K.-V., *Effect of film thickness on density and gas permeation parameters of glassy polymers*, *J. Memb., Sci.*, 112, 1996, pp. 275.
- [9] CHIRKOVA M.V., *Synthesis and investigation of properties of poly(1-trimethylsilyl-1-propyne) and poly(1-trimethylgermylpropyne) with different microstructure*, Ph.d. thesis, Topchiev Institute of Petrochemical Synthesis, 2004.
- [10] BORISEVICH O.B., SYRISOVA D.A., TEPLYAKOV V.V., KHOTIMSKII V.S., ROIZARD D., *Study of permeability process of organic substance vapors through poly(1-trimethylsilylpropyne)*, *Desalination*, 163, 2004, pp. 267–272.

*Keywords: volatile organic compounds (VOCs),
myristate cellulose membran,
sorption isotherms*

KAREL FRIESS*, JAROSLAVA MACHKOVÁ*,
MILAN SIPEK*, VLADIMIR HYNEK*,
YURII P. KUZNETSOV**

SORPTION OF VOCs AND WATER VAPORS IN MYRISTATE CELLULOSE MEMBRANE

The sorption of organic (benzene, toluene, cyclohexane, heptane, acetone, ethyl acetate, methanol and ethanol) and water vapors in myristate cellulose (MC) membrane in dependence of their activity is reported. Sorption experiments were carried out at 298 K by the use apparatus with Mc Bain spiral quartz balances and from experimental data the sorption isotherms were obtained. Sorption data of MC polymer revealed very low sorption for water and alcohols but essentially higher sorption for VOCs. All isotherms obtained are so-called Flory-Huggins type, only a water vapors isotherm has a linear (Henry type) character.

1. INTRODUCTION

The removal of VOCs from air or water is highly needed to protect environment and human health. However, the clean up of polluted environment is often difficult and expensive. In past decade the low-cost energy-saving techniques like the membrane separation processes constituted a hopefully alternative to the classical technologies of removing organic pollutants [1]–[4]. Just the shortcomings and limitations of VOCs removal methods compels to searching of new polymer materials with better parameters leading to the increasing of system performance. Many experimental studies of permeation, diffusion or sorption of gases and vapours in polymers enabled to design the polymer membranes with required parameters like high selectivity, long lifetime, mechanical

* Department of Physical Chemistry, Institute of Chemical Technology, Technická 5, 166 28 Prague 6, Czech Republic.

** Institute of Macromolecular Compounds, Russian Academy of Sciences, Bolshoy pr. 31, St. Petersburg 199004, Russia.

properties etc [3]–[6]. This work is focused on study of the effects of membrane composition on sorption (hydrophilic membrane matrix versus hydrophobic side chains) of benzene, toluene, heptane, cyclohexane, ethyl acetate, ethanol, methanol and water vapors in cellulose myristate membrane at temperature of 298 K.

2. THEORY

For description of transport of gases and vapors through non-porous polymer membranes the solution-diffusion model [7] is widely used. An association of permeation, diffusion and sorption together simplified the complex process of mass transport through polymer material, role of external driving forces (temperature, pressure and concentration gradients), nature of polymer material and penetrating component.

2.1. DETERMINATION OF DIFFUSION COEFFICIENT

For a polymer membrane of finite dimensions bounded by planes $z = L/2$ and $z = -L/2$ (where L is the membrane thickness) the solution of the 2nd Fick's law [8]

$$\frac{\partial c}{\partial t} = D \left(\frac{\partial^2 c}{\partial z^2} \right) \quad (1)$$

under the initial and boundary conditions $-L/2 < z < L/2$ $c = 0$ at $t = 0$ and $z = \pm L/2$ $c = c_1$ at $t > 0$ leads to infinite series given by equation (2),

$$\frac{Q_t}{Q_\infty} = 1 - \frac{8}{\pi^2} \sum_{m=0}^{m=\infty} \left[\frac{1}{(2m+1)^2} \exp \left(-D \frac{(2m+1)^2 \pi^2 t}{L^2} \right) \right] \quad (2)$$

where Q_t is the mass uptake at time t and Q_∞ is the mass uptake at infinite time.

For time interval, when the ratio Q_t/Q_∞ is still lower than 0.5, equation (2) could be replaced by equation (3):

$$\frac{Q_t}{Q_\infty} = 4 \sqrt{\frac{Dt}{\pi L^2}} \quad (3)$$

If the ratio D/L^2 in exponential terms of equation (2) is great enough then, even for relatively short time (for $m = 0$), we obtain equation (4):

$$\frac{Q_t}{Q_\infty} = 1 - \frac{8}{\pi^2} \exp \left(-\frac{\pi^2 Dt}{L^2} \right) \quad (4)$$

Equation (4) can be rearranged to the form:

$$\ln \left(1 - \frac{Q_t}{Q_\infty} \right) = -\frac{\pi^2 D}{L^2} t + \ln \left(\frac{8}{\pi^2} \right) \quad (5)$$

The appropriate value of diffusion coefficient D can be calculated from the linear part of the curve which is obtained by plotting of logarithm $(1 - Q_t/Q_\infty)$ versus time t .

2.2. FLORY–HUGGINS THEORY

The Flory–Huggins, Flory–Rehner and Free Volume theories [1], [9] are frequently used for description of swelling of polymer material caused by organic vapors penetration (Fig. 1). From Flory–Huggins theory a relation describing the dependence of equilibrium vapors pressure on polymer-penetrant composition can be presented in following form:

$$\ln a_1 = \ln \left(\frac{p_1}{p_1^0} \right) = \ln(1 - \varphi_2) + \varphi_2 + \chi \varphi_2^2 \quad (6)$$

where a_1 is activity of vapours, p_1 is equilibrium pressure of penetrant vapours around polymer membrane, p_1^0 is pressure of saturated vapours at given temperature, χ is Flory–Huggins interaction parameter, φ_2 is volume fraction of polymer.

Higher sorption for appropriate compound indicates higher range of polymer-solvent interactions and it means lower χ values [1], [10], [11]. When Flory–Huggins parameter is large ($\chi > 2$) the interactions between polymer and solvent are small and the sorption of penetrant in polymer systems could not reach high values. Strong polymer-solvent interactions exist for small values ($0.5 < \chi < 2$) and for $\chi < 0.5$ the polymer must be cross-linked to prevent the dissolution of polymer material.

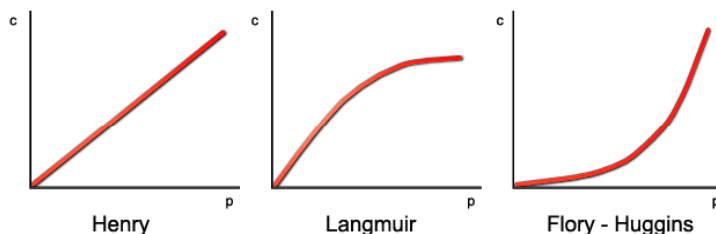


Fig. 1. Schematic drawing of sorption isotherms types

2.3. SOLUBILITY (SORPTION)

Solubility is a thermodynamic parameter and gives a measure of the amount of a penetrant sorbed by a polymer under equilibrium conditions [1]. Actually it is the equilibrium partition coefficient between a compound's concentration in a membrane and its concentration in liquid or gaseous phase in contact with the membrane. Different ways of expressions for solubility can be found in literature, depending on units used for membrane and gas phase concentrations [12].

3. EXPERIMENTAL

3.1. CHEMICALS AND MEMBRANE

All used chemicals (analytical grade – purchased from Penta, Czech Republic) and Milli-*Q* water (resistivity 18 MΩcm) were used without further purification. Cellulose myristate (MC) membrane was prepared by co-workers from Institute of Macromolecular Compounds, Russian Academy of Science. MC membrane (Fig. 2) is a result of reaction between cellulose and myristate acid which leads to substitution of OH groups in cellulose molecule by OC(O)-(CH₂)₁₂-CH₃ groups. Details about synthesis and transport properties (pervaporation) of MC membranes were published in Journal of Applied Chemistry (reference in Russian variant of J. of Appl. Chem., Vol. 18, No. 11, 1970, pp.2581–2583 and Vol. 76, No. 5, 2003, pp. 820–828).

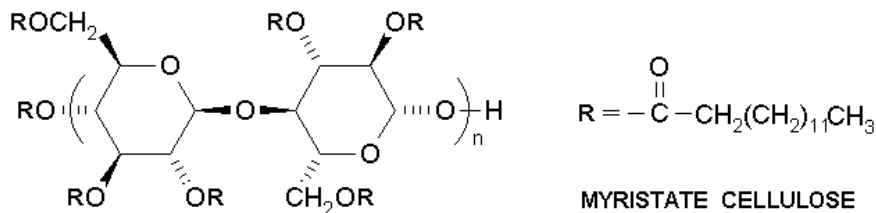


Fig. 2. Schematic structure of myristate cellulose

3.2. SORPTION APPARATUS

The sorption experiments have been performed gravimetrically. The sorption apparatus (Fig. 3), located in thermostated box, contains a calibrated quartz spiral (sensitivity ca. 9.477 mg/mm), so-called McBain's spiral balance. The stripe of sample polymer membrane (membrane weight 0.5–2 g) is hanged on ground glass joint of the tube evacuated by vacuum pumps. Stretching of quartz spiral was monitored by the camera at selected time intervals (0.1–100 s) from the beginning of measurement till the equilibrium state. The liquid sample (5–10 cm³) was dosed to a glass vessel. Dissolved gases from liquid sample were removed by consequent heating/cooling procedure. Selected vapour tension (i.e. activity) of each experiment was set by calibrated feed valve and determined by pressure gauge. The vapour reservoir served for pressure equalization. Before each experiment the apparatus was evacuated to pressure ca 0.001 Pa by rotary and turbo molecular pumps. The maximum error of mass determination reaches approximately 25–30 μg.

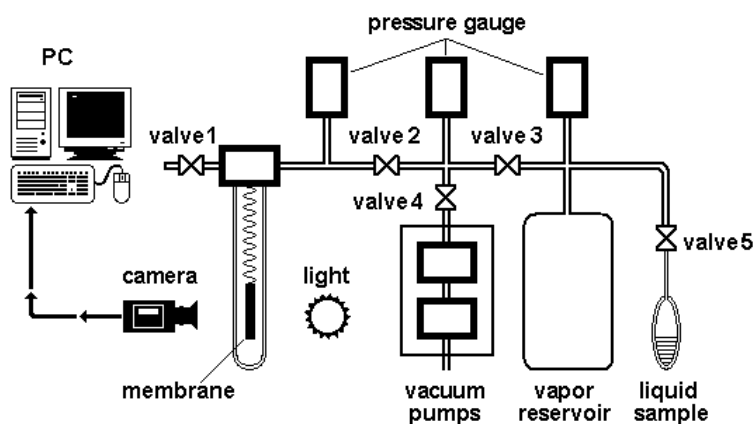


Fig. 3. Sorption apparatus

4. RESULTS

Determined sorption isotherms of all studied vapors increased with increasing relative pressure (activity) of the solvents (Fig. 4a and 4b). The shape of all isotherms, except water vapors which shows a linear dependence of sorbed amount on vapour pressure, can be successfully described by Flory-Huggins theory. Values of Flory-Huggins interaction parameter χ (Table 1) were obtained by fitting of experimental data by equation (6).

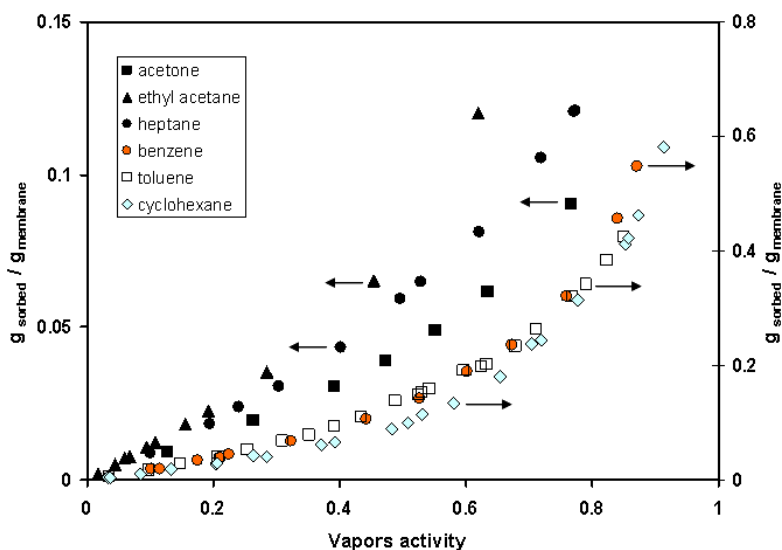


Fig. 4a. Sorption isotherms of benzene, toluene, cyclohexane, heptane, ethyl acetate and acetone vapors

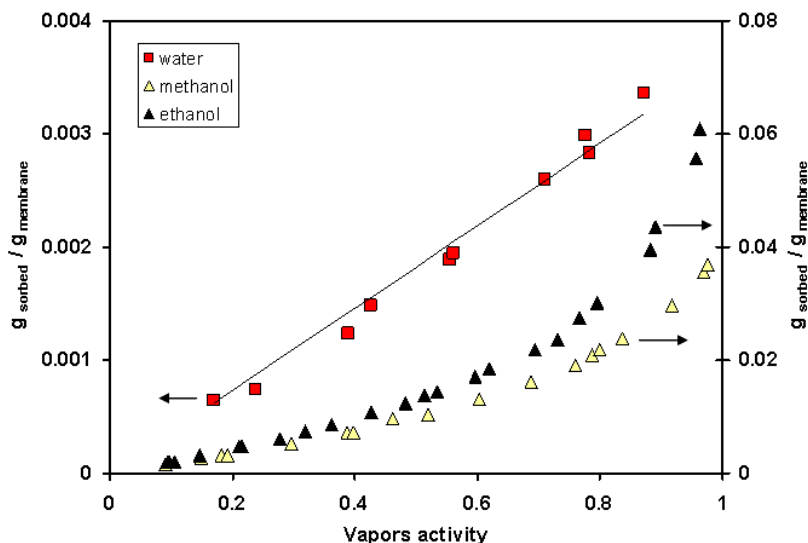


Fig. 4b. Sorption isotherms of methanol, ethanol and water vapors

It is obvious that the sorption of VOCs in MC membrane is essentially higher than the sorption of methanol and ethanol (low) and water (very low). Hence, the hydrophobic long side chains play a dominant role in our sorption experiments in comparison with competitive sorption of vapors in hydrophilic cellulose matrix. Otherwise the sorption of benzene > methanol > water in pure cellulose has an inverse order [13]. Likewise the interaction parameters χ in pure cellulose ($\chi_{\text{methanol}} = 1.18$, $\chi_{\text{benzene}} = 1.64$ and $\chi_{\text{toluene}} = 1.72$) [14] indicate another type of interactions between polymer and penetrant molecules or their sorption on specific sites.

Table 1. Values of vapors pressure and interaction parameters at 25 °C

	vapor pressure at 25 °C, kPa	Flory-Huggins parameter χ
benzene	12.68	0.40
toluene	3.80	0.33
cyclohexane	13.01	0.54
heptane	6.10	0.83
acetone	30.80	1.20
ethyl acetate	12.60	0.79
methanol	16.96	2.40
ethanol	7.87	2.18
water	3.17	≈ 4.35

Liquid phase sorption experiment revealed a stability of MC membrane in all studied compounds and results were corresponding with χ values and with their meaning. In accordance with that the total dissolution of MC membrane in liquid benzene and toluene (both have $\chi < 0.5$) took place. Sorption of other compounds were in order cyclohexane > ethyl acetate \geq heptane > ethanol > methanol > water.

The diffusion coefficients of vapors were determined on the basis of experimental data by equation (5). Fig. 5 shows the dependences of diffusion coefficient of selected vapors on their activity. It can be seen that the diffusion coefficients of all substances decrease with vapors activity. A decreasing of D with increasing concentration of the penetrating vapor molecules is usually attributed to sorption-induced changes in polymer structure, in particular to crystallization or a transition to another crystal modification. Structural changes may also take place in amorphous polymers when a presence of penetrant molecules caused a plasticizing of polymer structure and a rise of chains mobility. An increase of penetrant concentration leads to swelling of polymer and plasticization takes place. Lowering of D with increasing of water concentration has been recently attributed to molecule association via hydrogen bonding (clustering) [15]. Naturally, these effects will be most pronounced in sorption of water or alcohols by hydrophobic part in MC membrane. In hydrophilic part of polymer a clustering is either absent or sets is only in the region of high vapor activity. Since clusters may consist in many molecules, their mobility will be much smaller than that of free molecules, not bound to the functional groups on the polymer chain [16]. Barrer and Barrie found for system ethylcellulose+water that the decrease of D with increasing concentration was accounted for by the thermodynamics correction term $\gamma = \partial \ln a / \partial \ln C$ in 1st Fick's law [17].

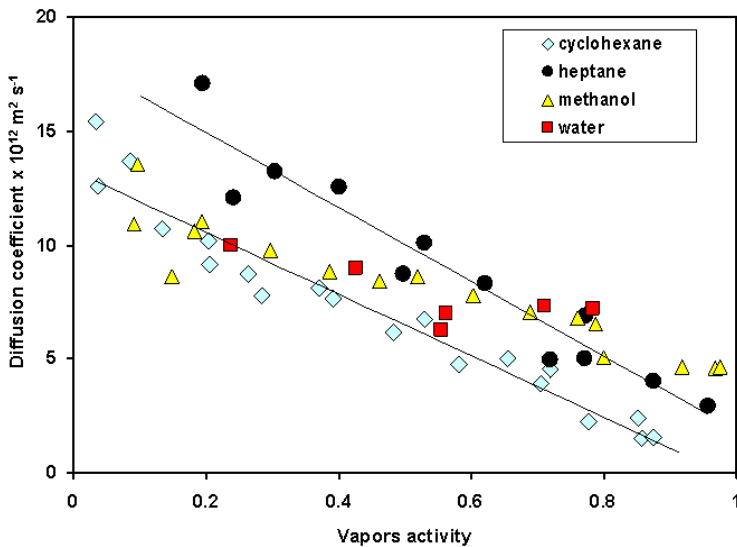


Fig. 5. Dependence of diffusion coefficient of selected vapours on activity

5. CONCLUSIONS

Based on the performed experiments the following conclusions can be drawn:

1. Myristate part in system determines a comprehensive sorption properties of MC membrane.

2. Sorption of VOCs in MC membrane can be described by Flory-Huggins theory and the strong non-polar interactions between MC and aromatic compounds lead to dissolution of MC in liquid benzene and toluene.

3. Sorption of water vapors in MC membrane is very low and almost has a linear (Henry's law) character.

4. Diffusion coefficients of all studied compounds decrease with increasing of penetrant activity.

ACKNOWLEDGEMENTS

This work was supported by the grant of MSM No. 6046137307 of Czech Ministry of Education, Youth and Sports.

REFERENCES

- [1] MULDER M.V.H., *Basic Principles of Membrane Technology*, Kluwer Academic Publisher, Dordrecht, 1998.
- [2] CRANK J., PARK G.S., *Diffusion in Polymers*, Academia Press, London, 1968.
- [3] HOFFMAN E.J., *Membrane Separations Technology*, Elsevier Science, USA, 2003.
- [4] OSADA Y., NAKAGAWA T., *Membrane Science and Technology*, Marcel Dekker Inc., New York, 1992.
- [5] KESTING R.E., FRITZSCHE A.K., *Polymeric Gas separation Membranes*, John Wiley & sons, New York, 1993.
- [6] BAKER R.W., WIJMANS J.G., KASCHEMEKAT J.H., *The design of membrane vapor-gas separation systems*, Journal of Membrane Science, 151, 1998, pp. 55–62.
- [7] WIJMANS J.G., BAKER R.W., *The solution-diffusion model: a review*, Journal of Membrane Science, 107, 1995, pp. 1–21.
- [8] CRANK J., *The Mathematics of Diffusion*, 2nd.edition. Clarendon Press, Oxford, 1975.
- [9] FLORY P.J., *Principles of Polymer Chemistry*, Cornell University Press, Ithaca, 1953.
- [10] VIETH.W.R., *Diffusion In and Through Polymers*, Hanser Publishers, New York, 1991.
- [11] BARTON A.F.M., *Polymer-Liquid Interaction Parameters and Solubility Parameters*, CRC Press, Boca Raton, 1990.
- [12] De BO I., Van LANGENHOVE H., De KEIJSER J., *Application of vapor phase calibration method for determination of sorption of gases and VOC in polydimethylsiloxane membranes*, Journal of Membrane Science, 209, 2002, pp. 39–52.
- [13] CHIRKOVA J., ANDERSONS B., ANDERSONE I., *Determination of standard isotherms of the sorption of some vapors with cellulose*, Journal of Colloid and Interface Science, 276, 2004, pp. 284–289.
- [14] MANDAL S., PANGARKAR V.G., *Separation of methanol-benzene and methanol-toluene mixtures by pervaporation: effects of thermodynamics and structural phenomenon*, Journal of Membrane Science, 201, 2002, pp. 175–190.

- [15] ZIMM B.H., LUNDBERG J.L., *Sorption of Vapors by High Polymers*, Journal of Physical Chemistry, 60, 1956, pp. 425–428.
- [16] TSILIPOTKINA M.V., TAGER A.A., KOLMAKOVA L.K., PEREVALOVA I.A., *Sorption and diffusion of water in cellulose and cellulose nitrate*, Polymer Science U.S.S.R., 31, 9, 1989, pp. 2201–2206.
- [17] BARRER R.M., BARRIE J.A., SLATER J., *Sorption and diffusion in ethyl cellulose*, Journal of Polymer Science, 27, 1958, pp. 117–197.

*Keywords: pervaporation, modelling,
membrane techniques*

AGNIESZKA STACHECKA*, WŁADYSŁAW KAMINSKI*

EMPIRICAL APPROACH TO DEWATERING OF ISOPROPANOL-WATER SYSTEM BY PERVAPORATION

The aim of the research was the evaluation of pervaporation process used for isopropanol-water mixture separation on a PERVAP 2210 hydrophilic membrane. Experiments were carried out in a Sulzer apparatus, at membrane surface area $A = 0.0177 \text{ m}^2$, temperatures 65 °C, 70 °C and 75 °C, for alcohol concentrations in the feed: 90, 92.5 and 95% and for three flow rates: 20, 40 and 60 dm^3/h . The process was conducted in steady conditions at constant pressure on the low-pressure side of the membrane (300–400 Pa). The experiments were made according to a three-level factorial design. Results of research based on the experiments were used to describe empirical model. This model was described using an Excel calculation sheet. To confirm the extrapolation ability, additional investigations were made for temperature 80 °C, concentration 80% and three flow rates. Data determined by mathematical models and experimental ones are compared.

1. INTRODUCTION

Quick development of research on industrial applicability of pervaporation process was observed at the beginning of the 80s of the 20th century, when the German company Deutsche Carbone AG GFT (now Sulzer Chemtech Membrantechnik) developed composite hydrophilic membranes with an active layer of polyvinyl alcohol. The membranes (commercial name PERVAP-1000) were applied in first industrial systems for ethanol dehydration [1]. At the end of the 20th century, successful attempts of using ceramic membranes in industrial installations also started [2]. At present, in the world there are about 100 industrial installations for pervaporation. They have different tasks and capacities ranging from 100 to 30000 dm^3/day . Pervaporation can be applied as a cheap and efficient method for dehydration of different solvents (Table 1) [3]–[6].

* Technical University of Łódź Faculty of Process and Environmental Engineering, ul. Wólczańska 215, 90-924 Łódź, Poland.

Table 1. Selected solvents dehydrated by pervaporation on industrial scale [3]–[6]

Solvent	Water content	
	in feed (% mass)	in permeate (ppm)
ethanol	4.50–12.0	100–10000
methanol	7.10	1650
<i>n</i> -butanol	5.40	800
<i>t</i> -butanol	10.40	580
THF	0.40	220
methyl ethyl ether	3.80	220
trichloroethane	0.01	8

The most important applications of pervaporation process include [2], [7]–[9]:

1. Dehydration of liquid water-organic mixtures:

- separation of azeotropic mixtures: water/EtOH, water/*i*-propanol, water/pyridine,
- dehydration of organic solvents, e.g. alcohols, esters, ketones, ethers, carboxylic acids, halogen derivative hydrocarbons.

2. Removal of liquid organic compounds from water, including:

- removal of hydrocarbons and their halogen derivatives from ground and surface water,
- dealcoholisation of wine and beer,
- concentration of odorous substances, e.g. aromas for food industry,
- removal of organic products during continuous fermentation.

3. Separation of mixtures of two or more liquid organic compounds, including:

- separation of isomers (e.g. *o*-, *m*-, *p*-xylenes),
- separation of azeotropes (e.g. methanol-methyl *t*-butyl ether (MTBE), methanol-dimethylcarbonate (DMC), ethanol-cyclohexane).

In pervaporation a serious problem to solve is selection of an appropriate membrane for a separated system and process parameters e.g. feed composition and temperature, and its flow velocity. To take advantage of the experience gained in a laboratory scale in designing industrial installations, it is necessary to describe the process mathematically which will allow us to predict mass flux and effect of separation.

Modelling of mass transport is based on three main approaches: physical, semi-empirical and empirical.

In empirical and semi-empirical methods experimental results can be utilised directly.

2. SUBJECT AND SCOPE OF RESEARCH

In experiments, a binary mixture was represented by isopropanol-water system because pervaporation has practical significance for it. Isopropanol is used to extract

vegetable oils, where it replaces the traditional solvents like hexane or petroleum benzine. Hexane is inconvenient to use because of its toxicity and explosiveness – the features which we do not observe in the case of isopropanol. The purity of isopropanol required for extraction exceeds 90% which is obtained as a result of pervaporation.

Basic data for isopropanol are given in Table 2 [10].

Table 2. Basic data for isopropanol [10]

Molar mass	60.096 g/mol
Melting temperature	185.28 K
Boiling temperature	355.41 K
Critical temperature	509.31 K
Critical pressure	4.764 MPa
Critical volume	220.1 cm ³ /mol
Critical density	0.2730 g/cm ³
Compressibility coefficient	0.248
Acentric factor	0.669

Experiments were made according to a three-level factor design. The variable process parameters were:

- feed flow rate, $u = 20, 40$ and $60 \text{ dm}^3/\text{h}$;
- feed temperature, $T = 65, 70$ and $75 \text{ }^\circ\text{C}$;
- feed composition (mass fraction of alcohol), $c = 90, 92.5$ and 95% .

Additionally, experiments were made for an isopropanol-water mixture at the temperature $T = 80 \text{ }^\circ\text{C}$ and feed composition $c = 80\%$ wt. alcohol in the feed.

3. EXPERIMENTAL SET-UP AND METHODS

3.1. EXPERIMENTAL SET-UP

The process of pervaporation was investigated using a Sulzer Chemtech system (Fig. 1) equipped with:

- temperature control system,
- feed circulation system,
- receiver.



Fig. 1. Sulzer Chemtech pervaporation system

Experiments were made on a PERVAP-2210 commercial hydrophilic membrane supplied by Sulzer Chemtech. The membrane was designed to dehydrate organic solvents that contain up to 20% water in the initial solution (feed) at the most. The active membrane surface was $A = 0.0177 \text{ m}^2$.

3.2. MEASUREMENTS AND ANALYSIS

The most popular and precise method used for the determination of pervaporated samples is the chromatographic method. It does not require big quantities of liquid for analysis which is very important in the case of permeate samples after pervaporation because the permeate is obtained in small amounts.

As it was mentioned earlier, the permeate samples were analysed in a Trace GC gas chromatograph (Thermo Finnigan), using the internal standard method.

4. EMPIRICAL MODEL

Experiments were carried out according to the three-level factorial design. Experimental results were used to determine empirical model coefficients for pervaporation. To estimate the effect of particular process variables they were normalised in the description according to the equation:

$$z_i = \frac{(x_i - x_{0i})}{\Delta x_i} \quad i = 1, 2, 3 \quad (1)$$

z_i – normalised process variable,

x_i – variable,

x_{0i} – central point of design,

$$\begin{aligned} \Delta x_i &- \text{variable increment, for } u \rightarrow \Delta u = 20 \text{ [dm}^3/\text{h]} \\ &T \rightarrow \Delta T = 5 \text{ [}^\circ\text{C]} \\ &c \rightarrow \Delta c = 2.5 \text{ [\%]}. \end{aligned}$$

Basing on the three-level factorial design, dependence of process variables on permeate flux can be described. Equation (2) is given in the form of the normalised variable system:

$$\begin{aligned} y_i = &c_0 + c_1 z_1 + c_2 z_2 + c_3 z_3 + c_{12} z_1 z_2 + c_{13} z_1 z_3 + c_{23} z_2 z_3 + c_{123} z_1 z_2 z_3 \\ &+ c_{11}(z_1^2 - z_{1 \text{ sr.}}^2) + c_{22}(z_2^2 - z_{2 \text{ sr.}}^2) + c_{33}(z_3^2 - z_{3 \text{ sr.}}^2). \end{aligned} \quad (2)$$

General formula of equation (2) can be presented in the following form:

$$y = \sum_{k=1}^M c_k \cdot \phi_k(z) \quad (3)$$

Taking into account that the factorial experiment is orthogonal, coefficients c_k can be obtained using equation (4):

$$c_k = \frac{\sum_{i=1}^p y_i \cdot \phi_k(z_i)}{\sum_{i=1}^p \phi_k^2(z_i)} \quad (4)$$

- c_k – coefficient in equation (2),
- z_i – normalised process variable,
- ϕ_k – function in equation (3) and (4),
- y_i – experimental data,
- p – number of experiments.

Coefficients of the equation were determined for two variants:

- variant I: when, y_i – permeate flux,
- variant II: when, y_i – enrichment factor β .

To describe the process of pervaporation, the permeate flux should be identified and permeate composition should be known. The proposed empirical model enables determination of the permeate flux (variant I) and calculation of water content in the permeate (variant II).

4.1. RESULTS AND DISCUSSION – VARIANT I

Using relation (4), 11 coefficients in equation (2) were calculated. They were used to calculate the permeate flux. Finally equation (2) has the form:

$$\begin{aligned}
y_i = & 0.308137 + 0.035644z_1 + 0.061167z_2 - 0.160883z_3 + 0.007825z_1z_2 - \\
& + 0.016317z_1z_3 - 0.048658z_2z_3 - 0.007288z_1z_2z_3 + 0.007089(z_1^2 - 2/3) - \\
& + 0.040378(z_2^2 - 2/3) - 0.018761(z_3^2 - 2/3)
\end{aligned} \quad (5)$$

It follows from the equation that the permeate stream is most affected by the feed composition. This is related to the value of coefficient “ c_3 ” ($c_3 = -0.160883$) that is responsible for the feed composition.

Fig. 2 shows a comparison of the permeate stream obtained experimentally with data calculated from the empirical model.

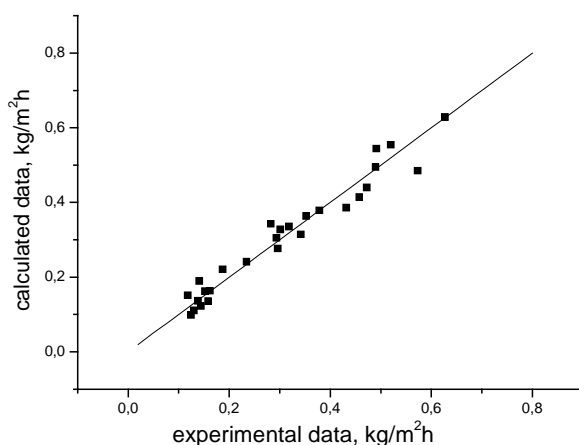


Fig. 2. Comparison of experimental and calculated data

When calculations and experiments are in ideal agreement, the points should be located on the diagonal. In the analysed case there is good agreement between experimental values and data obtained from the empirical model.

Using the empirical model, the permeate flux was determined depending on the temperature, flow rate and concentration of isopropanol in the feed, with one of the process variables being changed and two others taken at a constant level. In subsequent diagrams, the experimental and calculated data are compared.

In model calculations, beside equation (5) called further on the “full equation”, the same equation was used, however taken without square terms (equation 6).

$$\begin{aligned}
y_i = & 0.308137 + 0.035644z_1 + 0.061167z_2 - 0.160883z_3 + 0.007825z_1z_2 - \\
& + 0.016317z_1z_3 - 0.048658z_2z_3 - 0.007288z_1z_2z_3
\end{aligned} \quad (6)$$

Fig. 3 shows dependence of permeate stream on different temperatures and three isopropanol concentrations in feed using equation (6).

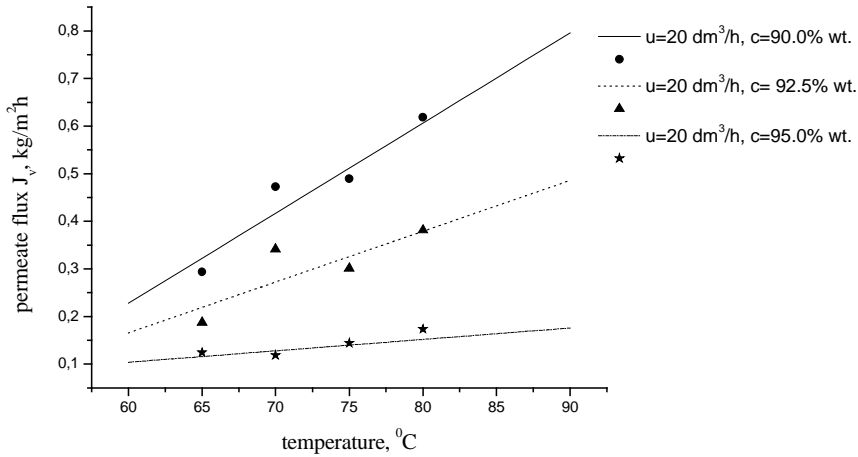


Fig. 3. Dependence of permeate stream on temperature for different isopropanol concentrations in the feed, for flow rate $u = 20 \text{ dm}^3/\text{h}$ (lines – empirical model, points – experimental data)

The empirical model provides good extrapolation of experimental data. Beside data from the factorial design, the diagrams contain additional points (at the temperature $T = 80 \text{ }^\circ\text{C}$). With an increase of isopropanol concentration in the feed, the permeate stream decreases which conforms to theoretical data.

It was shown that the permeate flux increased with a temperature rise. The lowest temperature impact is reported at high isopropanol content in the feed (95% wt. isopropanol concentration), the permeate flux ranges from 0.11 to 0.14 $\text{kg}/\text{m}^2\text{h}$.

Next, the effect of isopropanol concentration in the feed on the permeate flux, at different temperatures was investigated. Fig. 4 shows experimental and calculated data at three temperatures.

The model gives good description of the experimental data. A drop of the curve with an increase of concentration in the feed, follows immediately from the value of constant c_3 , which is responsible for alcohol concentration in the feed ($c_3 = -0.160883$) in the equation. Additionally, in the diagrams points were marked at $c = 80\% \text{ wt.}$, to confirm extrapolation data.

The smallest effect on the permeate flux is observed for high isopropanol concentrations in the feed. At 95% wt. concentration the flux for three considered temperatures is on the same level. This may be caused by transition of the isopropanol-water mixture through the azeotropic point.

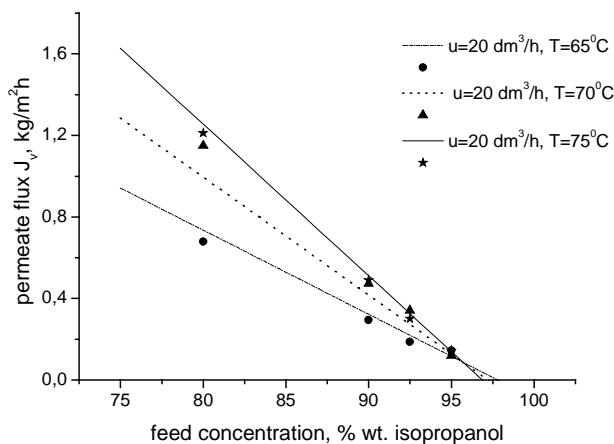


Fig. 4. Comparison of the dependence of permeate streams on isopropanol concentration in the feed, at constant flow rate $u = 20 \text{ dm}^3/\text{h}$ and three temperatures (lines – empirical model, points – experimental data)

The effect of flow rate on the permeate flux was also examined for constant isopropanol concentration in the feed and three temperatures (Fig. 5).

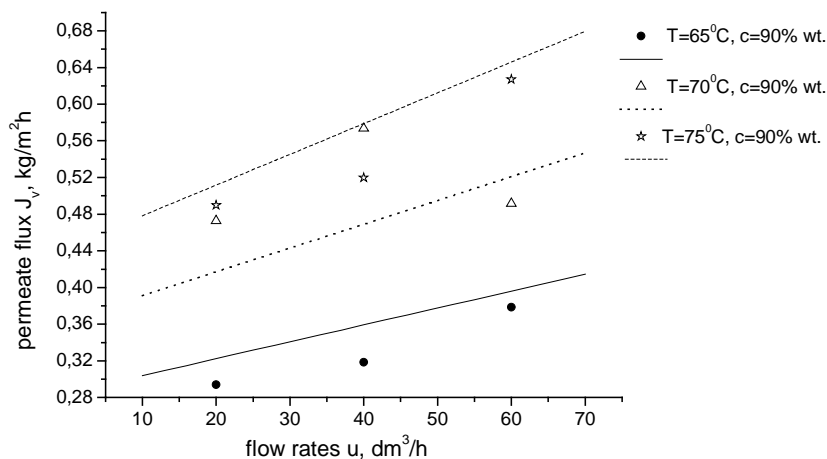


Fig. 5. Dependence of permeate flux on the flow rate at $c = 90\%$ wt. of isopropanol in the feed and three temperatures (lines – empirical model, points – experimental data)

It follows from the analysis of variant I, that the empirical model well describes the experimental data.

4.2. RESULTS AND DISCUSSION – VARIANT II

The empirical approach enables also estimation of an enrichment factor β . Constants of the equation (2) were determined according to equation (4) for enrichment factor β . They took the form:

$$y_i = 14.20113 + 6.259 \cdot 10^{-3} z_1 - 3.57 \cdot 10^{-3} z_2 + 4.850244 z_3 - 2.606 \cdot 10^{-2} z_1 z_2 + 2.35 \cdot 10^{-2} z_1 z_3 - 2.942 \cdot 10^{-2} z_2 z_3 - 4.875 \cdot 10^{-2} z_1 z_2 z_3 - 4.16 \cdot 10^{-3} (z_1^2 - 2/3) - 6.6 \cdot 10^{-4} (z_2^2 - 2/3) + 1.642356 (z_3^2 - 2/3) \quad (7)$$

Fig. 6 shows a comparison of enrichment factor β calculated and obtained experimentally.

Experimental points are located diagonally. It was observed that the data were not distributed evenly on the diagonal but accumulated in three clusters. Grouping depended on isopropanol concentration in the feed and flow rate.

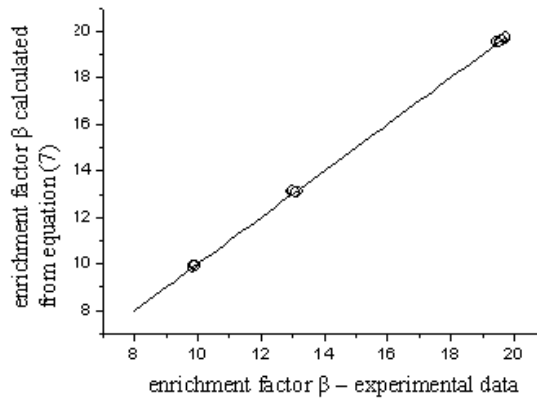


Fig. 6. Comparison of data obtained experimentally and calculated from equation (7)

Experimental and model points lie on the diagonal which shows good fitting, so further calculations were based on equation (7).

Basing on the empirical model, the effect of process parameters (temperature, flow rate and feed composition) on the enrichment factor β was investigated.

Subsequent diagrams illustrate the dependence of enrichment factor on water content in the feed at three temperatures and one flow rate (Fig. 7) and temperature $T = 65^\circ\text{C}$, and three flow rates (Fig. 8).

The diagram presenting three different flow rates and one temperature value confirms that with an increase of the flow rate, enrichment factor β decreases.

The empirical model well describes experimental data and can be used in the determination of the enrichment factor.

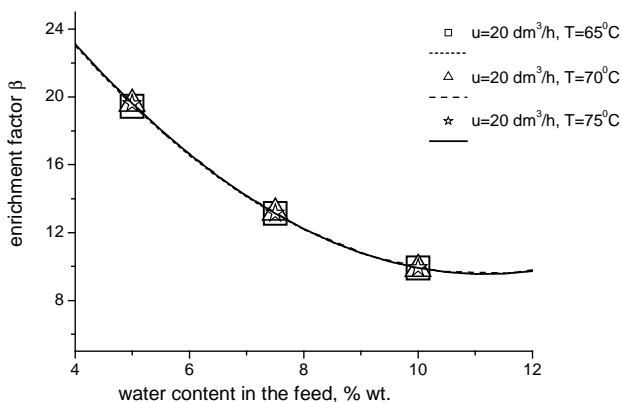


Fig. 7. Dependence of enrichment factor β on water content in the feed (lines – model data, points – experimental data)

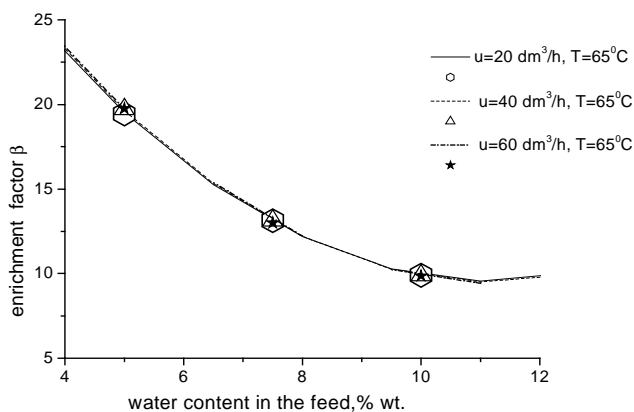


Fig. 8. Dependence of enrichment factor β on water content in the feed (lines – model data, points – experimental data)

5. CONCLUSIONS

The presented method of mathematical modelling of isopropanol-water system dehydration by pervaporation enables determination of streams and compositions of particular mixture components without the need to solve complex systems of equations. A comparison of calculated and experimental permeate streams shows good agreement of these values which makes possible to apply model calculations in designing the process of pervaporation.

REFERENCES

- [1] KUJAWSKI W., *Application of pervaporation and vapour permeation in environmental protection*, Polish Journal of Environmental Studies, 1, 2000, pp. 13–26.
- [2] KONDO M., KOMORI M., OKAMOTO K., *Tubular – type pervaporation module with zeolite NaA membrane*, Journal of Membrane Science, 133, 1997, pp. 133–141.
- [3] RAPIN J.L., *The Betheniville Pervaporation Unit – the first large – scale production plant for the dehydration of ethanol*, R. Bakish (Ed.), Proc. 3rd Int. Conf. on Pervaporation Processes in Chemical Industry, Bakish Materials Corp., Englewood, 1989, pp. 364–378.
- [4] SANDER U., JANSSEN H., *Industrial application of vapour permeation*, Journal of Membrane Science, 61, 1991, pp. 113–129.
- [5] BRUSCHKE H.E.A., *Industrial application of membrane separation processes*, Pure Appl. Chem., 67, 1995, pp. 993–1002.
- [6] SANDER U., SOUKUP P.B., *Practical experience with pervaporation systems for liquid and vapour separation*, Journal of membrane Science, 62, 199, pp. 67 – 89.
- [7] CHOPADE S.P., MAHAJANI S.M., *Pervaporation: membrane separations*, Encyclopedia of Separation Science, Academic Press, 8, 2000.
- [8] NÉEL J., *Introduction to pervaporation*, R.Y.M. Huang (Ed.), Pervaporation Separation Processes, Elsevier, Amsterdam, 1991, pp. 1–109.
- [9] KUJAWSKI W., *Pervaporation and vapour permeation – separation through nonporous membranes*, Polish Journal of Chemical Technology, 5, 2003, pp. 1–7.
- [10] YAWS M., *Yaws' Handbook of Thermodynamic and Physical Properties of Chemical Compounds*, ISBN: 0-07-073401-1 Electronic ISBN: 1-59124-028-X, Mc Graw-Hill, 2003.

*Keywords: bioethanol, distillery stillage,
membrane filtration, bioreactor*

KATERINA LAPIŠOVÁ*

EXPLOITATION OF CERAMIC MEMBRANE BIOREACTOR FOR THERMOPHILIC BACTERIA CULTIVATION

Food processing industries, such as distillery industry, produce a large amount of wastes. Distillery stillage is the most problematic waste from distillery. It contains a lot of organic compounds expressed as chemical oxygen demand (COD, up to 50 g O₂/dm³). This organic matter must be eliminated to protect the environment. Membrane bioreactor (MBR) is an effective wastewater treatment process in which the membrane separation technology is integrated with the activated sludge system. The suspended solids are completely separated from the treated water by the ceramic membrane unit, and all bio-mass is kept in the bioreactor. Because of such advantages as: good chemical stability, favourable mechanical strength, good antimicrobials ability, and high separation efficiency, the ceramic membrane is suitable for comprising ceramic membrane bioreactor (CMBR) with activated sludge.

1. INTRODUCTION

Membrane bioreactor (MBR) is an effective wastewater treatment process in which the membrane separation technology is integrated with the activated sludge system. The suspended solids are completely separated from the treated water by the ceramic membrane unit, and all bio-mass is kept in the bioreactor.

Because of such advantages as: good chemical stability, favorable mechanical strength, good antimicrobial ability, and high separation efficiency, the ceramic membrane play an ever increasing role in many applications. The ceramic membranes are suitable for comprising ceramic membrane bioreactor (CMBR) with activated sludge [1].

Ceramic membrane bioreactor has the advantage of compactness and high quality effluent without bacteria [2], [3]. In comparison with conventional activated sludge

* Institute of Chemical Technology in Prague, Technická 5, 166 28 Prague 6, Czech Republic. E-mail: katerina.lapisova@vscht.cz

process, the CMBR offers several advantages: reliability, compactness, high removal efficiency, bacteria free effluent, etc. The study on CMBR for wastewater reclamation has paid great attention since 1990s in the world. The stability and feasibility of ultra-filtration CMBR applied to urban wastewater treatment is investigated [4].

Stillage is the aqueous by-product from the distillation of ethanol following fermentation of carbohydrates. The enlarging production of bioethanol from biomass results in the concurrent production of stillage which exhibits a considerable pollution potential, especially for their large volume, liquid character and high chemical oxygen demand (COD), up to $100 \text{ g O}_2/\text{dm}^3$ [5].

One possibility to eliminate this organic matter is exploitation of thermophilic microorganisms. The thermophilic aerobic process represents a relatively new technology for high-strength and high-temperature wastewater effluents. The aim of our work is to establish a system for organic matter degradation and COD value minimization of distillers' stillage by connecting two processes: mixed thermophilic bacteria cultivation under aerobic conditions and external bio-mass recycle using semi-industrial microfiltration unit.

2. MATERIALS AND METHODS

2.1. MICROORGANISMS

The experiments were performed with mixed thermophilic bacteria culture obtained from activated sludge from wastewater treatment plant in Bystřice pod Hoštýnem (CZ). The bacterial culture was stored in Eppendorf's tube (1.5 cm^3) with glycerol as a cryoprotectant, in the deep freezing box (MDF-U3086S SANYO Japan), at the temperature of $-60 \text{ }^\circ\text{C}$ (storage can).

The adaptation and bacterial bio-mass propagation was necessary before the cultivation in the bioreactor. The inoculum was prepared from storage cans. The cultivation was performed on synthetic medium at $60 \text{ }^\circ\text{C}$, 200 rpm for 24 hours; the inoculum was consecutively resuspended to the medium in the bioreactor.

2.2. MEDIA

This paper presents the experiments made on synthetic medium. These tests were done to evaluate the ability of proposed process (aerobic cultivation with bio-mass recycle) realization on the real material (stillage). Synthetic medium consisted of: ammonium citrate $0.5 \text{ g}/\text{dm}^3$, glycerol $8 \text{ g}/\text{dm}^3$, $\text{MgSO}_4 \cdot 7\text{H}_2\text{O}$ p.a. $1 \text{ g}/\text{dm}^3$, $(\text{NH}_4)_2\text{SO}_4$ p.a. $0.2 \text{ g}/\text{dm}^3$, KH_2PO_4 p.a. $6 \text{ g}/\text{dm}^3$, yeast extract $2 \text{ g}/\text{dm}^3$, peptone $4 \text{ g}/\text{dm}^3$.

2.3. BIOREACTOR

The cultivations were performed in the 5 dm³ laboratory bioreactor AG MBR Switzerland (Fig. 1), facilitated by process control systems AG Switzerland. The bioreactor was connected with regulation and measuring unit IMCS 2000 monitoring values of pH, temperature, stirring, % of dissolved oxygen, concentration of outlet gases: O₂ (Magnos 16, Hartmann & Braun, Germany); CO₂ (Uras 14, Hartmann & Braun, Germany). An aerator was employed to maintain an aerobic environment for the normal growth of bacteria. To keep an optimal temperature, a heat exchanger was installed in the bioreactor. A stirrer was used to ensure complete mixing of the influent and the activated sludge. A level controller together with peristaltic pump was used in order to maintain a constant working volume.

The investigations were carried out in a CMBR apparatus as schematically presented in Fig. 2. The bioreactor, process pump and membrane module constituted a loop, where the medium was circulated at a high speed.

The bioreactor was filled with synthetic medium and inoculated by thermophilic bacteria. The substrate was taken from the feed tank to the bioreactor manually or by peristaltic pump. All the cultivations were performed at constant temperature of 55 °C and pH value 6.5 which was regulated by addition of 20% H₂SO₄ and 20 % NaOH automatically by pump. The CMBR system was monitored by measurement of permeate flux, chemical oxygen demand (COD) and suspended solids. The COD, suspended solids and other items were measured as per the standard methods for examination of water and wastewater [6].

2.4. CERAMIC MEMBRANES

The experiments were made with cross flow multi-channel ceramic membranes, manufactured by Tami-Deutschland, prepared from a mixture of Al₂O₃, TiO₂ and ZrO₂ with the length of 170 mm. The main characteristics of the ceramic membranes are: separation area 0.05, mechanical resistance 9 MPa, chemical stability pH 0–12, and thermal resistance up to 350 °C. The membrane pore size diameter corresponds to the micro filtration range (0.2 µm, 0.45 µm). The membranes were installed into two parallel modules at the semi industrial scale separation unit *ARNO 600-BIO* (Mikropur Ltd; Hradec Kralové, CZ). This regime enables the permanent process where one membrane is in separation regime and the other one in regeneration regime.



Fig. 1. Laboratory bioreactor AG MBR
Switzerland

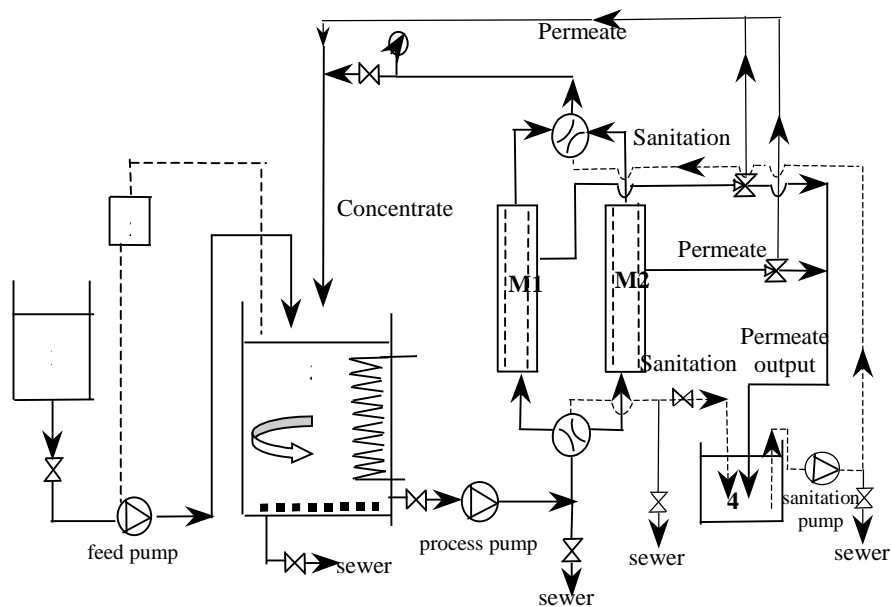

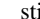


Fig.2. Schematic of ceramic membrane bioreactor. (1) feed tank, (2) level controller, (3) bioreactor, (4) cleaning tank, M1, M2 membrane module
 aerator,  stirrer,  heat exchanger,

3. RESULTS AND DISCUSSION

Figure 3 shows course of fed-batch cultivations. The values of dissolved oxygen (% O₂), outlet carbon dioxide (% CO₂) and biomass growth (g/dm³ X) are presented.

The course of the process varied, even the same cultivation conditions were applied. The process was stopped when the concentration of oxygen achieved at around 100% and did not change. The maximal value of dry matter was 2.67 g/dm^3 .

The COD values were reduced from $14\,700 \text{ mg O}_2/\text{dm}^3$ at the beginning of the cultivation to $3050 \text{ mg O}_2/\text{dm}^3$ at the end of the process, so the COD reduction achieved 80%.

During the process with biomass recycling, fouling effect occurred on the membranes used for separation, but this effect was not very severe and could be evaluated as stable. The flux decline was at around 40% of the initial water flux. The membranes were consequently regenerated by 5% H_2O_2 at 70°C for 2 hours in separate sanitation circle to achieve the initial flux.

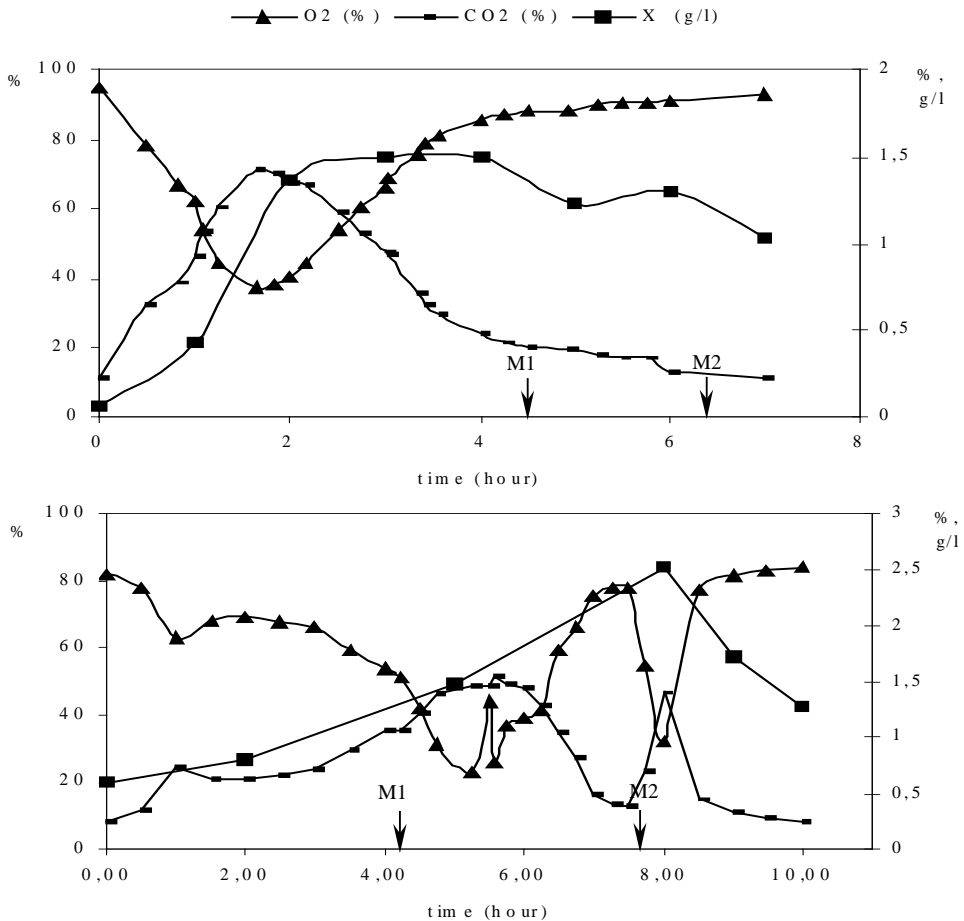


Fig. 3. Fed-batch aerobic cultivation on synthetic medium; arrows represent start of recycling on membrane module M1 ($0.45 \mu\text{m}$), M2 ($0.2 \mu\text{m}$)

The course of the continuous cultivation is shown in Fig. 4. Due to the lack of on-line analytical determination, the process was stopped owing to the value of oxygen, even the bio-mass increased (as was confirming optionally). Maximal value of dry matter achieved 6.4 g/dm^3 .

The COD values did not state about the degradation potential of thermophilic bacteria population and alternate according to the biomass growth.

The permeate flux decline was not measured. The permeate flux was regulated to constant discharge of $5 \text{ cm}^3/\text{min}$ as the substrate feed flow was regulated.

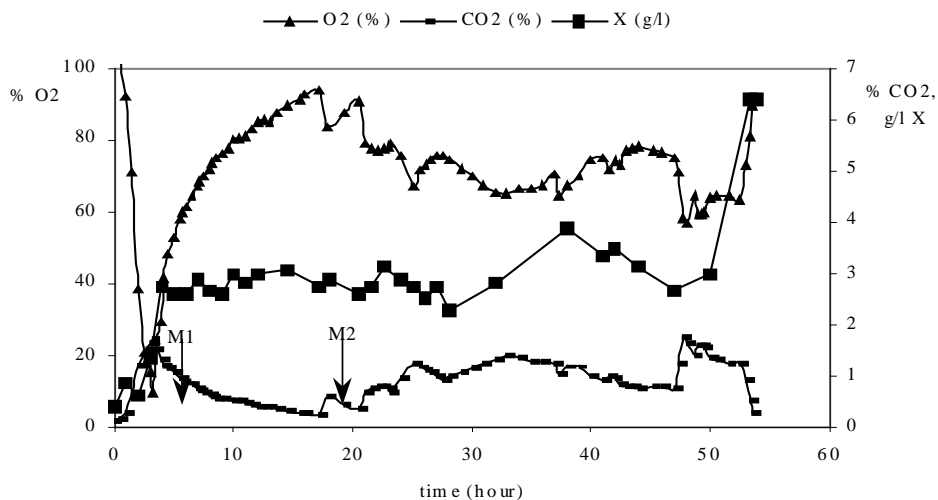


Fig.4. Continuous aerobic cultivation on synthetic medium; arrows represent start of recycling on membrane module M1 ($0.2 \mu\text{m}$), M2 ($0.45 \mu\text{m}$)

4. CONCLUSIONS

The thermophilic microorganisms are useful for utilization of organic compounds. Compared to other wastewater treatment technologies, thermophilic aerobic process is particularly advantageous for the treatment of high-strength wastewaters that can fully benefit from the high rate of degradation, large biodegradation range and low sludge formation. This biotechnology is also attractive due to the high temperature of treated material (stillage). The occurrence of pathogenic microorganisms in treated hazardous wastes, such as municipal water, is minimized at these high temperatures.

The mixed bacteria culture is changing and evolving during cultivation and the ratio of particular bacterial species is not constant within the whole cultivation. This can be explanation for different culture's behavior during the cultivation at same conditions.

Acetic acid was the primary metabolite from glycerol that was also used as a carbon source during cultivations. Rapid lysis of bio-mass started after utilization of the main part of glycerol, therefore COD values increased.

Considering the complexity of above-mentioned process, it is necessary to carry out more experiments in order to optimize the conditions and specifications of the aerobic cultivation with external recycling of bio-mass. The process with bio-mass recycling seems to be stable for a long period with no severe stress to the bacteria cells.

REFERENCES

- [1] NONG X., WEIHONG X., NANPING X., JUN S., *Study on ceramic bioreactor with turbulence promoter*, Separation and Purification Technology, 32, 2003, pp. 403–410.
- [2] GANDER M., JEFFERSON B., JUDD S., *Aerobic MBRs for domestic wastewater treatment: a review with cost considerations*, Separation and Purification Technology, 18, 2000, pp. 119–130.
- [3] MANEM J., SANDERSON R., *Membrane bioreactors*, [in:] J. Mallevialle, P.E. Odendaal, M.R. Wiesner (eds.), *Water treatment membrane process*, McGraw-Hill, New York, 1996.
- [4] XING C.-H., TARDIEU E., QIAN Y., WEN X.-H., *Ultrafiltration membrane bioreactor for urban wastewater reclamation*, Journal of Membrane Science, 177, 2000, pp. 73–78.
- [5] WILKIE A.C., RIEDESEL K.J., OWENS J.M., *Stillage characterization and anaerobic treatment of ethanol stillage for conventional and cellulosic feedstocks*, 19, 2000, pp. 63–102.
- [6] MALÝ J., MALA J., *Chemie a technologie vody*, NEOL 2000, 1996.

*Keywords: dialysis membrane, heparin,
anti-blood clotting*

JULIE MARCQ**, QUANG TRONG NGUYEN*,
KARINE GLINEL*, GUY LADAM¹

DIALYSIS MEMBRANES WITH IMMOBILIZED HEPARIN AND THEIR ANTI-BLOOD CLOTTING PROPERTIES

In this work the attention was focused on AN69TM membrane, a negatively charged polymer used for fast blood dialysis. The aim was to evaluate the immobilization of the negatively charged heparin, an anti blood clotting polymer, on the membrane support with the Layer-by-Layer (LbL) deposition technique. The cationic polyelectrolyte (polyethylenimine) (PEI) was used as the intermediate layer or “glue layer“. A dye staining method and a dissipative quartz crystal microbalance were used to study the required conditions for an effective PEI immobilization. It was observed an optimum adsorption for pH 8 and NaCl concentration within the range of 0.05–0.2 M. Ellipsometry measurements enabled to determine the thickness of the successive layers, namely 8 Å for PEI and 13 Å for heparin (pH 8, concentration of NaCl = 0.3 M). The preliminary results obtained with the dissipative quartz crystal microbalance technique (QCM-D) confirmed the presence of swollen layers in aqueous media. Finally, clotting experiments with whole blood were performed in order to assess the anti-blood clotting of the treated AN69TM membranes. The membrane surface was observed by optical microscopy at different blood-contact times on native AN69TM membrane, on AN69TM membrane treated with PEI and on heparin treated AN69TM membrane. Observations provide the evidence of an anti-blood clotting on the AN69TM membrane treated with heparin. The deposition of heparin by the LbL technique via a PEI layer leads to a membrane with a significant anti-blood clotting.

1. INTRODUCTION

AN69TM is a membrane used for fast blood dialyses of patients suffering from kidney deficiencies. This isotropic membrane, made from an acrylonitrile-methallyl sulfonate copolymer, exhibits negative charges on its surface and is thus hydrophilic. How-

* Polymers, Biopolymers, Membranes, UMR 6522, Rouen University, F-76821 Mont-Saint-Aignan Cedex, France.

¹ Laboratoire de biophysique et biomatériaux, Rouen University, 1 rue du 7ème chasseurs BP 281, F-27002 Evreux Cedex France.

ever, these surface charges may lead to anaphylactoid reactions within the first five minutes of hemodialysis [1] by generation of a highly active molecule, bradykinin. The immobilization of heparin, an anticoagulant polysaccharide, on the membrane is expected to bring about a better hemo-compatibility to the hemodialysis membrane.

In blood dialysis (or filtration) with membranes, heparin is systematically injected in blood to reduce the risk of thrombosis induced by the contact of the circulating blood with the large membrane surface area. Heparin is an anticoagulant polysaccharide which bears negatively charged groups. The anti-clotting effect of heparin is due to specific sequences of charged units in its structure. Its immobilization on the AN69TM membrane reduces the risk of coagulation during dialysis, making possible a cutback in the amount of injected heparin, which in turn reduces the risk of hemorrhage.

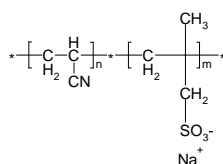
We used the negative charges present on the surface of the AN69TM membrane to adsorb successively poly(ethylenimine) (PEI) and heparin from an aqueous solution, in the so-called LbL deposition technique [2]. After the depositions of the polyelectrolytes, the outermost layer of the membrane mainly consists of heparin. The thickness and amount of adsorbed heparin and the surface charge density are expected to be critical parameters to control the anti-clotting property of the immobilized heparin molecules. The extreme simplicity and mildness of the deposition procedure motivated us to further prospect the influence of the immobilization conditions on the structure of the films and, in turn, on their anti-clotting properties. In fact, dialysis modules using PEI – treated AN69TM membranes are commercially available. The membrane inventors [3] claimed that the low blood coagulation activation during the contact phase is due to the reduction of the AN69TM surface charges by less than 10% of the overall ionic capacity after PEI fixation. A recent study showed that a heparin pre-immobilization onto PEI-treated AN69TM membrane allowed to dialyze patients with reduced or zero heparin administration [4].

Ellipsometry and quartz crystal microbalance (QCM-D) were used to study the layer deposition. The substrates used in our study were silicon wafers and gold-coated quartz crystal for ellipsometry and QCM-D, respectively. In the present work, deposition trials with different techniques were made until adequate layers of AN69 on those substrates were obtained for their correct study in ellipsometry and in QCM-D. We developed a spectrophotometric technique to study the surface charges by charge-site complexation with dye molecules bearing charges opposite to the surface charges. Thanks to the transparency of the AN69 dialysis membrane, such a staining with dye molecules that bear specific charges allowed us to reveal the accessible charged sites on the adsorbed layers. Finally, the extent of whole blood coagulation at surfaces with and without layers was analysed. The retention of erythrocytes within the *in vitro* coagulum on the membrane was observed directly under optical microscope. This test was chosen because the determination of the clot-promoting species released in blood after blood-membrane contact (e.g. the thrombin-antithrombin complex) is difficult [5], except in the case of an extra-corporal circulation of fresh blood in a large-membrane-area module.

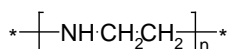
2. EXPERIMENTAL

2.1. CHEMICALS

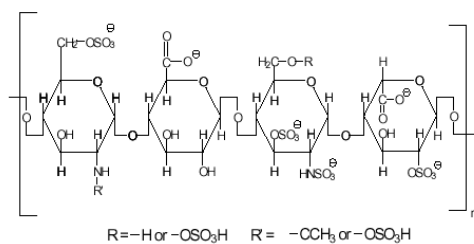
AN69™ dialysis membrane, a transparent microporous film, and AN69™ ($M_w = 50\,000$ g/mol) powder were kindly supplied by Rhodia Corp. AN69™ copolymer which is based on acrylonitrile and methallyl sulfonate exhibits negative charges. Branched poly(ethyleneimine) (PEI), ($M_w = 750\,000$ g/mol), heparin A from porcine intestinal mucosa (M_w within the range of 17 000 – 19 000 g/mol) and ponceau S red (an anionic dye stuff) were purchased from Sigma-Aldrich. Chemical structures are shown in Fig. 1. All other chemicals were purchased from Aldrich and used without further purification.



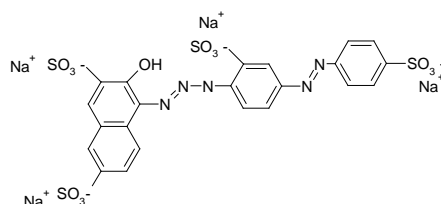
(a)



(b)



(c)



(d)

Fig. 1. Chemical structures of AN69™ (a), PEI (b), heparin (c) and ponceau S red (d)

2.2. SUBSTRATE PREPARATION

AN69TM membrane. The substrates used were AN69TM membranes cut into rectangular 2 cm x 2 cm samples. To be preserved from structure alteration due to drying, the original AN69TM film was glycerinated. The glycerinated samples were rinsed at least 4 times in 50 cm³ Milli-Q water baths and then stored in Milli-Q water before use.

Quartz sensors for QCM-D technique. A disc-shaped, 5 MHz AT-cut, optically polished, piezoelectric quartz crystal sensor with gold electrodes deposited on its two faces (supplied by Q-Sense). Since we wanted to study PEI adsorption onto AN69TM, the sensors were pre-treated as follows: they were first cleaned by treatment in a hot piranha solution (H₂O₂ (35%): H₂SO₄ (98%) 1:1 v/v) for 30 min and then thoroughly washed with pure water. Subsequently, substrates were treated with an aqueous solution of PEI (20 g/dm³, pH 8.75, NaCl concentration = 0.5 M) for 15 min, rinsed in water and then treated with an AN69TM solution in dimethylformamide (DMF, 5 g/dm³) for 15 min. Finally, they were rinsed with DMF and dried with a stream of nitrogen. This pre-treatment, based on the LbL technique, enabled us to obtain an uniform outermost layer of AN69TM on the QCM-D sensors.

Silicon substrates for ellipsometry. The substrates used were one-side polished silicon wafers (ACM, France) cut into 3 cm × 1 cm rectangles. The wafer cleaning and AN69TM coating procedures were similar to those used for QCM-D sensors, except for the compositions of the PEI (3.8 g/dm³, pH 8, NaCl concentration = 0.3 M) and AN69TM (25g/dm³) solutions. Thin films of AN69 were deposited onto cleaned silicon substrates by spin-coating in DMF. The concentration of the polymer solution (25 g/dm³), rotation speed (3000 rpm) and acceleration (500 rpm/s) were adjusted to produce samples with polymer film thickness of about 600 Å. Experiments were carried out to check the stability of this thin film in presence of aqueous solution (pH 8 and NaCl concentration = 0.3 M).

2.3. LAYER-BY-LAYER FILM DEPOSITION

AN69TM membrane. Multilayers were grown by alternately dipping the membrane in aqueous solutions of PEI and heparin for 1 hour each. Between each deposition step, the sample was thoroughly rinsed with pure Milli-Q water.

QCM-D sensors. In this case, the LbL films were built up within the measurement cell of the QCM device, by alternate flow of the PEI and heparin solutions in contact with the sensor.

Silicon wafer. Multilayers were grown by alternately dipping the substrate in aqueous solutions of PEI (3 g/dm³, pH 8, NaCl concentration = 0.3 M) and heparin (0.5 g/dm³, pH 8, NaCl concentration = 0.3 M) for 20 min each. Between each depo-

sition step, the substrate was rinsed by dipping ten times in three different beakers of pure Milli-Q water and dried with a stream of pure air.

2.4. ANALYTICAL TECHNIQUES

Dye staining method. The AN69TM samples were successively dipped in an aqueous solution of PEI (pH range of 2–10, NaCl concentration range of 0.005–1 M) then washed with pure MilliQ water and finally dipped into a solution of dye stuff, the ponceau S red (0.5 g/dm³), for 30 min. After thorough washing, the coloured samples were analysed with a UV-visible spectrophotometer in absorbance mode.

Quartz Crystal Microbalance with Dissipation Monitoring (QCM-D). The QCM-D technique (System D300, delivered by Q-Sense) was employed to follow the adsorption of PEI onto AN69TM. In this technique, the mass adsorbed (including material and hydrodynamically coupled water) onto the surface of a shear-mode oscillating quartz crystal causes a proportional change of its resonance frequency, f_n . For thin, uniform and rigid layers, the observed frequency shift (Δf_n) is related to the adsorbed mass (Δm) via the Sauerbrey relation:

$$\Delta M = -\frac{C}{n} \Delta f_n \quad (1)$$

where n is the overtone number and C denotes the mass sensitivity constant (for the QCM-D system $C = 17.7 \text{ ng/cm}^2\text{-Hz}^{-1}$) which depends on the properties of the crystal used. The QCM-D also allows one to measure the dissipation factor (D) which reflects frictional (viscous) losses induced by the deposited layer on the crystal surface. The QCM-D instrument and data processing software thus allow one to simultaneously determine the mass and the viscoelastic properties of an adsorbed film.

Ellipsometry. The thickness of the successive layers of PEI and heparin was measured by a null ellipsometer from Multiskop instrument (Optrel, Germany) at a fixed angle of 70° and fixed wavelength of 6328 Å. The optical set up consists of a polarized monochromatic laser beam source, a polarizer, a compensator, an analyser and a detector (Fig. 2). The changes in the light polarization with the thickness of films deposited on a substrate were detected via the determination of two characteristic angles psi and delta.

About nine spots were measured on each layer in order to have a relevant value. A model consisting of an isotropic film deposited on a flat isotropic substrate was used to analyze data. The refractive index of the silicon was taken to be 3.882-j0.019. A film refractive index of 1.5 was used to analyze the data.

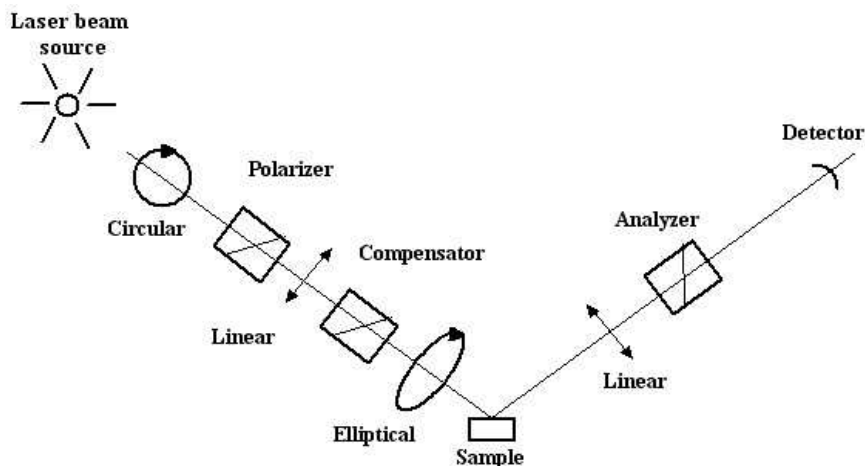


Fig. 2. Null ellipsometer principle

2.5. ANTI-BLOOD CLOTTING EXPERIMENTS

Optical microscopy observation of coagulum formation during blood-membrane contact. For all coagulation tests, blood sample collection in dry tube was performed by venipuncture according to the rules. Human blood with normal CK time (30 ± 2 s) was prepared for each series of tests. 0.1 cm^3 of a fresh blood sample was deposited on four series of three different samples of 1 cm^2 surface area (i.e. pristine AN69™ membrane, PEI-treated membrane, immobilized-heparin membrane, respectively) and incubated at $25 \text{ }^\circ\text{C}$ for different times. The surface of the spot in direct contact with blood was observed under a microscope (Leica DMLM™) equipped with a Sony 3CCD™ camera, after gently rinsing the samples with an isotonic sodium chloride solution for different given incubation times.

3. RESULTS AND DISCUSSION

Influences of pH and ionic strength on the PEI layer sorption. The absorbances of ponceau S red adsorbed on the AN69™ membranes treated with aqueous PEI solutions at various pH and NaCl concentrations are shown in Fig. 3 and 4, respectively. From Fig. 3 it appears that the amount of anionic dye sorbed onto the PEI layer exhibits two maxima depending on the pH (pH 3 and 9). Since all the components involved in the system are polyionic, all adsorption processes are likely to be driven by electrostatic interactions.

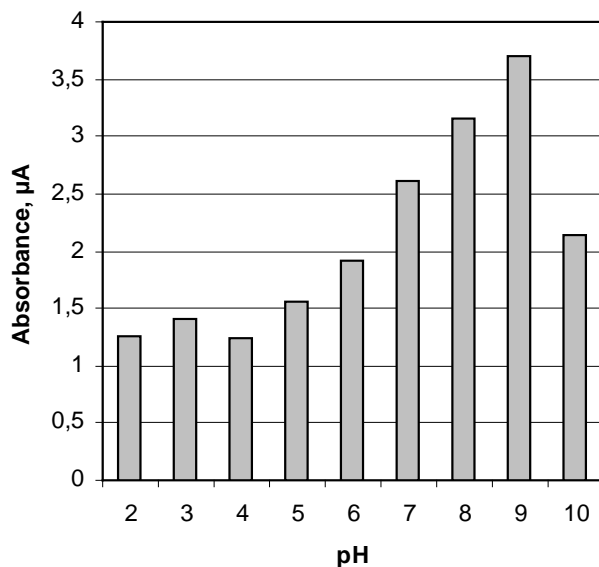


Fig. 3. Absorbance of ponceau S red adsorbed on AN69TM membranes treated with PEI solutions (20 g/dm³, NaCl concentration = 0.5 mol/dm³) of different pH

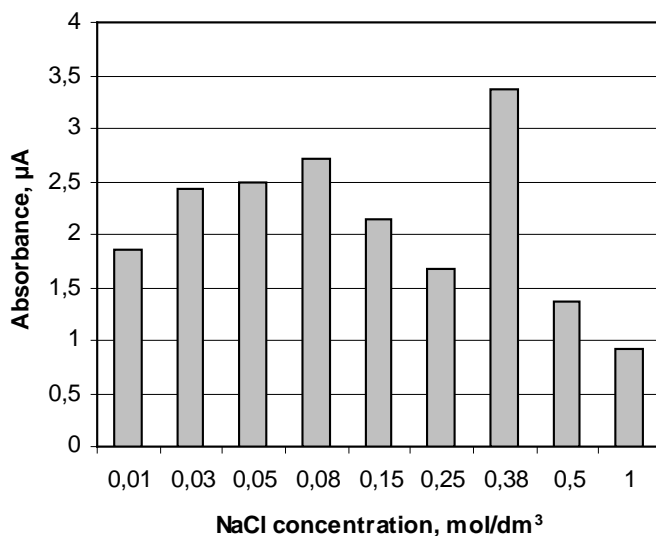


Fig. 4. Absorbance of ponceau S red adsorbed on AN69TM samples treated with PEI solution (20 g/dm³, pH 8) of different NaCl concentrations

With four anionic charges, the ponceau *S* dye is expected to be strongly repelled by the anionic pristine AN69TM membrane surface. However, due to the relatively low exchange capacity of AN69TM, one cannot exclude that the electrostatic repulsive interactions may not be strong enough to override the attractive Van der Waals interactions. Therefore, we verified that no ponceau *S* red was sorbed onto the pristine membrane within the ranges of pH and NaCl concentration studied. This confirmed that the dye molecules adsorb solely onto the PEI layer.

As parts of the PEI charges are involved in the interaction with underlying AN69TM membrane surface, ponceau *S* red molecules can interact only with free cationic charges. Considering the short length of the hydrocarbon segment in-between two consecutive PEI charges (two carbons), we assume that the hydrophobic interactions with the dye are negligible. The amount of adsorbed dye must thus reflect quantitatively the amount of positive charges available for on top of the PEI layer. In fact, competitive interactions of the dye and AN69TM for PEI must occur. As PEI is a weak base, its charge density decreases with pH increasing. Inversely, one expects an increase in the available positive charges at low pH. This may explain the maximum of PEI adsorption at pH 3. As far as the influence of NaCl concentration is concerned, the idea is a little bit different. For low concentrations, few counter-ions (Cl⁻) are present for the PEI. Thus more positive charges are available and PEI adopts a flat pancake-like conformation due to the repulsion of the positive charges and a great number of anchoring points on the AN69TM surface. We think that this scheme corresponds to NaCl concentration lower than 0.1 mol/dm³. Moreover, the attractive interactions between ponceau *S* red molecules and PEI are less screened at low NaCl concentration.

The maximum of ponceau *S* red absorbance at high pH (ca. 8.5) may come from the macromolecular nature of PEI. At such pH values, the number of PEI positive charges is low, leading to a small number of anchoring points on the AN69TM surface. The chains are coiled, with large tails and loops protruding into the solution, rather than as is the case at low pH values [6]. More dye molecules can thus be attached to those loops, in spite of a lower charge fraction per segments. In this hypothesis, the stoichiometry of PEI–ponceau *S* dye molecules must be different at low and high pH values. At high pH, due to the scarce distribution of the positive charges, the dye molecule would be attached by fewer points than at low pH values. In fact, the competition between AN69TM and ponceau *S* red for positive sites on PEI turns in favour of ponceau *S* red due to the number of configurations and positions that their molecules can adopt in solution, compared to the rigidly fixed charges on the AN69TM membrane surface. In other words, the optimum pH for obtaining a large number of accessible charged sites would be 8.5. Concerning the NaCl influence, for concentrations higher than 0.1 mol/dm³ we observed the highest absorbance intensity for salt concentration equal to 0.375 mol/dm³. As a matter of fact, we can suppose that, as it was the case for high pH values, counter-ions in large quantities make positive charges less available. Consequently PEI is more likely

to adopt the coiled conformation described at high pH, leading to the same process of ponceau S red adsorption. However, an excessive increase of NaCl concentration leads to a decrease of adsorbed dye molecules due to the screening of the attractive interactions. Finally the optimal NaCl concentrations for PEI adsorption range from 0.025 to 0.15 mol/dm³ or near 0.4 mol/dm³.

Influence of ionic strength studied by the QCM-D. These results, showed in Fig. 5, enable to complete the previous analysis with ponceau S red dye stuff. Considering the low dissipative coefficient of the adsorbed layers of PEI, one can assume that they are rigid and that the Sauerbrey relation is valid. Two maxima of sorbed amounts are obtained for NaCl concentrations within the range 0.025-0.15 mol/dm³ and around 0.4 mol/dm³, respectively, with the first maximum higher than the second one. These are consistent values with the results obtained from dye staining analysis. However, in QCM-D measurements, the difference between both maxima appears much higher. If we suppose that the amount of water coupled to the layer is independent of the NaCl concentration, this suggests that a NaCl concentration around 0.1 M is more efficient to adsorb the PEI layer. In fact, it is more reasonable to assume that the water quantity varies with PEI layer structure and therefore with the NaCl concentration. For low concentrations, the layer is thin and compact, and thus contains a low amount of water. When the NaCl concentration increases the layer is thicker and less compact, thus containing more water.

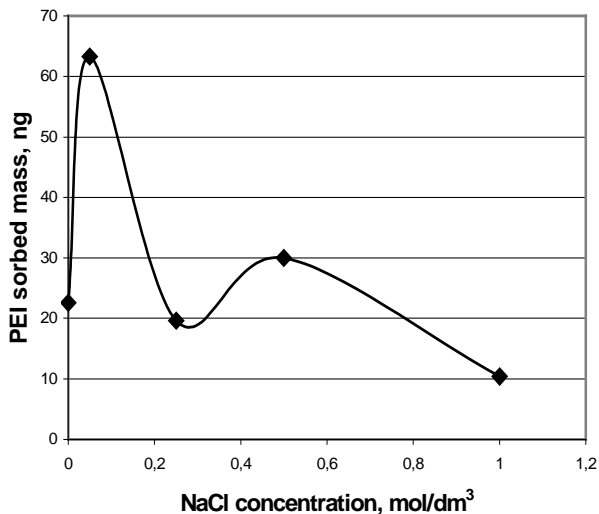


Fig. 5. QCM-D results of adsorbed PEI masses at pH = 8.75 for various NaCl concentrations

Thickness measurements of PEI and heparin layers by ellipsometry. Results are collected in Fig. 6. Ellipsometry measurements confirm the effective adsorption of

PEI on AN69TM and the effective adsorption of heparin on a PEI-treated AN69TM substrate. From these measurements, the thickness of each deposited layer was found to be namely 7 Å for PEI and 13 Å for heparin.

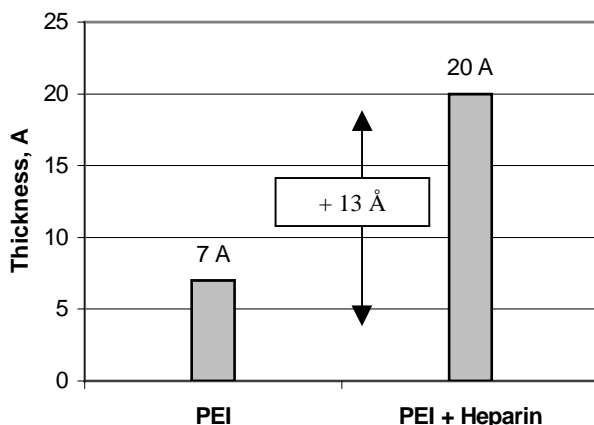


Fig. 6. Layer thicknesses obtained by ellipsometry

Influence of the surface nature on the coagulum formation during blood-membrane contact. The previous analyses of this work, in particular QCM-D and ellipsometry, consisted in studying the adsorption of PEI and heparin layers onto a modeled AN69TM membrane, since it was a thin layer of AN69TM deposited on a substrate and not a real membrane. In this last part of our work, we applied the conclusions deduced from the previous analyses to carried tests of blood coagulation onto three different substrates (Table 1) based on the pristine AN69TM dialysis membrane.

The coagulation time of blood on membrane surfaces strongly depended on the blood sample. Therefore, the comparison was only made on the basis of the same blood sample. Although some differences were detected in visual/photographic observations between the blood spot of each substrates tested, we also found that the observations under microscope were much more relevant. Indeed, we detected the formation of fibrils. Moreover, the coagulum with more and more erythrocytes on the spots with time was visible although no blood colours appear for a visual observation. In all cases, we observed a large difference in time for the onset of coagulation (as illustrated in Table 1.), i.e. the time at which coagulum attached to the membrane surface was clearly observed. An example of coagulum on the membrane surface is shown in Fig. 7. The coagulum mainly consists of erythrocytes in fibrin bundles. The fibrin fibers appeared well only at low erythrocyte density on the surface. In Fig. 7, the fibrin fibers are visible on the borders of the coagulum, and somehow under the erythrocyte cells in the zones of lower cell density.

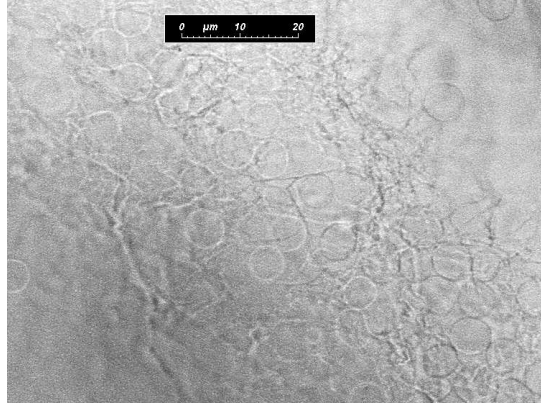


Fig. 7. Optical microscope photography of coagulum

Table 1. Coagulum onset times for three substrates with the same blood sample

Substrates	Coagulum onset time, minutes
Pristine AN69 TM membrane	15
PEI-treated AN69 TM membrane (with PEI concentration = 20 g/dm ³ in 0.5 M NaCl at pH 8)	7
PEI- and heparin-treated AN69 TM membrane (with heparin concentration = 1 g/dm ³ in 0.5 M NaCl at pH 7)	> 50

Our results agree qualitatively with those obtained by Serizawa et al. [7] with a surface of cell-culture poly(ethylene phthalate) disks coated with layer-by-layer assemblies of chitosan and dextrane sulfate. They observed that the assemblies with dextrane sulfate as the outermost layer were blood anticoagulant (i.e. with the longest coagulation time), while those with chitosan were blood procoagulant. We infer that the membrane with a cationic outermost layer (PEI, chitosan) is blood procoagulant, and that an anionic outermost layer (natural AN69TM surface, dextrane sulfate, heparin) is blood anticoagulant. However, the material with heparin as the outermost layer appears as the most anticoagulant. The coagulation onset time exceeded that of a correct preservation of fresh blood without added anticoagulant (like EDTA). It would be interesting to prospect the influence of different deposition parameters on the coagulum formation.

4. CONCLUSIONS

The main goal of this work was to prospect the immobilization of heparin on an AN69TM membrane via an intermediate PEI layer. We first studied the adsorption of

PEI to find optimal adsorption parameters (pH = 8.5 and NaCl concentration within the range 0.025–0.15 mol/dm³). We then controlled by an optical method (ellipsometry) the adsorption of PEI on AN69TM (7 Å) and heparin on PEI-treated AN69TM (13 Å). Finally blood and anti-blood clotting experiments were realized on various substrates. AN69TM membranes treated with PEI and heparin exhibit a significant anti-blood clotting.

REFERENCES

- [1] PARNES E., SHAPIRO W., *Anaphylactoid reactions in hemodialysis patients treated with the AN69 dialyser*, *Kidney Int.*, 40 (6), 1991, pp. 1148–1152.
- [2] DECHER G., *Fuzzy Nanoassemblies: Toward Layered Polymeric Multicomposites*, *Science*, 277, 1997, pp. 1232–1237.
- [3] THOMAS M., VALETTE P., *Use of a neutral or cationic polymer to prevent activation of the contact phase of blood or plasma in contact with a semi-permeable membrane*, US Patent 6,423,232, 2002.
- [4] LAVAUD S., CANIVET E., WUILLAI A., MAHEUT H., RANDOUX C., BONNET J.M., RENAUX J.L., CHANARD J., *Optimal anticoagulation strategy in hemodialysis with Heparin-coated polyacrylonitrile membrane*, *Nephrol. Dial. Transplant.*, 18, 2003, pp. 2097–2104.
- [5] NGUYEN Q.T., PING Z., NGUYEN T., RIGAL P., *Simple method for immobilization of biomacromolecules onto membranes of different types*, *J. Membr. Sci.*, 213, 2003, pp. 85–95.
- [6] NGUYEN Q.T., GLINEL K., PONTIE M., PING Z., *Immobilization of bio-macromolecules onto membranes via an adsorbed nanolayer. An insight into the mechanism*, *J. Membr. Sci.*, 232, 2004, pp. 123–132.
- [7] SERIZAWA T., YAMAGUCHI M., MATSUYAMA T., AKASHI M., *Alternating Bioactivity of polymeric layer-by-layer assemblies: anti- vs pro-coagulation of human blood on chitosan and dextrane sulfate layers*, *Biomacromolecules*, 1, 2000, pp. 306–309.

Keywords: biocatalytic membrane, membrane bioreactor, immobilized lipase, esterification, butyloleate

VICTOR KOCHKODAN*, NIDAL HILAL**,
RINAT NIGMATULLIN**, VLADISLAV GONCHARUK*

LIPASE-IMMOBILIZED BIOCATALYTIC MEMBRANES IN ENZYMATIC ESTERIFICATION

The performance of lipase immobilized membranes prepared by various approaches, viz. using the lipase adsorption on membranes, inclusion of enzyme in membrane structure by filtration as well as covalent attachment of lipase to membrane have been studied in reaction of butyloleate synthesis through esterification of oleic acid with n-butanol in isooctane. Ultrafiltration membranes made of regenerated cellulose (C030F) and polyethersulphone (PM30) were used for lipase immobilization. It was found that the lipase inclusion in the wide porous supporting layer of membrane was the most efficient method in preparing highly effective biocatalytic membranes. The degree of oleic acid conversion using these membranes was about 70–72% with a reaction time of 8 hours. It was shown that the distribution profile of the lipase in the membrane was important for the effective enzyme utilization. The profile imaging atomic force microscopy (AFM) technique was used to visualise surfaces of lipase immobilized biocatalytic membranes.

1. INTRODUCTION

Currently, lipases, also known as triacylglycerol ester hydrolases EC 3.1.1.3, have generated interest in fundamental and applied research [1]. Lipases catalyze a number of different reactions, although they were designed by nature to cleave ester bonds of triacylglycerols with the subsequent release of free fatty acids, diacylglycerols, monoacylglycerols and glycerol. Lipases are also able to catalyze reverse reactions under microaqueous conditions, viz. the formation of ester bonds between alcohol and carboxylic

* Institute of Colloid and Water Chemistry of National Academy of Science of Ukraine, Vernadskii Pr. 42, 03142 Kyiv, Ukraine. Tel.: 38 044 424 7521; fax: 38 044 423 82 24; e-mail: vkochkodan@hotmail.com

** Centre for Clean Water Technologies, School of Chemical, Environmental and Mining Engineering, University of Nottingham, University Park, Nottingham NG7 2RD, UK. Tel.: + 44 (0)115 9514168; fax: +44 (0)115 9514115; e-mail: nidal.hilal@nottingham.ac.uk

acid moieties (ester synthesis). Although ester synthesis can be done chemically with acid or base catalysis, the use of enzyme technology offers the advantages of mild conditions, high specificity including stereospecificity and reduced side reactions [1].

Generally, many lipase-catalyzed reactions studied were carried out in emulsion systems [2]. Currently, attempts are being made to avoid the use of emulsion systems because of difficulties not only in controlling the reaction but also in the re-use and stability of lipases [3]. Consequently, numerous efforts have been focused on the preparation of lipases in immobilized forms involving a variety of both immobilization methods and support materials [2]–[5].

Since lipases can be used in the wide variety of reaction systems, the preparation of immobilized lipase derivatives has to be made according to each synthetic process of interest. In this context, the combined evaluation of the complex mechanism of the biocatalytic membrane action as well as the special requirements for the membrane reactor performance should be taken into account. Thus, immobilization of lipases on or within membranes is far from an already solved problem. In this paper the catalytic behaviour of lipase-immobilized membranes prepared by both non-covalent and covalent immobilization methods using (i) lipase adsorption on membranes, (ii) loading of membranes with enzyme by filtration of lipase solution through active or support membrane layers (iii) covalent attachment of lipase to activated membrane, have been studied in the reaction of butyloleate synthesis through esterification of oleic acid with *n*-butanol.

2. EXPERIMENTAL

2.1. MATERIALS

Candida Rugosa lipase type VII with a ratio of 1:5.88 g proteins/g solids (raw lipase, 700–1500 units/mg solid, molecular weight 57–60 kDa), oleic acid, *n*-butanol, glutaric dialdehyde, isooctane, hexamethylenediamine (HMD) phosphate buffer (pH 7.0) were purchased from Sigma-Aldrich (Dorset, UK). All the chemicals were analytical grade and used without further purification. Molecular sieves (4–8 mesh) were supplied by Fisher Scientific (Loughborough, UK).

Two types of ultrafiltration membranes used (1) C030F membrane made of regenerated cellulose supplied by MICRODYN-NADIR GmbH (Wiesbaden, Germany) and (2) PM30 polyethersulfone membrane supplied by Millipore Express (Watford, UK) were used in this work. According to the manufactures' specifications, both membranes have the same MWCO of 30 kDa. These are composite membranes with thin-cellulose (C030F) or polyethersulfone (PM30) active layer supported by porous non-woven polymer materials in which pores are significantly larger than those in the active layer.

2.2. METHODS OF LIPASE IMMOBILIZATION ON MEMBRANES

2.2.1. NON-COVALENT IMMOBILIZATION

Lipase immobilization by adsorption:

A membrane sample 50 mm diameter was fixed in a special polymethylmethacrylate frame so that only active membrane layer was in contact with the lipase solution while the membrane supporting layer was prevented from contact by the enzyme solution. Membrane samples were placed in Petri dishes with 20 cm³ of 1–10 mg/cm³ lipase solution in phosphate buffer (pH 7.0). Membrane samples were shaken using a ABU-2 device (Mashprom, Tambov) for 1–12 hours at 20 °C. After sorption, membranes were removed from the Petri dishes and rinsed twice with 50 mM phosphate buffer (pH 7).

The amount of lipase adsorbed onto the membrane surface was determined as the total protein quantity from the difference between the amount of protein in solution before and after adsorption and in washing using QuantiPro™ BCA Assay kit (Sigma-Aldrich, Dorset, UK).

Lipase immobilization on membranes by filtration:

0.5–0.75 grams of crude lipase were dissolved in 50 cm³ of 50 mM phosphate buffer (pH 7.0) and the solution was gently stirred using a magnetic stirrer for 2 hours. Afterwards the solution was centrifuged at 3000 rpm for 10 minutes to remove the insoluble substances. 1–10 cm³ of the lipase solution was filtered through the active or support layers of the membranes in dead-end filtration cell (Amicon, model 8200, Fisher Scientific, Loughborough, UK) under a pressure of 2 kPa without stirring. After immobilization, membranes were rinsed twice with 50 mM phosphate buffer (pH 7).

2.2.2. COVALENT IMMOBILIZATION OF LIPASE ONTO MEMBRANES

The preliminary activation of the membrane surface *via* periodate oxidation was used for covalent immobilization of lipase on C030F cellulose Nadir membrane. The procedure for covalent lipase immobilization was as follows: a membrane sample was treated with 10 cm³ of 0.5 M sodium periodate solution for 90 minutes in the dark to activate the membrane surface. The activated membrane was thoroughly washed with distilled water and immersed in 10 cm³ of 10 g/dm³ lipase in a phosphate buffer (pH 7.0) for 24 hours.

For the insertion of HMD spacer, the membrane sample was activated with sodium periodate and placed in 10 cm³ of 1% (w/v) HMD solution for 18 hours. The membrane was then washed with distilled water, activated with 5% (v/v) glutaraldehyde for 1 hour and treated with the lipase as described above.

2.3. ENZYMATIC ESTERIFICATION IN MEMBRANE BIOREACTOR

The membrane bioreactor was designed on a base of membrane element described elsewhere [4]. The element consists of two identical cylindrical membrane channels of 2 mm width separated by biocatalytic membrane. Esterification started by pumping both phases through the membrane elements. Reactants diffuse through the biocatalytic membrane where the esterification reactions occurred as a result of catalytic action of immobilized lipase due to the difference in concentrations.

The degree of oleic acid conversion was determined using the following equation:

$$DC = \left(1 - \frac{C_s}{C_i}\right) \times 100\%$$

where C_i is the initial quantity of oleic acid in the feed stream and C_s is the sum of oleic acid quantities in the feed and receiving streams after given period of esterification reaction. Because of the possibility of oleic acid being transported into the receiving phase without transformation, samples of 1 cm³ volume were periodically withdrawn from both the feed and receiving reservoirs to evaluate degree of oleic acid conversion. Analysis of the oleic acid concentration into the samples was carried out by direct titration with 10 mM potassium hydroxide solution in *n*-butanol using phenolphthalein as an indicator.

The AFM used in this study was an Explorer (TMX 2000), a commercial device made by Veeco Instruments (USA). Profile imaging mode was selected to study the polymeric membranes [6].

3. RESULTS AND DISCUSSIONS

3.1. BIOCATALYTIC MEMBRANES WITH NON-COVALENT IMMOBILIZED LIPASE

Physical adsorption of lipases on the membrane surface provides the simplest approach for the preparation of membrane-immobilized lipases [7]. In this way, lipases become adsorbed on the membrane surface through a combination of Van der Waals, hydrophobic, electrostatic forces, hydrogen bonds and aromatic π - π binding.

Usually, adsorbed lipases are not very useful to work in high water-activity systems because of the possible desorption, however enzymes can remain adsorbed on the membrane surface in organic media due to practical insolubility in organic solvents.

It was found that 8 hours were required to reach the adsorption equilibrium in lipase-membrane system over the studied range of lipase concentration.

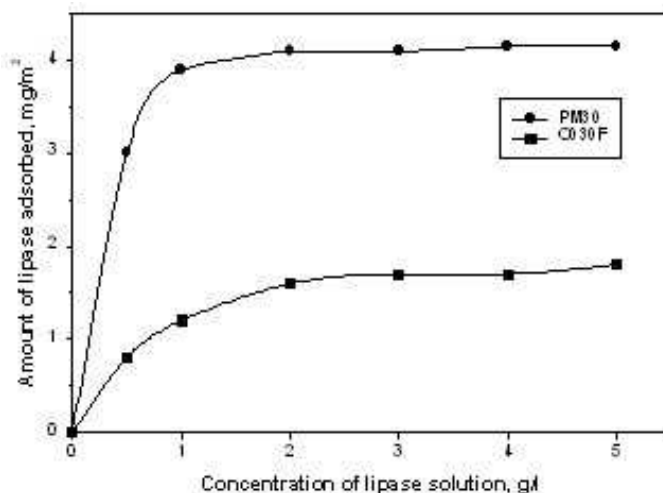


Fig. 1. Adsorption isotherms for lipase on C030F and PM30 membranes (pH 7, 25 °C, adsorption time of 8 h)

As can be seen from Fig. 1, the lipase adsorption isotherms have the typical Langmuir character for both cellulose C030F and PM30 polyethersulphone membranes. The lipase adsorption on polyethersulphone membrane is higher compared with a cellulose membrane. According to the chemical composition, PM30 polyethersulphone membrane has both polar and non-polar segments on its surface. As a result, polyethersulphone membrane is more hydrophobic than a cellulose membrane. It was previously shown that the more hydrophobic the membrane surface the more likely is the binding of proteins with the exposed non-polar regions of membrane polymer [8]. The amount of lipase adsorbed on the membranes studied is in the order of a monolayer, which has a surface density of 3.3 mg/m² for lipase from *C.rugosa* [9].

Reaction profiles of butyl oleate synthesis in membrane reactors with lipase-adsorbed biocatalytic membranes are shown in Fig. 2. Lipase-immobilized PM30 membrane provides about 28 % of substrate conversion for reaction time of 8 hours, whereas the lipase immobilized C030F membrane shows an oleic acid conversion of approximately 21 %. The better performance of PM30-based biocatalytic membrane is obviously due to a higher loading of enzyme on this membrane. It should be noted however, that the degree of oleic acid conversion was not high enough. This was due to low membrane loading with lipase. However, it can be seen from Table 1 that mass reaction rate (conversion vs protein loading) is higher in case of immobilization on the surface of cellulose membranes. Thus, we did not observe lipase activation by more hydrophobic polyethersulphone surface which was often claimed in research dealing with lipase immobilization on polymeric materials [5].

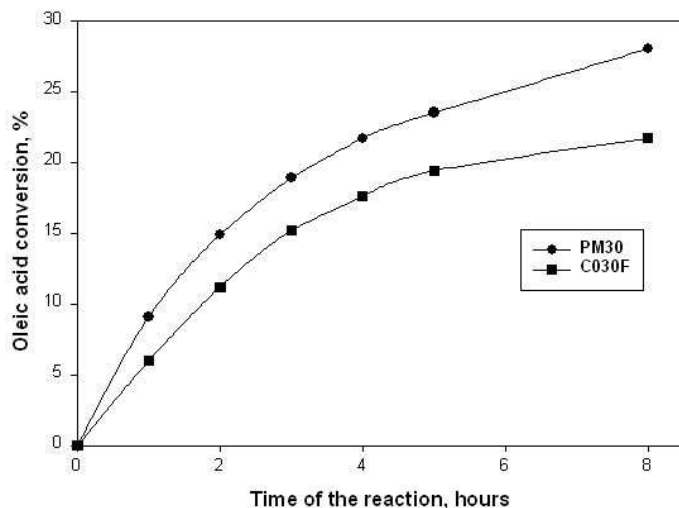


Fig. 2. Degree of oleic acid conversion versus time of esterification on membranes with adsorbed lipase. Lipase loading equals to $4.15 \text{ mg protein/m}^2$ for PM30 (●) and $1.7 \text{ mg protein/m}^2$ for C030F (■) membranes

To increase the membrane loading with lipase, the enzyme inclusion into the membrane body using the filtration technique was carried out. This procedure was based on the fact that PM30 and C030F are asymmetric composite ultrafiltration membranes and lipase molecules readily penetrate their supporting layers. The asymmetric membrane structure permits the lipase confinement by localizing it between the lipase-impermeable active layer (through which the lipase macromolecules cannot pass, for the chosen membrane cut-off) and the sponge support layer. Lipase is loaded into the porous membrane structure by ultrafiltration of an aqueous lipase solution in the direction from the support towards the active layer (reverse filtration mode).

According to Fig. 3, the highly effective biocatalytic membranes were prepared using the lipase inclusion in the membrane structure. Higher values of substrate conversion on lipase-immobilized membranes of this type compared to membranes with adsorbed lipases (Fig. 2), is due to higher lipase loading in the membrane. However, as shown in Table 1, higher values of specific lipase activity (conversion vs protein loading) were obtained for membranes with adsorbed lipase. This finding suggests that essential mass transfer limitation occurs when the immobilized enzyme is included in the membrane structure through the filtration technique. Therefore, immobilization by filtration results in biocatalytic membranes which provide higher transformation rate for the whole reactor due to higher reaction rate per membrane area. However, an effectiveness of lipase use in this case is lower than lipase immobilised by sorption.

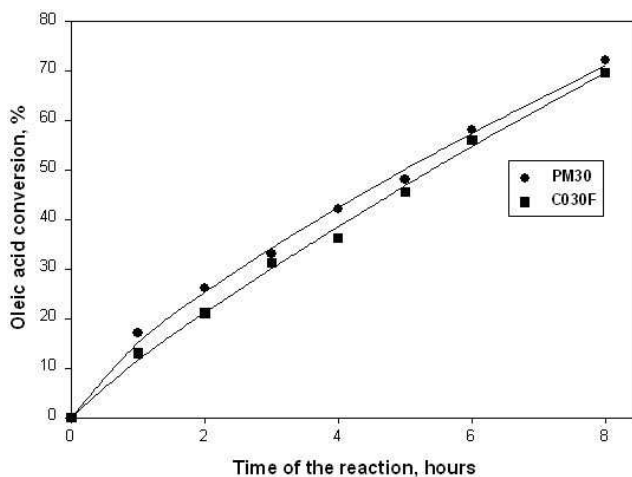


Fig. 3. Degree of oleic acid conversion versus time of esterification on lipase-immobilized membranes. Lipase loading equals to $4.15 \text{ mg protein/m}^2$ for PM30 (●) and $1.7 \text{ mg protein/m}^2$ for C030F (■) membranes

To study the effect of lipase loading on the degree of oleic acid conversion, membranes with various enzymes loading were prepared (Fig. 4). Lipase immobilization on an active membrane layer using a similar procedure was also carried out for comparison. This was carried out by the ultrafiltration of a lipase solution through the membrane in the direction from the active layer towards the support layer (normal filtration mode). The lipase retention on the membranes was found to be practically independent of the membrane orientation giving similar lipase loading after filtration of equal volumes of lipase solution.

Fig. 4 demonstrates that an increase in enzyme loading from $0.024 \text{ g of proteins/m}^2$ to $0.68 \text{ g of proteins/m}^2$ led to a slight increase in the conversion degree. This means that only a part of the enzyme immobilised within the membrane contributes to the reaction. These results indicate a decrease in specific activity of the lipase with increasing concentration when immobilized in the membrane. At high enzyme loading, the observed activity is lowered by an obstruction of pores, which decreases the mass transfer rate of the reagents through the membrane (Table 1) and by decreasing the accessibility of enzyme active sites within enzyme deposits.

Fig. 4 shows higher substrate conversion degree when lipase is immobilized in the support membrane layer. The higher rate of esterification with the enzyme immobilized within the wide porous support layer is most probably related to a better enzyme distribution through the porous structure of the membrane. In this case, the enzyme is more effective compared to the enzyme presented in the form of gel deposit on the surface of the active layer of the membrane. Thus the distribution profile of the lipase in the membrane is important in the effective enzyme utilization.

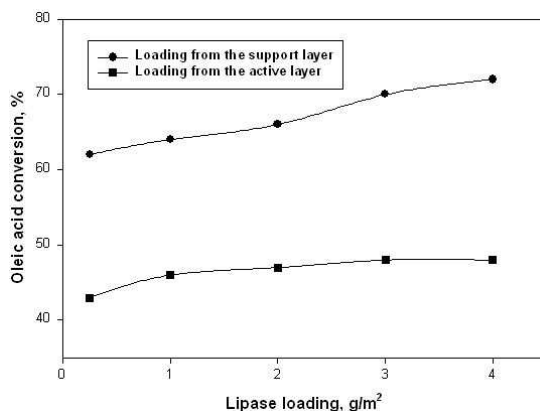


Fig. 4. Reaction profiles of butyloleate synthesis on biocatalytic membranes at various lipase loading. Immobilization by filtration technique in support (●) or active layer (■) of PM30 membrane. Esterification time equals to 8 hours

Table 1. Mass/area transport rates versus time of esterification reaction for biocatalytic membranes prepared by various immobilization methods

Biocatalytic membrane (method of lipase immobilization/lipase loading, mg protein/m ²)	Time of esterification reaction, hours				
	1	2	3	5	8
	Mass reaction rate, $\mu\text{mol/h}\cdot\text{mg protein}$				
	Area-reaction rate, $\mu\text{mol/h}\cdot\text{cm}^2\text{ membrane}$				
PM30 (adsorption/4.2)	$\frac{0.219}{0.046}$	$\frac{0.178}{0.038}$	$\frac{0.151}{0.032}$	$\frac{0.112}{0.023}$	$\frac{0.084}{0.018}$
C030 (adsorption/1.7)	$\frac{0.352}{0.030}$	$\frac{0.329}{0.028}$	$\frac{0.298}{0.026}$	$\frac{0.228}{0.019}$	$\frac{0.162}{0.014}$
PM30 (filtration through the support layer/680/1.7)	$\frac{1.31\cdot 10^{-3}}{0.045}$	$\frac{1.91\cdot 10^{-3}}{0.066}$	$\frac{1.62\cdot 10^{-3}}{0.084}$	$\frac{1.41\cdot 10^{-3}}{0.049}$	$\frac{1.31\cdot 10^{-3}}{0.045}$
C030 (filtration through the support layer/680)	$\frac{1.91\cdot 10^{-3}}{0.066}$	$\frac{1.54\cdot 10^{-3}}{0.031}$	$\frac{1.52\cdot 10^{-3}}{0.079}$	$\frac{1.34\cdot 10^{-3}}{0.046}$	$\frac{1.31\cdot 10^{-3}}{0.044}$
C030 (covalent immobilization without spacer/9.0 adsorption/1.7)	$\frac{0.110}{0.026}$	$\frac{0.044}{0.020}$	$\frac{0.041}{0.019}$	$\frac{0.031}{0.019}$	$\frac{0.025}{0.011}$
C030F (covalent immobilization with spacer/6.0 adsorption/1.7)	$\frac{0.101}{0.031}$	$\frac{0.083}{0.026}$	$\frac{0.074}{0.023}$	$\frac{0.058}{0.018}$	$\frac{0.043}{0.013}$

Surface characteristics derived from AFM image analysis software are shown in Table 2. It can be seen from Table 2, that the mean pore diameter of the initial membranes are very close. This is due to the fact that both membranes have the same MWCO. However, the surface of the PM30 membrane is smoother than the surface of the C030F membrane. As expected, lipase immobilization on the membrane surface leads to a decrease in pore size. Moreover, the deposition of lipase on the membrane surface results in a smoother surface and therefore gives less total contact area.

3.2. BIOCATALYTIC MEMBRANES WITH COVALENT IMMOBILISED LIPASE

Reaction profiles of butyl oleate synthesis with covalent immobilized lipases membranes are shown in Fig. 5. Comparisons between Fig. 2 and Fig. 5 shows that covalently immobilized lipases are less active in the esterification reaction compared with the adsorbed enzyme. Rigid enzyme attachment *via* covalent binding considerably modifies the protein tertiary structure leading to a loss of activity of the lipase.

Table 2. AFM surface characteristics of lipase immobilized PM30 and C030F membranes

Membrane type	Surface roughness, RMS, nm	Total contact area, Å ²	Mean pore diameter, Å
PM30 (active layer)	0.42	428420	13.85 ± 0.10
PM30 with lipase immobilized by filtration through the active layer	0.13	335080	8.25 ± 0.16
C030F (active layer)	0.76	468800	12.55 ± 0.15
C030F with lipase immobilized by filtration through the active layer	0.36	436190	5.43 ± 0.18
C030F with covalent immobilized lipase (without spacer)	0.29	487500	4.52 ± 0.13
C030F with covalent immobilized lipase (with HMD spacer)	0.30	652200	5.61 ± 0.17

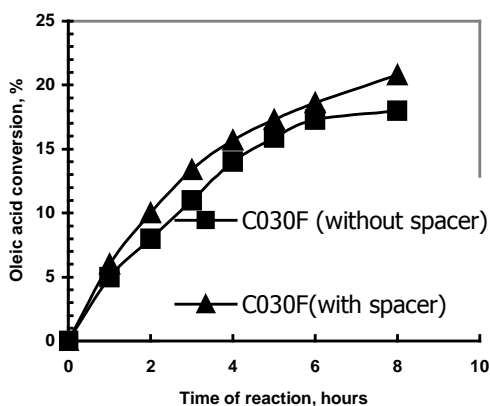


Fig. 5. Reaction profiles of butyloleate synthesis on biocatalytic membranes with covalent immobilized lipases without (■) and with HMD spacer (▲)

Fig. 5 shows, that the degree of oleic acid conversion on biocatalytic membrane with covalent immobilized lipase with a HMD spacer is higher comparing with membrane without spacer. It should be noted that the amount of covalent immobilized proteins was $9 \pm 1 \text{ mg/m}^2$ and $6 \pm 0.5 \text{ mg/m}^2$ with and without spacer, respectively.

Thus, membranes with lipase immobilized *via* spacer gave a higher conversion degree even at lower loading level. This phenomenon is probably due to the fact that the spacer stretches out of the bulk phase and minimizes the interactions between the enzyme and membrane surface, which could affect the lipase structure [10].

Comparison of surface characteristics of lipase-immobilised membranes presented in Table 2 shows that the mean pore diameter for covalently immobilized biocatalytic membranes is similar to that of C030F immobilized membranes prepared through a filtration technique. However, the amount of covalently bounded lipase is much lower than that loaded by filtration (9 ± 1 mg protein/m² and 0.68 ± 0.05 g protein/m², respectively). The decrease in pore size for lipase-immobilized membranes is a result of alteration of membrane porous structure due to binding of bulky protein molecules. The reason of virtually the same decrease in membrane pore size due to binding lower quantity of enzyme for covalent immobilization and for immobilization *via* filtration is not established. Obviously, irrespective of the method of lipase immobilization (covalent or filtration), both PM30 or C030F membranes were covered with a layer of immobilized enzyme. At these conditions the various lipase loading determines mainly the thickness of the immobilized layer and to a lesser extent affects the other surface characteristics of immobilized layer, including the pore size.

Moreover, surface roughness for the membranes with covalently immobilized lipase was lower than that in the case of immobilization by filtration (Fig. 6). Probably rigid multipoint binding due to covalent immobilization results in the spreading of protein macromolecules across the surface smoothing it. Such a distortion in protein structure has a detrimental effect on the enzyme activity. Spacer introduction, as mentioned above, contributes to better preservation of the protein structure. That was confirmed by less pronounced smoothing of the membrane surface when lipase was immobilized with the spacer. Lipase immobilized by filtration preserves the globular structure even better and surface roughness in this case is the highest among the membranes with immobilized lipase.

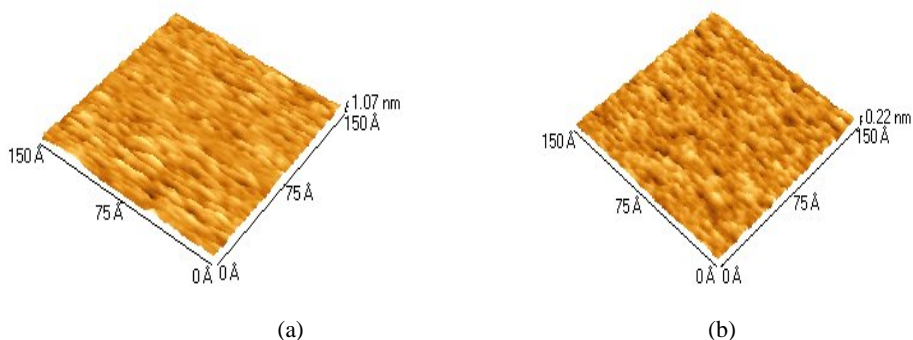


Fig. 6. 3-D AFM images of C030F membranes with covalently immobilized lipase without spacer (a) and with HMD spacer (b)

4. CONCLUSIONS

It was found that lipase inclusion in the wide porous support membrane layer provides highly active membranes able to convert 70–72% of oleic acid in 8 hours of reaction time. On the contrary, the biocatalytic membranes with adsorbed or covalently bounded lipase give the substrate conversion of 22–28% and 18–21%, respectively, at the same conditions. Higher values of substrate conversion on membranes with filtration-immobilized lipase compared to membranes with adsorbed lipases is due to higher lipase loading in the membranes. However, the data on mass- and area reaction rates indicate essential mass transfer limitation at high enzyme loadings, which were achieved by the filtration technique.

It was shown that lipase immobilization by filtration in the sponge layer of the asymmetric membranes allowed higher catalytic activity with respect to the enzyme immobilized on the active membrane layer. Thus the distribution profile of the lipase in the membrane is important for the effectiveness of immobilised enzyme.

Covalent immobilized lipases on membrane C030F were found less active in esterification reaction compared with the adsorbed enzyme on this membrane, this is probably due to conformational changes in tertiary structure of lipase during the covalent attachment to the membrane, which results in a partial loss of the lipase activity. An introduction of a HMD spacer between the membrane surface and covalently immobilized enzyme mitigates to some extent the detrimental effect of covalent immobilization and increases the rate of esterification reaction.

ACKNOWLEDGEMENTS

We thank the Royal Society (UK) for the financial support of this work (GR 15335).

REFERENCES

- [1] VILLENEUVE P., MUDERHWA J.M., GRAILLE J., HAAS M.J., *Customizing lipases for biocatalysis: a survey of chemical, physical and molecular biological approaches* (a review), *Journal of Molecular Catalysis B: Enzymatic*, 9, 2000, pp. 113–148.
- [2] BALCAO V.M., PAIVA A.L., MALCATA F.X., *Bioreactors with immobilized lipases: State of the art*, *Enzyme and Microbial Technology*, 18, 1996, pp. 392–416.
- [3] SAKAKI K., GIORNO L., DRIOLI E., *Lipase-catalyzed optical resolution of racemic naproxen in biphasic enzyme membrane reactors*, *Journal of Membrane Science*, 184, 2001, pp. 27–38.
- [4] HILAL N., NIGMATULLIN R., ALPATOVA A., *Immobilization of cross-linked lipase aggregates within microporous polymeric membranes*, *Journal of Membrane Science*, 238, 2004, pp. 131–141.
- [5] FERNANDEZ-LAFUENTE R., ARMISEN P., SABUQUILLO P. et al., *Immobilization of lipases by selective adsorption on hydrophobic supports*, *Chemistry and Physics of Lipids*, 93, 1998, pp. 185–197.
- [6] BOWEN W.R., HILAL N., LOVITT R.W., WILLIAMS P.M., *Atomic force microscope studies of membranes: surface pore structures of Diaflo ultrafiltration membranes*, *Colloid and Interface Science*, 180, 1996, pp. 350–359.

- [7] TSAI S.-W., SHAW S.-S., *Selection of hydrophobic membranes in the lipase-catalyzed hydrolysis of olive oil*, Journal of Membrane Science, 146, 1998, pp. 1–8.
- [8] MATTHIASSEN E., *The role of macromolecular adsorption in fouling of ultrafiltration membranes*, Journal of Membrane Science, 16, 1983, pp. 23–32.
- [9] PRONK W., VAN RIET K., *The interfacial behaviour of lipase in free form and immobilized in a hydrophilic membrane reactor*, Biotechnology and Applied Biochemistry, 14, 1991, pp. 146–153.
- [10] STARK M.B., HOLMBERG K., *Covalent immobilization of lipase in organic media*, Biotechnology and Bioengineering, 34, 1989, pp. 942–954.

*Keywords: polysulfone, surface modification,
Friedel-Crafts reaction, water flux,
FTIR, SEM*

ANJA CAR*, GREGOR FERK*, CHRTO MIR STROPNIK*

EFFECT OF SURFACE MODIFICATION WITH FRIEDEL–CRAFTS REACTION WITH (1,3)-PROPANE SULTONE ON THE PHYSICAL PROPERTIES OF POLYSULFONE MEMBRANES

Asymmetric porous membranes were prepared from polysulfone (PSf) by wet-phase separation procedure. Chemical modification was applied to the upper membrane surface, which was exposed to interaction with nonsolvent (water) in the coagulation bath during the membrane formation. The membrane surface was modified by the series of Friedel–Crafts electrophilic substitutions of aromatic rings in the polysulfone molecules. As the surface reactive reagent (1,3)-propane sultone and AlCl_3 as catalyst were used. With this procedure a new functional groups $\text{CH}_2\text{-CH}_2\text{-CH}_2\text{SO}_3^-$ were introduced on the surface of conventional ultrafiltration membranes. The measurements of the membrane thickness, deionized water flux through the membrane and the FTIR/ATR spectroscopy as characterization method of chemical modification of the membrane surface were applied. The morfologies of membranes were characterized with SEM.

1. INTRODUCTION

The polysulfone (PSf) membranes have been developed for variety of industrial applications, such as: microfiltration, ultrafiltration, reverse osmosis and gas separations. In recent years, ultrafiltration technology has recived tremendous importance for concentration, purification and fractionation of various products in diverse fields. Most of the commercial ultrafiltration membranes are made from hydrophobic polymers like different polysulfones, polypropylene and polyethylene due to their excellent properties. PSf is one of the most important polymeric materials in this group for

* University of Maribor, Faculty of Chemistry and Chemical Engineering, Smetanova 17, 2000 Maribor, Slovenia. E-mail: anja.car@uni-mb.si

membrane manufacturing, because of thermal and hydrolytic stability as well as good mechanical and film-forming properties [1]. A common technique for the preparation of polymeric membranes with asymmetric structure is the phase separation process where the thin layer of polymer solution is cast on a suitable support and the phase separation is introduced by a non-solvent [2], [3]. The phase separation method has been widely used for the preparation of different synthetic polymeric membranes. During the process, the polymer casting solution is immersed into a bath with non-solvent. The solvent diffuses out of the cast film and the non-solvent diffuses into it, which results in phase separation and polymer precipitation to form a membrane. In the formation process of a membrane, two types of phase separation can be distinguished. The dry phase separation takes place in the atmosphere by evaporation of a volatile solvent and the wet phase separation is induced by non-solvent. In order to obtain membranes with special properties, additional additives can be dissolved in the casting solution. The final membrane structure and its properties are influenced by different physical and chemical parameters [4]. Polymer membranes with well-defined pore structures and specifically functionalized surfaces play key role in advanced separations, high performance ultrafiltration fractionation [5] or affinity filtration of proteins [6]. But hydrophobic surface of PSf membranes has a severe fouling during water solutions ultrafiltration of containing different substances [7]. There are many factors contributing to fouling such as surface properties (chemistry, morphology), hydrodynamic conditions, ionic strength, and solute concentration [8]. The fouling resistance on membrane surface can be reduced by introducing various functional groups, which can change the surface charge density and surface hydrophilicity/hydrophobicity. Thus, the ideal membrane would combine the superior bulk properties of hydrophobic polymers with the surface chemistry of hydrophilic materials for variety of separation applications. Surface modification of membrane is an attractive approach to change the surface properties of the membrane in a defined selective way, while preserving its macroporous structure. Several techniques have been used to impart surface hydrophilicity to conventional hydrophobic membranes to improve their fouling resistance. These techniques include: chemical oxidation [9], [10], radiation and photochemical grafting [11], [12], low plasma treatment [13], [14], covalent attachment [15], [16] and coating of a thin layer [17].

In this paper we present a study of chemical modification of the PSf membrane surface in order to change its physical properties with respect to the surface charge density. The PSf membrane surface was modified by the Friedel–Crafts electrophilic substitution of aromatic rings in PSf molecules with (1,3)-propane sultone. We applied the measurements of the membrane thickness, deionized water flux through the membrane, the FTIR/ATR and SEM as the characterization methods of chemical modification of the membrane surface and morphology. Measurements of the FTIR/ATR, SEM and water flux are in a qualitative agreement with the physical and chemical properties of the membrane surface changed by application of the specific chemical modification.

2. EXPERIMENTAL

Materials. In the experiments the following chemicals were used: Udel A Polysulfone (PSf) (Aldrich 18,244-3), N,N-dimethylacetamide (DMA) (Fluka), (1,3)-propane sultone (Aldrich), AlCl_3 (Fluka), methanol (Fluka), butanol (Fluka), hexane (Fluka). Chemicals were applied without further purification with the exception of AlCl_3 that was sublimed before used.

Membrane preparation and surface modification. Asymmetric porous membranes were prepared from polysulfone by the wet-phase separation method. 15% PSf solution in N, N-dimethylacetamide (DMA) with the nominal thickness of 300 μm was immersed in a coagulation bath of pure water at the room temperature. Membranes were left in pure water for 24 hours. The modification was applied to the upper membrane surface, which was exposed to interaction with non-solvent (water) in the coagulation bath during the membrane formation (Fig. 1). Reaction mixture was slowly agitated and the membrane was left in the reaction mixture for appropriate time. The PSf membranes were modified by Friedel–Crafts electrophilic substitution [18] of aromatic rings in PSf molecules with (1,3)-propane sultone, AlCl_3 was used as a catalyst. The membrane surface was previously conditioned in different solvents: water, methanol, butanol and hexane, i.e. a sequence of a polar to less polar and finally a non-polar solvent. Exposition time to the chemical reaction was 1, 5 and 10 minutes at the room temperature. Different mole ratio of AlCl_3 catalyst to (1,3) propane sultone was applied. After reaction membranes were washed with methanol and water.

Table 1. Surface-modified conditions of PSf membranes

Reaction time, min	Catalyst mole ratio AlCl_3 /(1,3) propane sultone
1	0.005
5	
10	
1	0.01
5	
10	
1	0.02
5	
10	

Membrane characterization. The surface of chemically modified membranes was characterized with FTIR/ATR (Fourier transform infrared spectroscopy/Attenuated total reflectance). FTIR/ATR spectroscopy was used to confirm the pendant functional groups on membrane surface. Measurements were recorded using

Spectrum One (Perkin Elmer) spectrometer. The morphology of native and chemically modified membranes was followed with SEM microscopy. The membrane thickness was measured by magnetic probe MINIMER HD1. The deionized water flux through the membranes was measured in AMICON 8400 cell under the ultrafiltration pressure of nitrogen at 0.4 and 0.6 MPa.

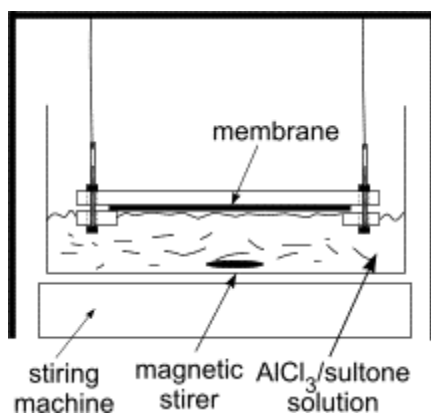


Fig. 1. Device for chemical surface modification

3. RESULTS AND DISCUSSION

Polysulfone asymmetric porous membranes were chemically modified at their upper surface according to the conditions shown in the Table 1. The modification of surface was obtained by a simple method, namely being dipped into the active reagents. The anticipated product by Friedel–Crafts reaction is shown in Fig. 2. The mechanism of the reaction is postulated as alkylation of benzene using Friedel–Crafts catalyst [19].

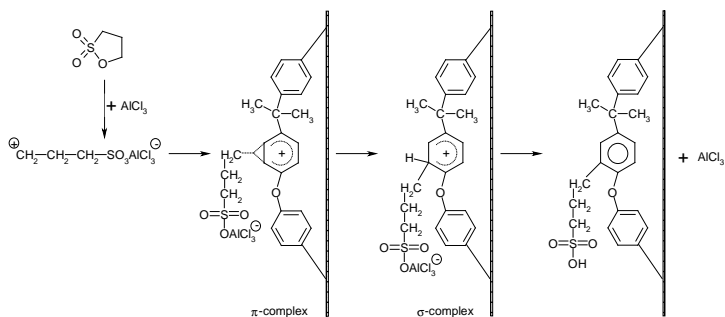


Fig. 2. The Friedel–Crafts electrophilic substitution of aromatic rings in polysulfone molecule

The results of membrane thickness measurements and deionized water fluxes of modified and unmodified membranes are presented in the Table 2 and Figs. 3 and 4.

Rate of reduction of water flux describes the equation 1:

$$R = 1 - \frac{\text{flux of modified membrane}}{\text{flux of unmodified membrane}} \quad (1)$$

Differences between water fluxes of modified and unmodified membranes can be observed. Bonding new functional group-CH₂-CH₂-CH₂SO₃⁻ via (1,3)-propane sultone on PSf membrane surface can be obtained. A hydrophilic sulfonate unit can be located to the polymer main chain having a joint segment of (-CH₂-)_n groups. The long side chains will contribute to enhanced mobility of -SO₃H moiety and decrease the pore size on the surface. These groups sterically hinder the water flux along the membrane surface, which can cause increased thickness of immobile water layer at the surface. Reduction of the water flux through the membrane can be observed at all reaction conditions after modification.

Table 2. Membrane thickness and deionized water flux trough the unmodified and modified PSf membranes

Reaction time, min	Catalyst mole ratio AlCl ₃ /(1,3) propane sultone	Thickness, μm		Deionized water flux, dm ³ /m ² h			
				at 0.4 MPa		at 0.6 MPa	
		Before reaction	After reaction	Before reaction	After reaction	Before reaction	After reaction
1	0.005	118	120	59.18	33.21	90.54	51.51
5		124	125	59.86	31.49	93.77	48.47
10		118	117	59.36	29.58	90.88	45.72
1	0.01	110	114	58.57	28.03	91.88	42.91
5		111	112	60.13	27.83	92.37	42.63
10		127	125	61.19	27.11	94.93	41.57
1	0.02	117	116	59.61	26.16	91.77	40.15
5		122	124	58.26	24.64	88.45	38.17
10		118	114	62.60	26.25	97.36	40.75

On the other hand we can observe the effect of the increased mole ratio of AlCl₃/(1,3) propane sultone on the water flux. AlCl₃ is known as the strongest catalyst for Friedel-Crafts reaction [19]. Increasing the mole ratio of catalyst causes vigorous reaction what could be effecting the morphology. Some experiments were made also with mole ratio of AlCl₃/(1,3)-propane sultone (1:1) and this caused defects

in the morphology of the membrane. Measurements of water fluxes through these membranes are not relevant. These experiments were made for SEM pictures to show the difference between the damaged and undamaged morphology of the membrane. SEM's of cross-section are shown in Figs. 5–8. The modified membranes show essentially no difference in morphology to the unmodified membranes. There is a possibility of slight degradation due to melting of the skin layer because of AlCl_3 catalyst as well as low concentration of catalyst. These could be well perceived in membrane cross-section in Fig. 5b, which represents the modification at catalyst mole ratio (1:1). Defects in morphology and also degradation of melting skin layer can be observed. SEM cross-sections were made at the highest catalyst mole ratio (0.02) of AlCl_3 /(1,3)-propane sultone.

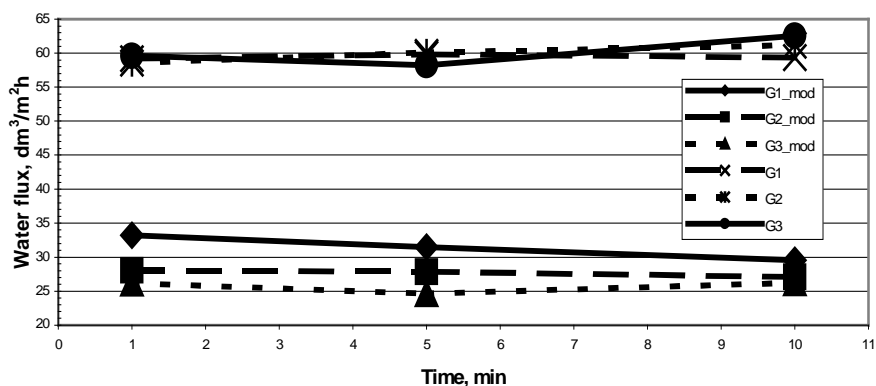


Fig. 3a. Water flux at 0.4 MPa for modified and unmodified membranes at different mole ratio of AlCl_3 /(1,3)-propane sultone (G1_Mod at 0.005:1 mole ratio, G2_Mod at 0.01:1 mole ratio and G3_Mod at 0.02:1 mole ratio; G1, G2 and G3 unmodified membranes)

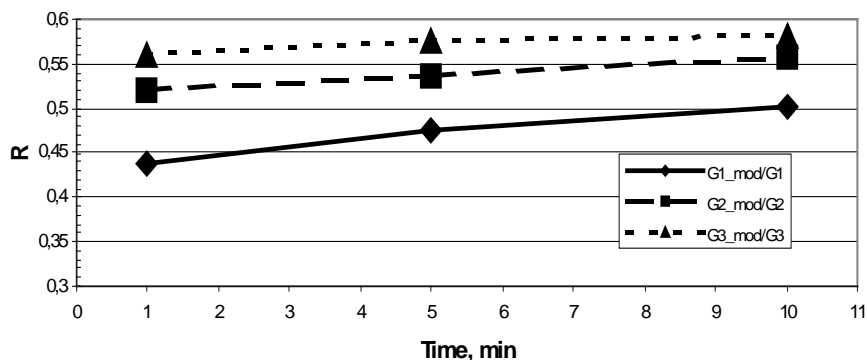


Fig. 3b. Rate of reduction of water flux at 0.4 MPa

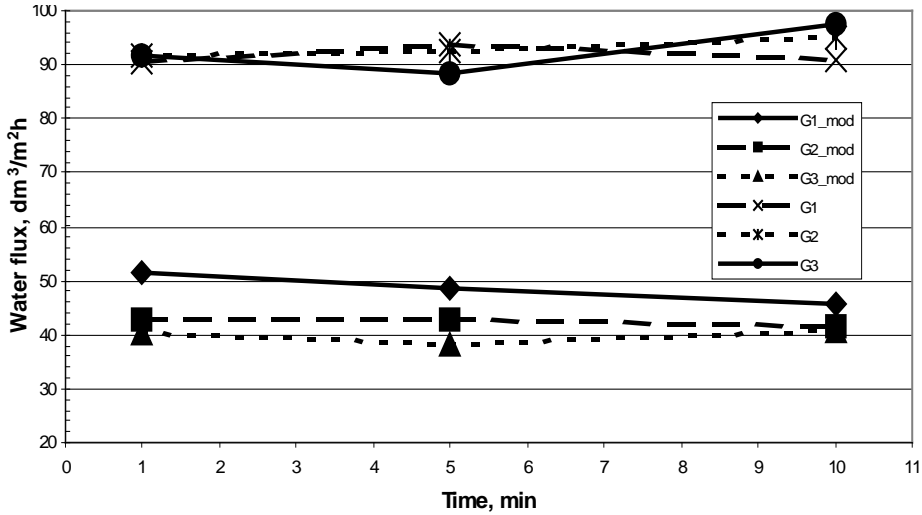


Fig. 4a. Water flux at 0.6 MPa for modified and unmodified membranes at different mole ratio of AlCl_3 /(1,3)-propane sultone (G1_Mod at 0.005:1 mole ratio, G2_Mod at 0.01:1 mole ratio and G3_Mod at 0.02:1 mole ratio; G1, G2 and G3 unmodified membranes)

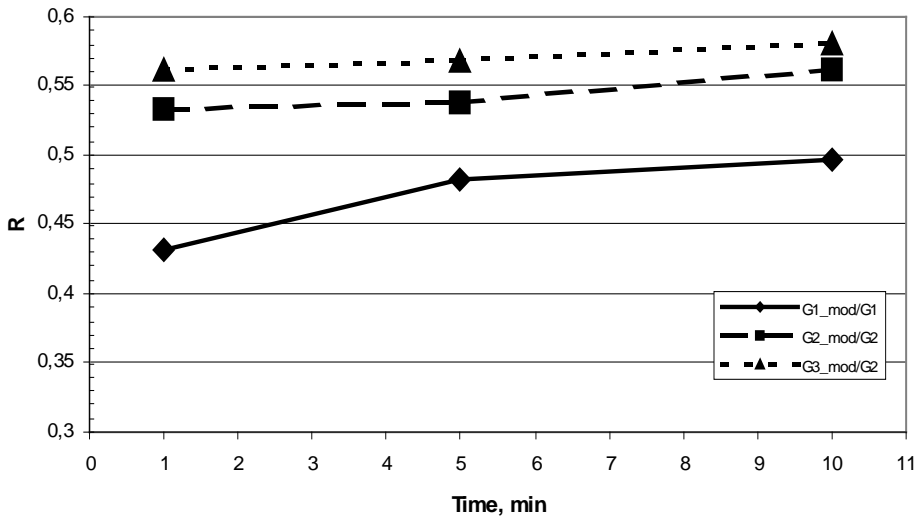


Fig. 4b. Rate of reduction of water flux at 0.6 MPa

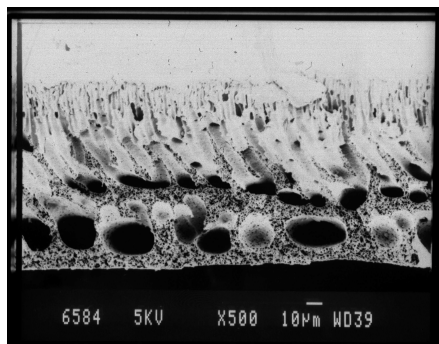


Fig. 5a. SEM micrograph of cross-section of PSf membrane

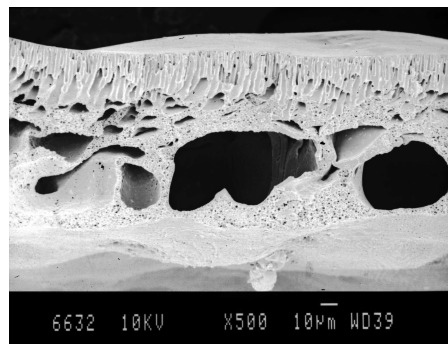


Fig. 5b. SEM micrograph of cross-section of PSf membrane modified with (1:1) mole ratio of catalyst

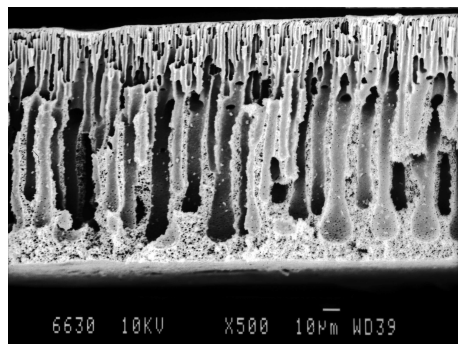


Fig. 6a. SEM micrograph of cross-section of PSf membrane modified for 1 minute

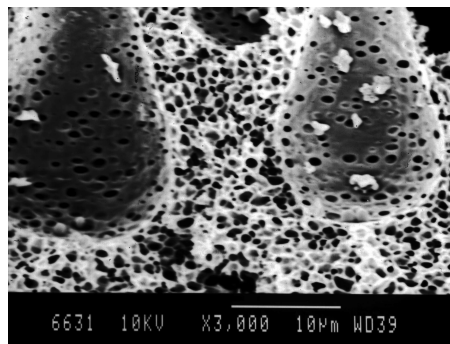


Fig. 6b. SEM micrograph of cross-section of macrovoids of PSf membrane modified for 1 minute

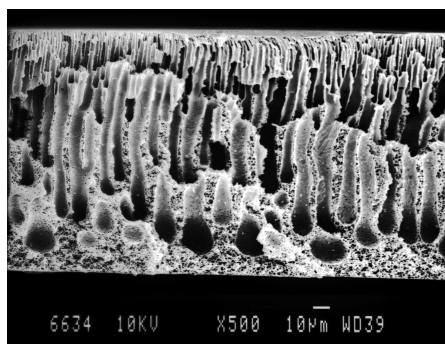


Fig. 7a. SEM micrograph of cross-section of PSf membrane modified for 5 minutes

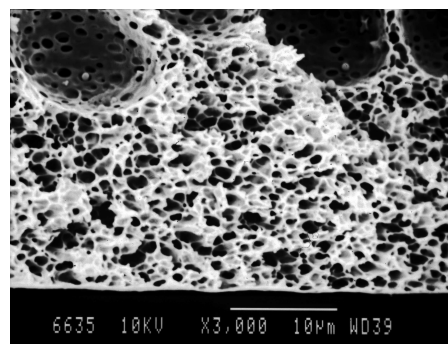


Fig. 7b. SEM micrograph of cross-section of macrovoids of PSf membrane modified for 5 minutes

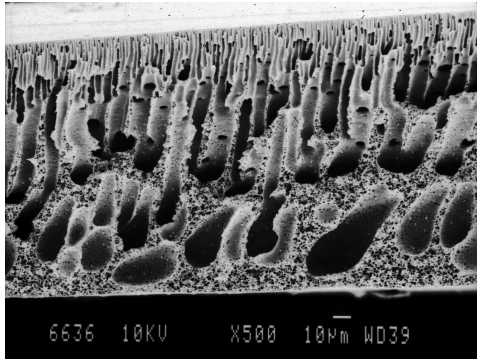


Fig. 8a. SEM micrograph of cross-section of PSf membrane modified for 10 minutes

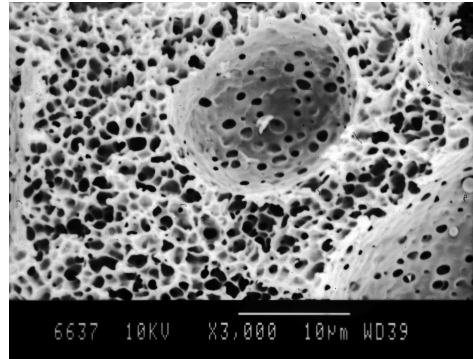


Fig. 8b. SEM micrograph of cross-section of macrovoids of PSf membrane modified for 10 minutes

Fig. 9 presents the main difference between unmodified and modified PSf membranes at reaction time 10 minutes and 0.02 mole ration of catalyast. In the FTIR/ATR spectrum a minimum intensity difference could be observed in area of aromatic rings [20] ($1590\text{--}1400\text{ cm}^{-1}$). The new peaks appeared at 1042 cm^{-1} and 1192 cm^{-1} in curve b) that is the asymmetric $S=O$ streching vibration. Identification of other $S=O$ peak at about 1240 cm^{-1} is difficult because of presence $S=O$ groups in unmodified PSf membrane.

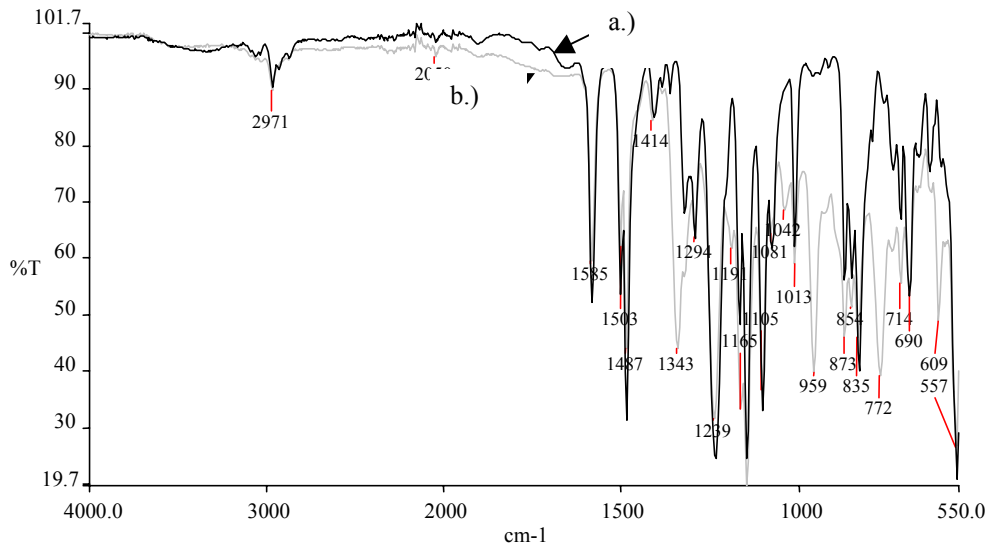


Fig. 9. FTIR/ATR spectra of a) PSf and b) modified PSf

Fig. 10 presents the difference according to different reaction time conditions at 0.02 mole ration of catalyast. Spectra show the different length of peaks according to reaction time what indicates the different quantity of product on the membrane surface. The above results suggest that the surface reaction occurred according to Fig. 2 under applied conditions of modification.

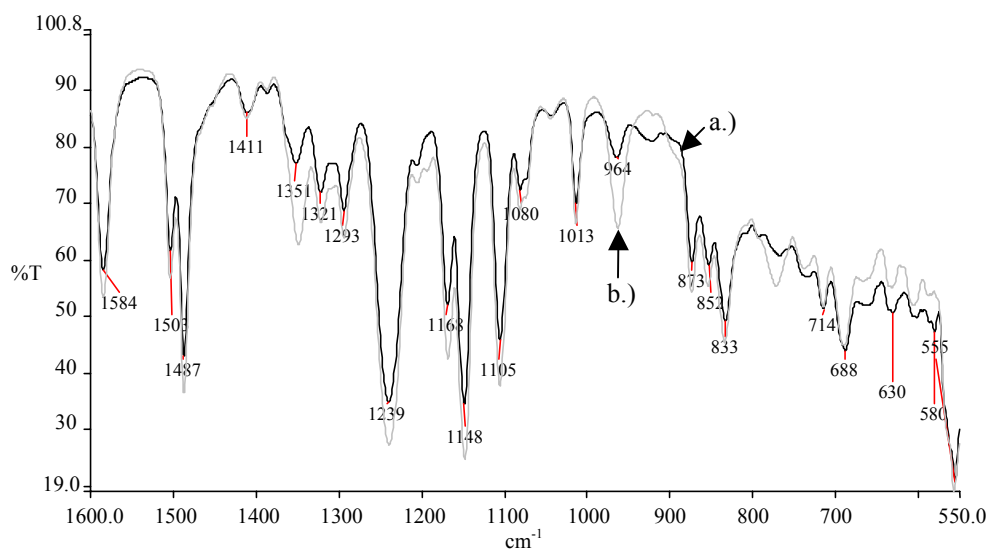


Fig. 10. FTIR/ATR spectra of a) PSf modified for 5 min and b) PSf modified for 10 min

REFERENCES

- [1] RIVATON A., GARDETTE J.L., *Photodegradation of polyethersulfone and polysulfone*, *Polymer Degradation and Stability*, 66, 1999, pp. 385–403.
- [2] Van de WITTE P., DIJKSTRA P.J., Van den BERG J.W.A., FEIJEN J., *Phase separation processes in polymer solutions in relation to membrane formation*, *J. Membrane Sci.*, 117, 1996, pp. 1–31.
- [3] STROPNIK Č., GERMIC L., ŽERJAL B., *Morphology variety and formation mechanisms of polymeric membranes prepared by wet phase inversion*, *J. Appl. Polym. Sci.*, 61, 1996, pp. 1821–1830.
- [4] BARHT C., GONCALVES M.C., PIRES A.T.N., ROEDER J., WOLF B.A., *Asymmetric polysulfone and polyethersulfone membranes: effects of thermodynamic conditions during formation on their performance*, *J. Membrane Sci.*, 169, 2000, pp. 287–299.
- [5] FEINS M., SIRKAR K.K., *Novel internally staged ultrafiltration for protein purification*, *J. Membrane Sci.*, 248, 2005, pp. 137–148.
- [6] ROPER D.K., LIGHTFOOT E.N., *Separation of biomolecules using adsorptive membranes*, *J. Chromatogr. A*, 702, 1995, pp. 3–26.
- [7] MOK S., WORSFOLD D.J., FOUDA A., MATSUURA T., *Surface modification of polyethersulfone hollow fiber membranes by γ -ray irradiation*, *J. Appl. Polym. Sci.*, 51, 1994, p. 193.

- [8] KIM K.J., FANE A.C., FELL C.J.D., JOY D.C., *Fouling mechanisms of membranes during protein ultrafiltration*, J. Membrane. Sci., 68, 1992, p. 79.
- [9] BAMFORD C.H., AL-LAMEE K.G., *Functionalization of polymers*. US Pat 5618887, April 1997.
- [10] PIERACCI J., CRIVELLO J.V., BELFORD G., *Photochemical modification of 10 kDA polyethersulfone ultrafiltration membrane for reduction of biofouling*, J. Membrane Sci., 156, 1999, pp. 223–240.
- [11] ULBRICHT M., RIEDEL M., *Ultrafiltration membrane surface with grafted polymer 'tentacles' preparation, characterization and application for covalent protein binding*, Biomaterials, 19, 1998, pp. 1229–1237.
- [12] LI J., ICHIZURO S., ASANO S., MUTOU F., IKEDA S., IIDA M., MIURA T., OSHIMA A., TABATA Y., WASHIO M., *Surface analysis of the proton exchange membranes prepared by pre-irradiation induced grafting of styrene/divinylbenzene into crosslinked thin PTFE membranes*, Appl. Surface Sci., 245, 2005, p. 260–272.
- [13] ULBRICHT M., BELFORD G., *Surface modification of ultrafiltration membranes by low temperature plasma. II Graft polymerization onto polyacrylonitrile and polysulfone*, J. Membrane Sci., 111, 1996, p. 193.
- [14] BELFORD G., ULBRICHT M., *Surface modification of ultrafiltration membranes by low temperature plasma. I. Treatment of polyacrylonitrile*, J. Appl. Polymer Sci., 56, 1995, p. 325.
- [15] SEIFER B., MIHANETZIS G., GROTH T., ALBRECHT W., RICHAU K., MISSIRLIS Y., PAUL D., VON SENGBUSCH G., *Polyetherimide: A New Membrane-Forming Polymer for Biomedical Application*, Artificial Organs, 26(2), 2002, pp. 189–199.
- [16] KUKOVIČIĆ I., ŠOSTER R., BRUMEN M., RIBITSCH V., WIEGEL D., ARNOLD K., STROPNIK Č., *Chemical modification and characterization of the surface of polysulfone membranes*, Acta Chim. Slov., 47, 2000, pp. 339–347.
- [17] HAMZA A., CHOWDHURY G., MATSUURA T., SOURIRAJAN S., *Sulphonated poly(2,6-dimethyl-1,4-phenylene oxide)-polyethersulphone composite membranes. Effects of composition of solvent system, used for preparing casting solution, on membrane-surface structure and reverse-osmosis performance*, J. Membrane. Sci., 129, 1997, pp. 55–64.
- [18] HIGUCHI A., IWATA N., TSUBAKI M., NAKAGAWA T., *Surface-modified polysulfone hollow fibers*, J. Appl. Polym. Sci., 36, 1988, pp. 1753–1767.
- [19] OLAH G.A., *Friedel–crafts alkylation chemistry*, John Wiley & Sons, New York, 1984.
- [20] SOCRATES G., *Infrared characteristic group frequencies*, John Wiley & Sons, Inc., New York, 1994.

*Keywords: diffusion coefficient, input non-perfect step,
evaluation correction*

JIRINA CERMAKOVA*, KATERINA FIALOVA*,
ROMAN PETRYCHKOVYCH*, VLADIMIR KUDRNA*,
PETR UCHYTEL*

EFFECT OF INPUT NON-PERFECT STEP CONCENTRATION FUNCTION ON DIFFUSION COEFFICIENT EVALUATION

Diffusion coefficients of vapour permeating through polymer membranes were evaluated from dynamic permeation experiments. The measurements were made in an apparatus, which was divided by membrane into two parts - upstream and downstream sides. The input step function of concentration in upstream side is usually supposed for the diffusion coefficients evaluation by the solution of the Fick's second law. But in real system the input concentration function often differs from the step function. This work deals with the description of the input concentration and its influence on the evaluated diffusion coefficients. The mathematical model was developed, where the non-perfect step input concentration function was included in the description of the transport through a polymer. The influences of the upstream volume and the flow rate of permeating vapours on errors of the diffusion coefficient evaluation were discussed.

1. INTRODUCTION

The transport of gases or vapours through a polymeric membrane can be described by Fick's law in an ideal case, e.g. in non-swelling system of a membrane and a permeate. The solution of Fick's second law which is widely used in papers dealing with the vapour transport in polymeric membranes was derived on the basis of simplifications of the experimental arrangement i.e. the input step concentration function and zero output concentration. But for some experimental arrangements the reality is far away from these assumptions and the evaluation models need modification. Morliere et al. [1] authors deal with problem of the non-perfect pressure step function and the time lag method of diffusion experiment evaluation.

* Institute of Chemical Process Fundamentals, Academy of Sciences of the Czech Republic, 165 02 Prague. E-mail: cermakovaj@icpf.cas.cz

Corrected diffusion coefficient in the case of non-perfect step was 2.5 times higher than with the assumption of the perfect step function.

We measured in contrast to paper [1] not the pressure but the concentration of a permeant in the upstream side membrane by chromatographic method. The input function was realized by a change of the input stream to the cell. In the real state the volume of the cell and its design intensely affect the shape of the input concentration function to the membrane, because of the non-immediately renewal volume in the upstream parts of the cell. The non-perfect step input concentration in upstream part of a membrane has to be then taken into account for the diffusion coefficient evaluation. The results of our study enable to estimate the magnitude of the diffusion coefficient evaluation errors in the dependence on experimental arrangements.

2. EXPERIMENTAL

Dynamic permeation experiments were carried out in a diffusion cell which is depicted in the Fig. 1. The cell consists of two parts – upstream and downstream sides divided by a polymeric membrane (low-density polyethylene (LLDPE)). The diameter of a circular membrane sample was 24 mm. As a permeate vapours of propan-1-ol were used. The cell was placed in thermostat and the streams of vapours (inputs, outputs) were conducted by tubes with inner diameter of 2 mm.

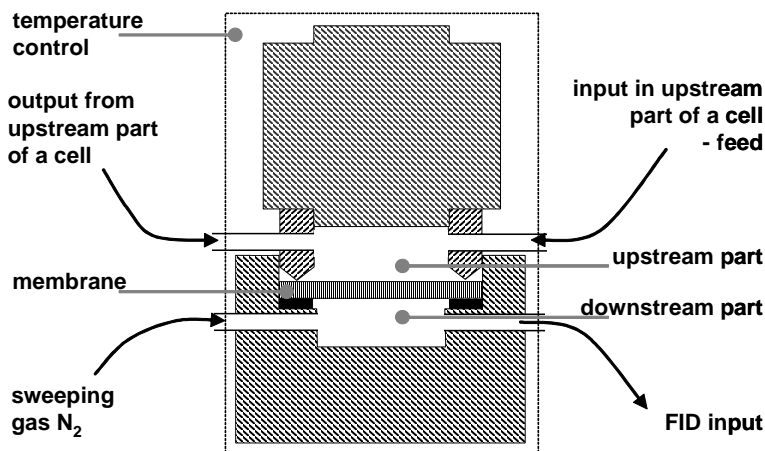


Fig. 1. Diffusion apparatus for measurement of steady state permeation process

The vapours of demanded concentrations were prepared by nitrogen percolation through the liquid permeant and by dilution with nitrogen. The gas mixture was fed to the upstream part and flowing along the membrane surface. At the start of the experi-

ment the concentration was changed by the substitution of the input stream of pure nitrogen to the upstream part by the stream of the permeant vapours.

Another side of the membrane was wash-out by pure nitrogen to a continual chromatographic detection. The flow rates in the upstream and the downstream parts were maintained constant. The driving force of the process could be only the chemical potential gradient.

The input concentration function was experimentally obtained by a blind measurement, where the membrane was replaced by the perforated aluminium foil. The negligible resistance to the diffusion through pores in the aluminium foil is assumed in comparison with the diffusion in the polymeric membrane. To specify the effect of the volume of the upstream part and the gas flow rate a series of experiments were performed. The two volumes were used (1 cm^3 and 21 cm^3) and the gas flow rate was in range $24\text{--}200 \text{ cm}^3/\text{min}$.

How the downstream side volume of the permeation cell contributes to the overall dilution effect was separately investigated in another experiments in which drop of volatile liquid (pentane) was put directly on the upstream side of the aluminium foil perforation. In this case the response of FID was immediate and practically rectangular. It means that the effect of the downstream side volume of permeation apparatus on the value of the calculated diffusion coefficient is negligible in comparison with the upstream one. The flow in this part is practically piston.

3. THEORY

Permeation of vapours (vapour permeation) and liquids (pervaporation) through a non-porous polymeric films is driven by the chemical potential gradient across a membrane. The sorption-diffusion model is generally used for the description of the mass transport through polymeric membranes. This model supposes three steps of the transport: the sorption of molecules of vapours or liquids at the upstream membrane surface, the diffusion of the permeants through the membrane and the desorption of the permeated species in the vapour form at the downstream membrane side. The diffusion through the dense polymeric membrane is considered as the rate limiting step of the process.

Analysis of the experimental data is based on the solution of the Fick's second law (equation. (1)). The experimental arrangement is represented by boundary and initial conditions.

$$\frac{\partial c}{\partial t} = D \frac{\partial^2 c}{\partial x^2} \quad (0 < x < l, t > 0), \quad (1)$$

$$c = c_1, \quad \text{when } x = 0, \quad (2)$$

$$c = c_2, \quad \text{when } x = l, \quad (3)$$

$$c = 0, \quad \text{when } t = 0 \quad (4)$$

where c is concentration of a permeant in a polymer of thickness l in the distance x at time t . D is diffusion coefficient. The surfaces of a membrane ($x = 0$ and $x = l$) are maintained at constant concentration c_1 , c_2 . The thickness l has to be negligible compared to the other dimensions of membrane. The solution of the unsteady dimensionless flow under condition of the step input concentration and neglecting retardation and/or immobilisation of the permeating molecules is described by Crank [2]:

$$\frac{J}{J_{\max}} = 1 + 2 \sum_{n=1}^{\infty} (-1)^n \exp(-D_s n^2 \pi^2 t / l^2). \quad (5)$$

The solution of the Fick's second law with a concentration independent diffusion coefficient D_s is fitted to the dimensionless flux (the ratio of the flux of permeate $J(t)$ at time t to its steady state flux J_{\max} (infinite t)) versus the time dependence. This solution of equation (1) supposes the shape input function not far from the step signal. We tested experimentally the acceptability of this simplification. When the input function is far from the type of the step function, the necessity of a evaluation correction takes place. In this case we changed one boundary condition to the following form:

$$c = c_1 \varphi(t), \quad \text{when } x = 0, \quad (1)$$

$$\varphi(t)_{t \rightarrow \infty} = 1 \quad \varphi(t) \in \langle 0, 1 \rangle \quad (2)$$

where $\varphi(t)$ is the dimensionless function of time and c_1 is a concentration constant. Taking into account solution of the modified case in the book written by Carslaw and Jaeger [3] (equation (1)), after rearrangement we obtained:

$$\frac{J}{J_{\max}} = -\frac{2D_{ns}\pi^2}{l^2} \int_{\lambda=0}^t \varphi(\lambda) \sum_{n=1}^{\infty} n^2 (-1)^n \exp(D_{ns} n^2 \pi^2 (\lambda - t) / l^2) d\lambda \quad (3)$$

where: D_{ns} is the corrected diffusion coefficient for the non-perfect step input function, λ is the integration variable time from 0 to t . The input function can be modelled [4] on the base of a hydromechanical behaviour in the upstream cell part or the experimentally obtained input function may be directly substituted to equation (8). The relation (8) implies the dependence of the correction on the ratio of D/l^2 and a mean residence time of a gas in the upstream cell part, which is represented by the ratio of the volume and the flow rate.

4. RESULTLS AND DISCUSSION

Theoretical simulations and experimental verifications were made to quantify the influence of non-perfect input function.

The diffusion coefficient D_s , D_{ns} were obtained by minimization of the difference between the experimental response and calculated curves from equations (5) and (8). D_s represents the situation with the ideal step input concentration function and D_{ns} is more reliable diffusion coefficient from the modified evaluation equation (8) with the non-step input function. Examples of the different experimental arrangements are shown in Figs. 2 and 3. When the mean residence time in the upstream part is higher, the use of equation (5) caused the underestimation of the diffusion coefficient value. The difference in mean residence time equal to 26 s between experiments in Figs. 2 and 3 caused underestimate 20.6%. With respect to the diffusion transport, the errors increase also with increasing value D/l^2 .

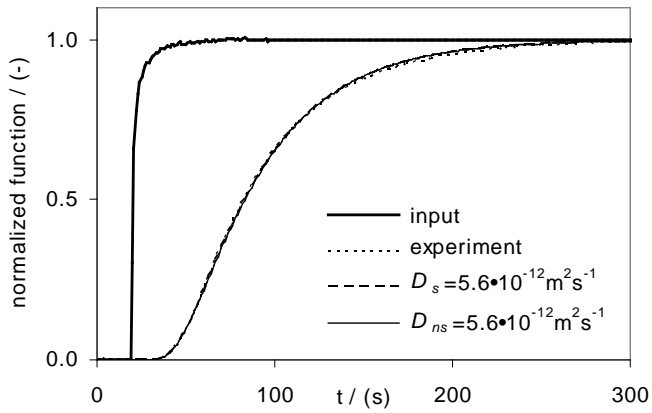


Fig. 2. Effect of input function on the diffusion coefficient if the mean residence time is negligible ($V/Q = 1.34 \text{ s}$, $V = 1 \text{ cm}^3$, $Q = 44.8 \text{ cm}^3/\text{min}$, $l = 50 \text{ }\mu\text{m}$)

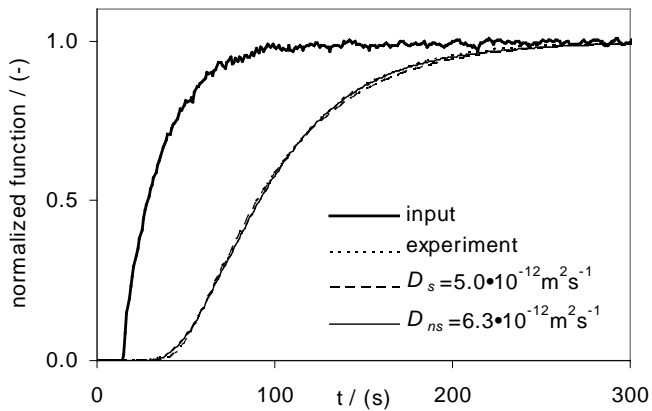


Fig. 3. Effect of input function on the diffusion coefficient if the mean residence time is not negligible ($V/Q = 27.4 \text{ s}$, $V = 21 \text{ cm}^3$, $Q = 46 \text{ cm}^3/\text{min}$, $l = 50 \text{ }\mu\text{m}$)

5. CONCLUSIONS

The experimental realization of the ideal step input function or the experimental determination of the input concentration function could be sometimes very difficult. The use of the assumption of the ideal step input concentration for the high mean residence time in the upstream part of the permeation cell leads to the underestimation of the diffusion coefficients. Presented model, which takes in the account the input step concentration function, enables to evaluate the correct diffusion coefficients and to estimate the error of the evaluation of diffusion coefficients with the step input function. In this case the proposed model could be used to design the measurement arrangement and to choose appropriate conditions.

REFERENCES

- [1] MORLIERE N., CORRIOU J.P., FAVRE E., ROIZARD D., *Characterization of film transport properties for organic vapours using the time-lag method – interest and limitations*, Desalination, 144, 2002, pp. 109–113.
- [2] CRANK J., *The Mathematics of Diffusion*, Clarendon Press, Oxford, 1975.
- [3] CARSLAW H.S., JAEGER J.C., *Conduction of Heat in Solids*, Clarendon press, Oxford, 1959.
- [4] KUDRNA V., JAHODA M., SIYAKATSHANA N., ČERMÁKOVÁ J. MACHOŇ V., *General Solution of the Dispersion Model for a One Dimensional Stirred Flow System Using Danckwerts' Boundary Conditions*, Chem.Eng. Sci., 59, 2004, pp. 3013–3020.

*Keywords: computer modelling, Monte Carlo simulation,
ion beam irradiation, fluoropolymer membranes,
SRIM/TRIM program*

ZOLTAN A. FEKETE*, EUGENE WILUSZ**,
FRANK E. KARASZ***, CSABA VISY*

ION BEAM IRRADIATION OF FLUOROPOLYMERS FOR PREPARING NEW MEMBRANE MATERIALS – A THEORETICAL STUDY

In determining the permselectivity of dense membranes, the surface and subsurface layer at the interface play a crucial role. This outer few micrometer region can be manipulated by medium energy (up to a few hundred keV) ion beam irradiation in a controlled way to modify permeation properties – similarly to the traditional polymer engineering method for integral skin preparation – as it has been demonstrated in our previous work on ionomer membranes. The technique is also well suited for preparing modified surface layers on conjugated polymers. A systematic mathematical modelling approach to describing the process was developed. Building upon previous work on the perfluorinated ionomer Nafion[®] dense membranes, theoretical investigations on other fluorinated membrane materials such as PTFE and PVDF have been continued.

1. INTRODUCTION

Fluoropolymers, e.g. polytetrafluoroethylene (PTFE) and polyvinylidenedifluoride (PVDF), are traditionally used for making porous membranes with high chemical and thermal stability. It is well known that even low energy ion beam impact may drastically alter the surface of polymers [1]–[6], and medium energy irradiation modifies the sub-surface layer down to tens of microns [7]–[9] (i.e., comparable to the skin depth of asymmetric polymer membranes). Given that diffusibility and permeability of polymers can be modified by ion beam treatment [7], [10]–[16], this technique is

* Department of Physical Chemistry, University of Szeged, POB Szeged, H-6701 Hungary.

** U.S. Army Natick Soldier Center, Natick, MA 01760 USA.

*** Department of Polymer Science and Engineering, University of Massachusetts, Amherst, MA 01003 USA.

a promising tool to control the gas-solid interface, which is crucial in determining permeation behavior [17].

During ion implantation a beam of positive ions, typically with energies between 20–200 keV, is used to uniformly bombard the target polymer. This causes the projectile ions to be trapped in the substrate and the target to undergo structural changes due to the large amount of energy taken up from the penetrating ions [7], [18].

The use of Monte Carlo simulation to model the effect of ion implantation into various polymers (such as polyethylene, polypropylene, polytetrafluoroethylene and polyamide) has been demonstrated in the literature [19]–[21]. The main purpose of these calculations was to estimate the penetration depths. The results from applying the simulation implemented in the SRIM/TRIM program [22]–[24] showed near-quantitative agreement with implant profiles measured by the Rutherford back-scattering technique [19]–[21].

A comprehensive quantum mechanical based treatment of ion–atom collisions is implemented in the SRIM/TRIM program (Stopping / Transport and Range of Ions in Matter) [22]–[25]. In this contribution it has been applied to understand the effect of selected ion beam implantations into polytetrafluoroethylene (PTFE) or polyvinylidenedifluoride (PVDF) membrane materials. The calculations have been augmented by statistical analysis of the damage distribution, thus allowing an assessment of the dependence of surface layer changes on the implantation parameters. The target material forms considered include dense isotropic membranes, as well as simplified models for porous media.

2. TARGET MATERIALS

2.1. POLYTETRAFLUOROETHYLENE (PTFE)

Polytetrafluoroethylene (PTFE) is the simplest fluoropolymer:



that is often used as a hydrophobic membrane material, and is a common ion irradiation target material as well. Its density used in the calculations is 2.20 g/cm³.

2.2. POLYVINYLIDENEDIFLUORIDE (PVDF)

Another traditional hydrophobic membrane material, used both in micro- and ultrafiltration applications, is polyvinylidenedifluoride (PVDF):



Its density used in the calculations is 1.70 g/cm³.

3. CALCULATION

For dense membranes, details of applied methodology have been reported earlier [9]. Briefly, penetration of projectile ions as well as the full recoil cascades are calculated by the TRIM module of the SRIM program package [22], [23], [25] (version 2003.26). At each combination of projectile ion and energy investigated, statistical analysis is carried out from the raw results on both the implant ion and so-called vacancy (*i.e.* collisional damage) positions, to determine the moments of depth distributions [22], [23], [26]. The first moment is conventionally called (longitudinal) range (R_p) for the implanted ions, and we have analogously defined the range for collisional damage (R_d) [9].

The projectile ions chosen for these studies are the noble gases He through Rn. This covers the atomic number range 2–86. Fitting over our results allows to predict range data for arbitrary ions from the entire periodic table.

In order to summarize all the results from the different ions, converting to dimensionless units based on the Ziegler-Biersack-Littmark formalism [22], [23] is performed. This utilizes scaling with the characteristic energy E_c and length R_c , defined according to equations 1–3:

$$a_s = 0.8853 a_B / (Z_1^{0.23} + Z_2^{0.23}), \quad (1)$$

$$E_c = Z_1 Z_2 e^2 (M_1 + M_2) / M_2 4\pi \varepsilon_0 a_s, \quad (2)$$

$$R_c = (M_1 + M_2)^2 / M_1 M_2 N_d 4\pi a_s^2 \quad (3)$$

where a_s is the Ziegler-Biersack-Littmark screening length, $a_B = 0.529 \text{ \AA}$ is the Bohr radius, Z_1 and Z_2 are the atomic numbers of the incident ion and target atom, respectively, M_1 and M_2 are their atomic masses, $e = 1.6 \cdot 10^{-19} \text{ C}$ is the electron's charge, $\varepsilon_0 = 8.85 \cdot 10^{-12} \text{ C}^2/\text{N m}^2$ is the permittivity of vacuum, and N_d is the number density of the target.

For porous membranes, two methods to approximately describe porous media are used. The cruder approach simply uses an isotropically “diluted” target material, *i.e.* one with proportionally decreased density corresponding to the porosity. We are also developing a novel methodology that transforms the problem of random fibrous medium into one with a random stratified structure. Hopefully this model preserves the simplicity of planar layer target description utilized in SRIM/TRIM, while at the same time statistically describes the gross effects of the ion beam impact on the stochastically arranged membrane medium. The fibrous structure modeling is controlled by a preprocessing script, which takes as input the fibre diameter and medium porosity. From this the average separation for material contained in cylindrical shapes is determined. Then pathlengths of beams, arriving from random directions, are calculated both within and between the fibers. These are input as layer thickness and interlayer distances, respectively, for the SRIM/TRIM simulation.

Job control, which involves queuing multiple SRIM/TRIM runs over sets of input data prepared, as well as evaluating and summarizing raw output, is handled by in-house developed scripts that we release to the public domain [27].

4. RESULTS AND DISCUSSION

Fig. 1 displays the logarithms of scaled ranges for implant ions ($\lg(R_p/R_c)$), versus the logarithm of scaled energy ($\lg(E/E_c)$), with the PTFE and PVDF data plotted together. It can be seen that all results (combined for both target materials) fall on a linear master curve, when expressed in this scaled form. The logarithms of scaled ranges for collisional damage ($\lg(R_d/R_c)$) in PVDF, versus the logarithm of scaled energy ($\lg(E/E_c)$), are presented in Fig. 2.

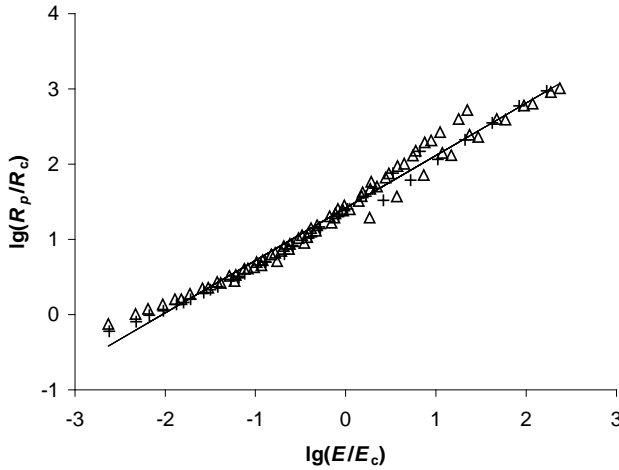


Fig. 1. Scaled ranges for implantation in PTFE (triangles) and PVDF (crosses)

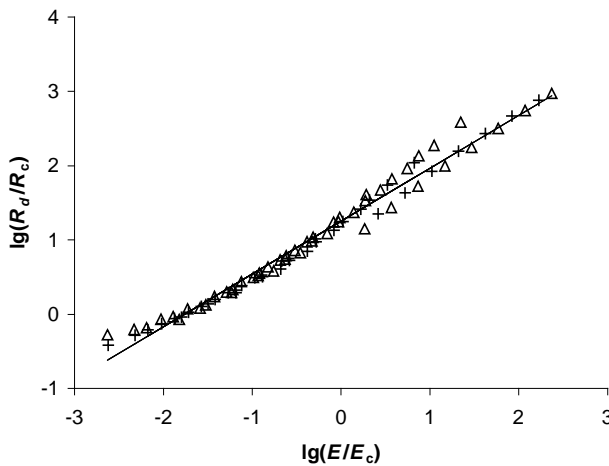


Fig. 2. Scaled ranges for collisional damage in PTFE (triangles) and PVDF (crosses)

Double logarithmic fits of the scaled ranges, equations 4–5 below (where the standard errors of the fitted slope and intercept are also shown in parentheses), show good linearity as indicated by their regression coefficient r near unity:

$$\lg(R_p/R_c) = (0.698 \pm 0.009) \lg(E/E_c) + (1.418 \pm 0.011), r = 0.990, \quad (4)$$

$$\lg(R_d/R_c) = (0.712 \pm 0.011) \lg(E/E_c) + (1.253 \pm 0.013), r = 0.991. \quad (5)$$

These equations allow calculating what R_p and R_d values would be yielded by a SRIM/TRIM calculation on a polymer, provided that the dimensionless energy falls in the covered range 0.002–236. Ranges for projectile ions with arbitrary Z_1 , M_1 can be calculated, aiding a rational design of ion irradiation experiments.

Finally, for the rarified material modeling some preliminary data are shown in Fig. 3. Here again it is seen that the close master curve for the whole dataset is promising for an overall fit to be effective.

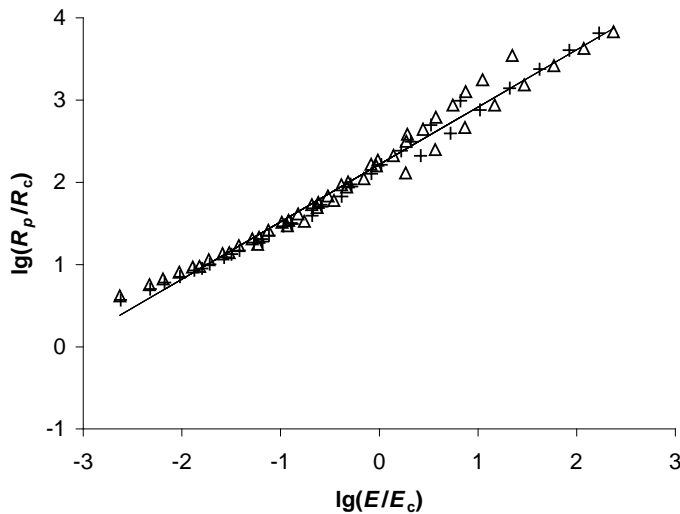


Fig. 3. Approximate scaled ranges for implantation in 85% porosity material: PTFE (triangles) and PVDF (crosses)

ACKNOWLEDGEMENTS

The authors of this paper thank Dr. Thomas J. Tate for assistance with setting up the TRIM simulations, and acknowledge funding by Army Research Grant DAAD 16-01-P-0389. FEK is also partially supported by the Air Force Office of Scientific Research, and ZAF by the Hungarian Scientific Research Fund (OTKA grant no. T 032190 and T 042539).

REFERENCES

- [1] EVERETT M.L., HOFUND G.B., *Chemical Alteration of Poly(Tetrafluoroethylene) Teflon Induced by Exposure to Vacuum Ultraviolet Radiation and Comparison with Exposure to Hyperthermal Atomic Oxygen*, Journal of Polymer Science Part a-Polymer Chemistry, 43, 2005, p. 552.
- [2] HOFUND G.B., EVERETT M.L., *Chemical Alteration of Poly(Vinyl Fluoride) Tedlar by Hyperthermal Atomic Oxygen*, Applied Surface Science, 239, 2005, p. 367.
- [3] BRYJAK M., POZNIAK G., GANCARZ I., TYLUS W., *Microwave Plasma in Preparation of New Membranes*, Desalination, 163, 2004, p. 231.
- [4] BRYJAK M., GANCARZ I., POZNIAK G., *Plasma-Modified Porous Membranes*, Chemical Papers-Chemicke Zvesti, 54, 2000, p. 496.
- [5] BRYJAK M., GANCARZ I., *Plasma Treatment of Polyethylene Ultrafiltration Membranes*, Angewandte Makromolekulare Chemie, 219, 1994, p. 117.
- [6] HAN S., CHOI W.K., YOON K.H., KOH S.K., *Surface Reaction on Polyvinylidene fluoride (Pvdf) Irradiated by Low Energy Ion Beam in Reactive Gas Environment*, Journal of Applied Polymer Science, 72, 1999, p. 41.
- [7] KORUGIC-KARASZ L.S., HOFFMANN E.A., *Polymer Ion Implantation: Present and Future Prospects*, Nonlin. Opt. Quant. Opt., 32, 2004, p. 135.
- [8] WILUSZ E., ZUKAS W., FEKETE Z.A., KARASZ F.E., *Ion Beam Modification of Permselective Membranes for Chemical Biological Protective Clothing*, Polymer Preprints Polymer Preprints (American Chemical Society, Division of Polymer Chemistry), 45, 2004, p. 7.
- [9] FEKETE Z.A., WILUSZ E., KARASZ F.E., *Modeling of Displacement Damage in an Ion-Beam-Modified Perfluorosulfonate Ionomer*, Journal of Polymer Science Part B-Polymer Physics, 42, 2004, p. 1343.
- [10] DAVENAS J., XU X.L., *Diffusion of Iodine into Polyimide Films Modified by Ion-Bombardment*, Nuclear Instruments & Methods in Physics Research, Section B: Beam Interactions with Materials and Atoms, B 71, 1992, p. 33.
- [11] XU X.L., COLEMAN M.R., MYLER U., SIMPSON P.J., *Postsynthesis Method for Development of Membranes Using Ion Beam Irradiation of Polyimide Thin Films*, ACS Symposium Series, 744, 2000, p. 205.
- [12] XU X.L., DOLVECK J.Y., BOITEUX G., ESCOUBES M., MONCHANIN M., DUPIN J.P., DAVENAS J., *Ion-Beam Irradiation Effect on Gas Permeation Properties of Polyimide Films*, Journal of Applied Polymer Science, 55, 1995, p. 99.
- [13] XU X.L., COLEMAN M.R., MYLER U., SIMPSON P.J., *Ion Beam Irradiation-an Efficient Method to Modify the Subnanometer Scale Microstructure of Polymers in a Controlled Way*, Materials Research Society Symposia Proceedings, 540, 1999, p. 255.
- [14] SVORCIK V., PROSKOVA K., RYBKA V., HNATOWICZ V., *Water Diffusion in Polyethylene Modified by Ion Irradiation*, Polymer Degradation and Stability, 60, 1998, p. 431.
- [15] WILUSZ E., FEKETE A.Z., KARASZ F.E., *Permeability of Ion Beam Treated Nafion*, in press, 2003.
- [16] ESCOUBES M., DOLVECK J.Y., DAVENAS J., XU X.L., BOITEUX G., *Ion Beam Modification of Polyimide Membranes for Gas Permeation*, Nuclear Instruments & Methods in Physics Research, Section B: Beam Interactions with Materials and Atoms, 105, 1995, p. 130.
- [17] ROBESON L.M., BURGGOYNE W.F., LANGSAM M., SAVOCA A.C., TIEN C.F., *High-Performance Polymers for Membrane Separation*, Polymer, 35, 1994, p. 4970.
- [18] LEE E.H., LEWIS M.B., BLAU P.J., MANSUR L.K., *Improved Surface-Properties of Polymer Materials by Multiple Ion-Beam Treatment*, Journal of Materials Research, 6, 1991, p. 610.
- [19] SVORCIK V., RYBKA V., MICEK I., POPOK V., JANKOVSKIJ O., HNATOWICZ V., KVITEK J., *Structure and Properties of Polymers Modified by Ion- Implantation*, European Polymer Journal, 30, 1994, p. 1411.

-
- [20] HNATOWICZ V., HAVRANEK V., KVITEK J., PERINA V., SVORCIK V., RYBKA V., *Modifications of Polypropylene Induced by the Implantation of Iodine Ions*, Japanese Journal of Applied Physics, Part I: Regular Papers and Short Notes, 32, 1993, p. 1810.
- [21] HNATOWICZ V., KVITEK J., SVORCIK V., RYBKA V., *Oxygen Incorporation in Polyethylene and Polypropylene Implanted with F⁺, as⁺ and I⁺ Ions at High-Dose*, Applied Physics A: Solids and Surfaces, 58, 1994, p. 349.
- [22] ZIEGLER J.F., BIRSACK J.P., LITTMARK U., *The Stopping and Range of Ions in Solids*, Pergamon Press, New York, 1985.
- [23] ZIEGLER J.F., Srim-2003, *Nuclear Instruments & Methods in Physics Research Section B-Beam Interactions with Materials and Atoms*, 219–20, 2004, p. 1027.
- [24] ZIEGLER J.F., MANOYAN J.M., *The Stopping of Ions in Compounds*, Nuclear Instruments & Methods in Physics Research, Section B: Beam Interactions with Materials and Atoms, B35, 1988, p. 215.
- [25] ZIEGLER J.F., BIRSACK J.P., *Srim/Trim: Stopping/Transport and Range of Ions in Matter, Version 2003.26; Pc-Compatible Program*, 2003. Available via <http://www.srim.org/>
- [26] BURENKOV A.F., KOMAROV F.F., KUMAKHOV M.A., TEMKIN M.M., *Tables of Ion Implantation Spatial Distributions*, Gordon and Breach, New York, 1986.
- [27] FEKETE Z.A., *Srim-Scripts: Scripts for Driving and Evaluating Ion Implantation Simulations by Ziegler's Srim/Trim Software*, 2005. Available via http://www.staff.u-szeged.hu/~fekete/srim_trim-scripts/

*Keywords: Monte Carlo simulation, computer modeling,
polymers, ion beam irradiation, SRIM/TRIM
program*

ZOLTAN A. FEKETE*, EUGENE WILUSZ**,
FRANK E. KARASZ***

INTEGRALLY SKINNED BARRIER LAYER PREPARATION BY ION BEAM IRRADIATION OF IONOMERS

Irradiation by medium energy ion beams is found to be useful for controlling permselectivity, by modifying the sub-surface layer down to tens of microns. The method can also be useful for preparing membranes of varied selectivity, useful e.g. as sensor elements. Our theoretical investigation based on Monte Carlo simulations is presented, with a detailed statistical analysis of the implantation and damage distributions. The systematic mathematical modeling approach yields a simple equation to quantitatively predict implantation and damage depths in any given polymer, for any ions with arbitrarily chosen atomic number and energy. This provides a theoretical tool for rational design of irradiation parameters. The results presented here cover the perfluorinated hydrophilic ionomer Nafion, as well as the simple hydrophobic membrane material Teflon. Both sets of data fit together in the general mathematical model developed, which gives confidence for extending it to describe other materials too.

1. INTRODUCTION

Ion implantation into polymer membranes [1]–[3] is a novel technique for developing barrier layers selectively permeable for water and other vapors. It is well known that even low energy ion beam impact may drastically alter the surface of polymers [4]–[9], and medium energy irradiation modifies the sub-surface layer down to tens of microns [1]–[3] (i.e. comparable to the skin depth of asymmetric polymer membranes). Since the gas-solid interface is crucial in determining permeation behavior [10], the technique modifying the sub-surface layer is well-suited for its control. There is experimental evidence that ion beam treatment of polymers profoundly alters

* Department of Physical Chemistry, University of Szeged, POB 105 Szeged, H-6701 Hungary.

** U.S. Army Natick Soldier Center, Natick, MA 01760 USA.

*** Department of Polymer Science and Engineering, University of Massachusetts, Amherst, MA 01003 USA.

diffusibility and permeability [11]–[17]. Surface irradiation has been used to treat, primarily, hydrocarbon-based polymers [18]–[21]. Little is known, however, about the ion implantation of more complex fluorinated polymers [22]–[24] such as the hydrophilic ionomer Nafion[®]. The latter is an ion exchange polymer widely used in fuel cells as an electrolyte membrane because of its proton transport capability and chemical inertness [25]–[27]. Ion implantation can further modify these properties by developing barrier layers selectively permeable to water or other vapors.

During ion implantation a beam of positive ions, typically with energies between 20–200 keV, is used to uniformly bombard the target polymer. This causes the projectile ions to be trapped in the substrate and the target to undergo structural changes due to the large amount of energy taken up from the penetrating ions [1], [28].

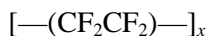
The use of Monte Carlo simulation to model the effect of ion implantation into various polymers (such as polyethylene, polypropylene, polytetrafluoroethylene and polyamide) has been demonstrated in the literature [19], [29], [30]. The main purpose of these calculations was to estimate the penetration depths. The results from applying the simulation implemented in the SRIM/TRIM program [31]–[33] showed near-quantitative agreement with implant profiles measured by the Rutherford back-scattering technique [19], [29], [30].

A comprehensive quantum mechanical based treatment of ion–atom collisions is implemented in the SRIM/TRIM program (Stopping / Transport and Range of Ions in Matter) [31]–[34]. In this contribution it has been applied to understand the effect of selected ion beam implantations of Nafion[®]. The calculations have been extended by statistical analysis of the damage distribution, thus allowing an assessment of the dependence of surface layer changes on the implantation parameters.

2. TARGET MATERIALS

2.1. POLYTETRAFLUOROETHYLENE

Polytetrafluoroethylene (PTFE) is the simplest fluoropolymer:



often used as a hydrophobic membrane material, and is a common ion irradiation target material as well. Its density used in the calculations is 2.20 g/cm³.

2.2. NAFION[®]

Nafion[®] (E. I. Du Pont de Nemours) is a perfluorosulfonic-acid type ionomer mainly used as a proton exchange membrane in fuel cells. It consists of a hydrophobic polytetrafluoroethylene (PTFE) backbone with pendant side chains of perfluorinated

vinyl ethers terminated by hydrophilic ion-exchange groups that take up several molecules of water under ambient humidity [26], [27]. Its general chemical structure in the protonated form is given as [25]:



It is conventionally characterized by its equivalent weight (EW), which is defined as the mass of dry polymer (in grams) that contains 1 mol of exchangeable sulfonate ion. The most often used material has a nominal EW = 1100, corresponding to about $n = 6.5$. This material is known to retain some water even after intensive drying; a substrate with one adsorbed water molecule per sulfonate group, with an overall empirical formula $C_{20}F_{39}SO_6H_3$ has been assumed here. The density of dry Nafion® is 2.0 g/cm^3 , for the minimally hydrated (3% v/v) substrate a volume-weighted average value of 1.97 g/cm^3 has been used in the present calculations.

3. CALCULATION

Details of our methodology have been reported earlier [3]. Briefly, penetration of projectile ions as well as the full recoil cascades are calculated by the TRIM module of the SRIM program package [31], [32], [34] (version 2003.26). At each combination of projectile ion and energy investigated, statistical analysis is carried out from the raw results on both the implant ion and so-called vacancy (*i.e.* collisional damage) positions, to determine the moments of depth distributions [31], [32], [35]. The first moment is conventionally called (longitudinal) range (R_p) for the implanted ions, and we have analogously defined the range for collisional damage (R_d) [3]. The second moments are called straggling parameters; in the figures below these variance type quantities will be shown plotted in place of error bars (which would be smaller than the symbols used, due to the ranges calculated with sufficient accuracy).

The projectile ions chosen for this study are the noble gases He through Rn. This covers the atomic number range 2–86. Fitting over our results allows to predict range data for arbitrary ions from the entire periodic table.

In order to summarize all the results from the different ions, converting to dimensionless units based on the Ziegler-Biersack-Littmark formalism [31], [32] is performed. This utilizes scaling with the characteristic energy E_c and length R_c , defined according to equations 1–3:

$$a_s = 0.8853 a_B / (Z_1^{0.23} + Z_2^{0.23}), \quad (1)$$

$$E_c = Z_1 Z_2 e^2 (M_1 + M_2) / M_2 4\pi \epsilon_0 a_s, \quad (2)$$

$$R_c = (M_1 + M_2)^2 / M_1 M_2 N_d 4\pi a_s^2, \quad (3)$$

where a_s is the Ziegler-Biersack-Littmark screening length, $a_B = 0.529 \text{ \AA}$ is the Bohr radius, Z_1 and Z_2 are the atomic numbers of the incident ion and target atom, respectively, M_1 and

M_2 are their atomic masses, $e = 1.6 \cdot 10^{-19}$ C is the electron's charge, $\varepsilon_0 = 8.85 \cdot 10^{-12}$ C²/N m² is the permittivity of vacuum, and N_d is the number density of the target.

Job control, which involves queueing multiple SRIM/TRIM runs over sets of input data prepared, as well as evaluating and summarizing raw output, is handled by in-house developed scripts that we release to the public domain and make available as supplementary material (http://www.staff.u-szeged.hu/~fekete/srim_trim-scripts/).

4. RESULTS AND DISCUSSION

Fig. 1 displays the logarithms of scaled ranges for implant ions ($\lg(R_p/R_c)$), versus the logarithm of scaled energy ($\lg(E/E_c)$), with the PTFE and Nafion data plotted together. It can be seen that all results (combined for both target materials) fall on a linear master curve, when expressed in this scaled form. The corresponding straggling parameters, marked by error bar symbols are also shown on these plots. The logarithms of scaled ranges for collisional damage ($\lg(R_d/R_c)$) in Nafion, versus the logarithm of scaled energy ($\lg(E/E_c)$), are presented in Fig. 2.

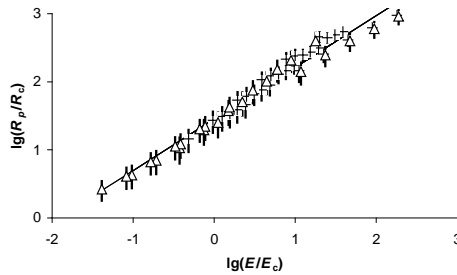


Fig. 1. Scaled ranges for implantation in PTFE (crosses) and Nafion (triangles); error bar symbols mark corresponding straggling parameters

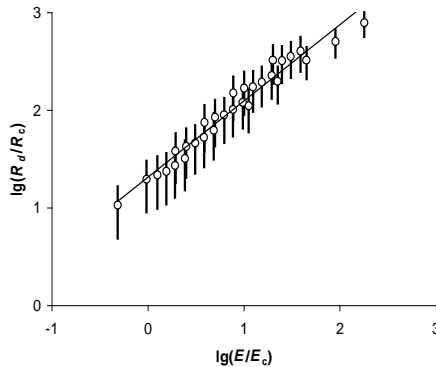


Fig. 2. Scaled ranges for collisional damage in Nafion error bar symbols mark corresponding straggling parameters

Double logarithmic fits of the scaled ranges, equations 4-5 below (where the standard errors of the fitted slope and intercept are also shown in parentheses), show good linearity as indicated by their regression coefficient r near unity:

$$\lg(R_p/R_c) = (0.759 \pm 0.016) \lg(E/E_c) + (1.453 \pm 0.017), r = 0.988, \quad (4)$$

$$\lg(R_d/R_c) = (0.781 \pm 0.028) \lg(E/E_c) + (1.314 \pm 0.030), r = 0.982. \quad (5)$$

These equations allow calculating what R_p and R_d values would be yielded by a SRIM/TRIM calculation on a polymer, provided that the dimensionless energy falls in the covered range 0.041–179. Ranges for projectile ions with arbitrary Z_1 , M_1 can be calculated, aiding a rational design of ion irradiation experiments.

A representative example of the membrane permeation behavior of water vapor in untreated and treated membranes of Nafion[®] 117 (178 μm thick) is shown in Fig. 3. The treated specimens were implanted with either $10^{15} \text{ cm}^{-2} \text{ N}^+$ or $10^{15} \text{ cm}^{-2} \text{ F}^+$. Significant reduction of the water flux through this particular membrane was observed, more for the fluorine implanted than the nitrogen implanted. This result illustrates the profound effect of irradiation on the permeability of dense membranes.

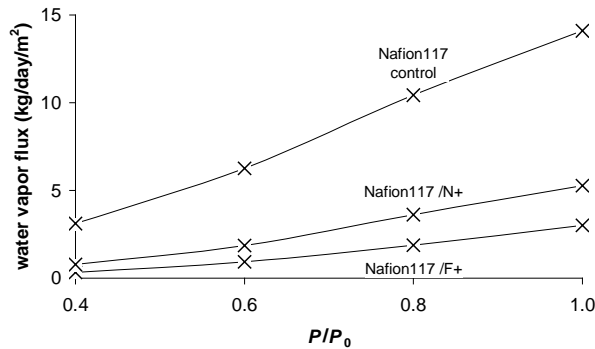


Fig. 3. Water flux for untreated and treated Nafion[®] 117 (top curve: untreated control; lower curve: irradiated with $10^{15} \text{ cm}^{-2} \text{ N}^+$; bottom curve: irradiated with $10^{15} \text{ cm}^{-2} \text{ F}^+$)

ACKNOWLEDGEMENTS

The authors of this paper thank Dr. Thomas J. Tate for assistance with setting up the TRIM simulations, and acknowledge funding by Army Research Grant DAAD 16-01-P-0389. FEK is also partially supported by the Air Force Office of Scientific Research, and ZAF by the Hungarian Scientific Research Fund (OTKA grant no. T 032190 and T 042539).

REFERENCES

- [1] KORUGIC-KARASZ L.S., HOFFMANN E.A., *Polymer Ion Implantation: Present and Future Prospects*, Nonlin. Opt. Quant. Opt., 32, 2004, p. 135.

- [2] WILUSZ E., ZUKAS W., FEKETE Z.A., KARASZ F.E., *Ion Beam Modification of Permselective Membranes for Chemical Biological Protective Clothing*, Polymer Preprints Polymer Preprints (American Chemical Society, Division of Polymer Chemistry), 45, 2004, p. 7.
- [3] FEKETE Z.A., WILUSZ E., KARASZ F.E., *Modelling of Displacement Damage in an Ion-Beam-Modified Perfluorosulfonate Ionomer*, Journal of Polymer Science Part B-Polymer Physics, 42, 2004, p. 1343.
- [4] EVERETT M.L., HOF LUND G.B., *Chemical Alteration of Poly(Tetrafluoroethylene) Teflon Induced by Exposure to Vacuum Ultraviolet Radiation and Comparison with Exposure to Hyperthermal Atomic Oxygen*, Journal of Polymer Science Part a-Polymer Chemistry, 43, 2005, p. 552.
- [5] HOF LUND G.B., EVERETT M.L., *Chemical Alteration of Poly(Vinyl Fluoride) Tedlar by Hyperthermal Atomic Oxygen*, Applied Surface Science, 239, 2005, p. 367.
- [6] BRYJAK M., POZNIAK G., GANCARZ I., TYLUS W., *Microwave Plasma in Preparation of New Membranes*, Desalination, 163, 2004, p. 231.
- [7] BRYJAK M., GANCARZ I., POZNIAK G., *Plasma-Modified Porous Membranes*, Chemical Papers-Chemicke Zvesti, 54, 2000, p. 496.
- [8] BRYJAK, M., GANCARZ, I., *Plasma Treatment of Polyethylene Ultrafiltration Membranes*, Angewandte Makromolekulare Chemie, 219, 1994, p. 117.
- [9] HAN S., CHOI W.K., YOON K.H., KOH S.K., *Surface Reaction on Polyvinylidene fluoride (Pvdf) Irradiated by Low Energy Ion Beam in Reactive Gas Environment*, Journal of Applied Polymer Science, 72, 1999, p. 41.
- [10] ROBESON L.M., BURGOYNE W.F., LANGSAM M., SAVOCA A.C., TIEN C.F., *High-Performance Polymers for Membrane Separation*, Polymer, 35, 1994, p. 4970.
- [11] DAVENAS J., XU X.L., *Diffusion of Iodine into Polyimide Films Modified by Ion-Bombardment*, Nuclear Instruments & Methods in Physics Research, Section B: Beam Interactions with Materials and Atoms, B 71, 1992, p. 33.
- [12] XU X.L., COLEMAN M.R., MYLER U., SIMPSON P.J., *Postsynthesis Method for Development of Membranes Using Ion Beam Irradiation of Polyimide Thin Films*, ACS Symposium Series, 744, 2000, p. 205.
- [13] XU X.L., DOLVECK J.Y., BOITEUX G., ESCOUBES M., MONCHANIN M., DUPIN J.P., DAVENAS J., *Ion-Beam Irradiation Effect on Gas Permeation Properties of Polyimide Films*, Journal of Applied Polymer Science, 55, 1995, p. 99.
- [14] XU X.L., COLEMAN M.R., MYLER U., SIMPSON, P.J., *Ion Beam Irradiation-an Efficient Method to Modify the Subnanometer Scale Microstructure of Polymers in a Controlled Way*, Materials Research Society Symposia Proceedings, 540, 1999, p. 255.
- [15] SVORCIK V., PROSKOVA K., RYBKA V., HNATOWICZ V., *Water Diffusion in Polyethylene Modified by Ion Irradiation*, Polymer Degradation and Stability, 60, 1998, p. 431.
- [16] WILUSZ E., FEKETE A.Z., KARASZ F.E., *Permeability of Ion Beam Treated Nafion*, in press, 2003.
- [17] ESCOUBES M., DOLVECK J.Y., DAVENAS J., XU X.L., BOITEUX G., *Ion Beam Modification of Polyimide Membranes for Gas Permeation*, Nuclear Instruments & Methods in Physics Research, Section B: Beam Interactions with Materials and Atoms, 105, 1995, p. 130.
- [18] SVORCIK V., RYBKA V., JANKOVSKIJ O., HNATOWICZ V., *Free Volume-Limited Diffusion in Ion-Modified Polymers*, Journal of Applied Polymer Science, 61, 1996, p. 1097.
- [19] SVORCIK V., RYBKA V., MICEK I., POPOK V., JANKOVSKIJ O., HNATOWICZ V., KVITEK J., *Structure and Properties of Polymers Modified by Ion- Implantation*, European Polymer Journal, 30, 1994, p. 1411.
- [20] MYLER U., XU X.L., COLEMAN M.R., SIMPSON P.J., *Ion Implant-Induced Change in Polyimide Films Monitored by Variable Energy Positron Annihilation Spectroscopy*, Journal of Polymer Science, Part B: Polymer Physics, 36, 1998, p. 2413.

- [21] WON J., KIM M.H., KANG Y.S., PARK H.C., KIM U.Y., CHOI S.C., KOH S.K., *Surface Modification of Polyimide and Polysulfone Membranes by Ion Beam for Gas Separation*, Journal of Applied Polymer Science, 75, 2000, p. 1554.
- [22] HOBSON L.J., OZU H., YAMAGUCHI M., MURAMATSU M., HAYASE S., *Nafion(R) 117 Modified by Low Dose Eb Irradiation: Surface Structure and Physical Properties*, Journal of Materials Chemistry, 12, 2002, p. 1650.
- [23] HOBSON L.J., OZU H., YAMAGUCHI M., HAYASE S., *Does Low Dose Electron Beam Exposure Make Nafion (R) Film a Suitable Candidate for Improved Dmfcc Performance?* Journal of New Materials for Electrochemical Systems, 5, 2002, p. 113.
- [24] HOBSON L.J., OZU H., YAMAGUCHI M., HAYASE S., *Modified Nafion 117 as an Improved Polymer Electrolyte Membrane for Direct Methanol Fuel Cells*, Journal of the Electrochemical Society, 148, 2001, p. A1185.
- [25] ROBERTSON M.A.F., YEAGER H.L., *In Ionomers: Synthesis, Structure, Properties and Applications*, Tant M.R.; K.A., M.; Wilkes, G. L., (eds.), Chapman & Hall: London, 1997, p. 290.
- [26] RIVIN D., KENDRICK C.E., GIBSON P.W., SCHNEIDER N.S., *Solubility and Transport Behavior of Water and Alcohols in Nafion (Tm)*, Polymer, 42, 2001, p. 623.
- [27] REUCROFT P.J., RIVIN D., SCHNEIDER N.S., *Thermodynamics of Nafion (Tm)-Vapor Interactions. I. Water Vapour*, Polymer, 43, 2002, p. 5157.
- [28] LEE E.H., LEWIS M.B., BLAU P.J., MANSUR L.K., *Improved Surface-Properties of Polymer Materials by Multiple Ion-Beam Treatment*, Journal of Materials Research, 6, 1991, p. 610.
- [29] HNATOWICZ V., HAVRANEK V., KVITEK J., PERINA V., SVORCIK V., RYBKA V., *Modifications of Polypropylene Induced by the Implantation of Iodine Ions*, Japanese Journal of Applied Physics, Part I: Regular Papers and Short Notes, 32, 1993, p. 1810.
- [30] HNATOWICZ V., KVITEK J., SVORCIK V., RYBKA V., *Oxygen Incorporation in Polyethylene and Polypropylene Implanted with F⁺, as⁺ and I⁺ Ions at High-Dose*, Applied Physics A: Solids and Surfaces, 58, 1994, p. 349.
- [31] ZIEGLER J.F., BIRSACK J.P., LITTMARK U., *The Stopping and Range of Ions in Solids*, Pergamon Press, New York, 1985.
- [32] ZIEGLER J.F., *Srim-2003, Nuclear Instruments & Methods in Physics Research Section B-Beam Interactions with Materials and Atoms*, 219–20, 2004, p. 1027.
- [33] ZIEGLER J.F., MANOYAN J.M., *The Stopping of Ions in Compounds, Nuclear Instruments & Methods in Physics Research, Section B: Beam Interactions with Materials and Atoms*, B35, 1988, p. 215.
- [34] ZIEGLER J.F., BIRSACK J.P., *Srim/Trim: Stopping/Transport and Range of Ions in Matter, Version 2003.26; Pc-Compatible Program*, 2003. Available via <http://www.srim.org/>
- [35] BURENKOV A.F., KOMAROV F.F., KUMAKHOV M.A., TEMKIN M.M., *Tables of Ion Implantation Spatial Distributions*, Gordon and Breach, New York, 1986.

*Keywords: coagulation, MIEX[®] resin, ultrafiltration,
natural organic matter*

MAŁGORZATA KABSCH-KORBUTOWICZ*,
ANDRZEJ BIŁYK*, MAREK MOŁCZAN*

IMPACT OF WATER PRETREATMENT ON THE PERFORMANCE OF ULTRAFILTRATION MEMBRANES

The objectives were to investigate the effect of water pretreatment by mean of coagulation, or MIEX[®] resin adsorption on the removal of natural organic matter and on the fouling of membranes during the ultrafiltration process. In all cases water pretreatment resulted in the increase of permeate quality and the decrease of membrane fouling. However, the results indicated that treatment with MIEX[®] resin is much more effective than the coagulation in organic substances removal. That was especially true for its low-molecular fractions, which are responsible for the membrane fouling.

1. INTRODUCTION

Increasing water scarcity and the stringent water quality legislation result in the expansion of membrane-based technologies in the water treatment sector. The low-pressure membrane processes (microfiltration and ultrafiltration) receive increased attention due to the quality of water and the cost reduction caused by improvements in membrane technology. Application of those techniques can simplify the treatment process by eliminating coagulation, flocculation and sedimentation processes. These processes have also been considered to be suitable for the conventional drinking water treatment.

A more widespread application of membrane processes is limited by the decrease in membrane performance that occurs during potable water treatment as a result of fouling through the accumulation of particles and adsorption of the NOM [1]–[4]. Extensive research has been carried out to understand the factors influencing the intensification of membrane fouling, but these results are either not conclusive, or sometimes even con-

* Wrocław University of Technology, Institute of Environment Protection Engineering, Wybrzeże Wyspiańskiego 27, 50-370 Wrocław, Poland. E-mail: malgorzata.kabsch-korbutowicz@pwr.wroc.pl

tradictory. Generally, it might be said that the decrease in membrane permeability during the water treatment depends on the type of the membrane used as well as on the amount and properties of the organic substances fractions in the treated water.

The water pretreatment process used to remove foulants (mainly particles and organic matter) prior to the membrane process has become an important aspect of any membrane operation. Moreover, water pretreatment, prior to membrane filtration, can improve the final quality of water. A variety of pretreatment processes for water ultrafiltration have been recently investigated. Among them, the most frequently applied were coagulation [5]–[10], or activated carbon adsorption [3], [11]–[14]. Pretreatment process may cause a significant increase in the total cost of the water production and sometimes the expected results, i.e. reduction of membrane fouling, may not be achieved. For example Carroll et. al. [15] stated that a small molecular weight and hydrophilic fraction of the NOM, which is responsible for membrane fouling, was not removed during the coagulation step, and after the coagulation pretreatment no decrease of membrane flux was observed. Bian et. al. [16] reported that adsorption by PAC does not remove the NOM fractions which are highly responsible for fouling.

Since neither coagulation, nor carbon adsorption can remove all the organic foulants from the treated water prior to membrane filtration, many research is carried out to find new and effective method of the organic matter removal. Ion exchange process seems to be a very effective solution to this problem.

The first studies demonstrating a strong potential of the anion exchange resin for the natural matter removal appeared at the end of the 1970s [17] and were followed by numerous research works [18]–[20]. It has been proved that anion exchange resins can effectively eliminate the NOM from the treated water and are much more efficient in eliminating the low organic NOM fraction when compared to conventional processes [21], [22].

The interest in the ion exchange process application in the water treatment increased when the new Magnetic Ion EXchange resin, MIEX[®] was developed. The MIEX[®] resin was developed by Orica, an Australian Company, and optimized for the removal of negatively charged organic particles from the water [23], [24]. The MIEX[®] resin is a micro size, macroporous, and strong base ion exchange resin made from a moderately cross-linked acrylic skeleton. The resin has a magnetic component incorporated into its polymeric structure. This makes individual resin beads behave like small magnets capable of agglomerating into large and heavy agglomerates. In this form they can be easily removed from water by sedimentation. The process for the DOC removal based on the MIEX[®] resin includes resin contacting with water, resin separation and recycle, and resin regeneration with NaCl. The process differs from the conventional ion exchange technology in the way that the ion exchange part of the process is continuous.

The MIEX[®] resin has a very small particle size – the diameter of a particle is only 150–180 μm . With a specific surface area comparable to other conventional macropo-

rous resins, this resin has a lot more external bead surface. This benefits in the DOC exchange kinetics (less controlled by the particle diffusion) and the resistance to fouling (less DOC exchanged into the particles, shorter diffusion paths with smaller beads).

The literature of MIEX[®] indicated high efficiency of the process in the DOC removal. UV₂₅₄ and DOC removal ranged from 50 to 85%, respectively, depending on the raw water quality [18], [25], [26]. The process is especially effective in separating the low molecular weight organic particles [27]. MIEX[®] does not remove turbidity and even may generate secondary pollution, since a small part of a resin might be carried away from the system. In order to eliminate water turbidity and remove larger organic particles from water it is required to use coagulation with low doses of coagulants as a post-treatment of water.

The aim of this work was to evaluate the suitability of process composed of the MIEX[®] treatment or coagulation and membrane ultrafiltration on the final water quality and to assess the influence of this pretreatment method on the membrane fouling.

2. EXPERIMENTAL

2.1. WATER SAMPLES

Raw water (RW), pure water from Mokry Dwor waterworks (MD) and raw water treated with the MIEX[®] resin followed by the sand filtration were collected between March and April 2005.

The Mokry Dwór waterworks takes its raw water from Olawa river and produces about 40% of the distributed drinking water for the city of Wroclaw, Poland. The plant has an average water flow of about 80000 m³/h. The treatment process at Mokry Dwór include the coagulation with Al₂(SO₄)₃, and the sand filtration. The characteristics of raw (RW) and pure water (MD) are given in Table 1.

Table 1. Results of raw and pure water quality at Mokry Dwór waterworks plant

	Raw water	MD pure water
Colour, g Pt/m ³	15.0	9.2
DOC, g C/ m ³	4.8	3.9
UV ₂₅₄ , m ⁻¹	13.0	10.0

2.2. THE MIEX[®] PROCESS DESCRIPTION

The experiments with MIEX[®] resin were performed at a semi-automatic pilot plant (Fig. 1) module delivered by ORICA WATERCARE which was installed on raw wa-

ter intake of Mokry Dwor waterworks. The main parts of the installation set-up of the system included the following major parts: contactor (250 dm³), settler (260 dm³), regeneration vessel (45 dm³), fresh resin tank (120 dm³), brine tank (30 dm³), overflow tank (55 dm³), compressor, pumps, mixers and a distribution/control box. Parameters of the MIEX[®] process performance were determined in jar tests [28] and are presented in table 2.



Fig. 1. MIEX[®]DOC pilot plant

Table 2. The operating parameters of the MIEX[®] pilot plant trial

Parameter	unit	Value	
		for trial range	for UF samples
Raw water flow	dm ³ /h	500	500
Resin concentration	cm ³ _{resin} / dm ³ _{suspension}	10–29	20
Resin/water contact time	min	30	30
Resin bed volumes	dm ³ _{water} / dm ³ _{resin}	1000–3000	1230
Regeneration rate	%	4–8	5
Fresh resin concentration	cm ³ _{resin} / dm ³ _{suspension}	180–240	210
Recycle resin concentration	cm ³ _{resin} / dm ³ _{suspension}	60–150	120
Regeneration frequency	day ⁻¹	1	1
Brine dosage	dm ³ _{brine} / dm ³ _{resin}	2.5–3,0	2.5

2.3. THE ULTRAFILTRATION MODULE AND TESTING SET-UP

In the ultrafiltration experiments we made use of hollow-fibre UF modules (prepared in Institute of Biocybernetics and Biomedical Engineering PAS, Warsaw, Poland) with polysulfone (PS 1700 NT-LCD) membranes of cut-off 30 kDa (the membrane cut-off was determined using dextrans). The module consisted of 127 hollow fibres with an internal diameter of 0.96 mm. The effective surface area of the membranes in the module amounted to 0.0567 m².

In the ultrafiltration experiments Millipore ProFlux M12 (Fig. 2) cross-flow system was used. During membrane filtration tests the feed solution volume amounted to 2 dm³ and, in order to maintain constant feed parameters, permeate was recirculated to the feeding tank.



Fig. 2. Millipore Proflux M12 ultrafiltration system

2.3.1. METHODS OF PROCESSES INVESTIGATION

Prior to each ultrafiltration cycle, the membrane module has been treated with distilled water at 0.03 MPa until a constant volume flux was established.

Transport properties of membranes were investigated at 0.03 MPa by measuring the rate of permeate flow through the capillaries under steady conditions.

Permeate volume flux (J) was calculated as follows:

$$J = \frac{V}{t \cdot A}, \quad \text{m}^3/\text{m}^2 \text{ day}$$

where V is permeate volume (m^3), t stands for time (day), and A denotes the effective membrane surface area (m^2).

The efficiency of the examined processes was determined by measuring the amount of the organic matter in the samples before and after each process. The NOM concentration was monitored by the measurement of the DOC (TOC 5050 Analyser, Shimadzu), the absorbance of UV at 254 nm (UV_{254}), and the colour intensity (Shimadzu UV1240 spectrophotometer). The retention coefficient of the measured water parameters was determined using the following expression:

$$R = \frac{c_0 - c_p}{c_0} \cdot 100, \quad \%$$

where R is the retention coefficient, and c_0 and c_p are the parameter values of the feed and permeate, respectively.

The high-performance size exclusion chromatography (HPSEC) has been used to determine the molecular weight distribution of the organic substances in the water samples. In the HPSEC analysis, organic substances are separated primarily on the basis of differences in the molecular sizes, i.e. the largest molecules are eluted first in the column, while the smallest molecules are eluted last.

The HPSEC was carried out using the HPLC system with an UV detector (Shimadzu) equipped with a BIOSEP-SEC-S2000 column (7.5 x 300 mm, Phenomenex). The column packing consisted of a hydrophilic bonded silica with particle size of $5\mu\text{m}$ and pore size of 145 \AA . The eluent that has been used was a 0.1 M NaCl solution buffered at pH 6.8 with 2 mM phosphate solution. A water sample of $20 \mu\text{l}$ was injected into the column. The flow rate was $1 \text{ cm}^3/\text{min}$ and the analysis time was 15 min. All solutions were prepared using analytical grade chemicals and the MiliQ water. The absorbance at 254 nm was used for detection. As the pretreatment for the HPSEC fractionation of the NOM, water samples were filtered through a $0.45 \mu\text{m}$ membrane. The HPSEC column was calibrated with protein standards such as insuline (5.7 kDa), ovalbumin (45 kDa), bovine serum albumine (69 kDa), and γ -globuline (150 kDa).

The area of the peak in the chromatogram refers to the amount of UV absorbing fraction of the DOM in a specific molecular size fraction.

3. RESULTS AND DISCUSSION

3.1. THE MIEX[®] PROCESS EFFECTIVENESS

One month pilot trial of the MIEX[®]DOC process gave average results as shown in Fig. 3 [29]. The average effectiveness of UV_{254} , colour and the DOC removal were very close to these obtained in the jar tests a year before [28], although ranges of the

results were rather wide. This was not only due to the raw water quality and the NOM fractions changes, but also to the programmed changes of the main process parameters like resin concentration and resin bed volumes (see table 2).

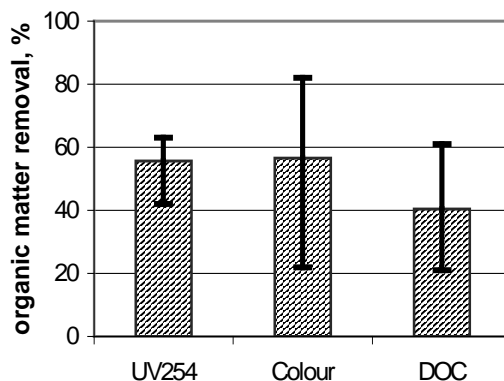


Fig. 3. The average efficiency of organic matter removal in pilot MIEX[®]

3.2. THE INFLUENCE OF PRETREATMENT METHOD ON PERMEATE QUALITY

The plots of Fig. 4 demonstrate how the quality of water has changed after application of the investigated methods of pretreatment. As shown by these data a commonly applied method of surface water treatment, i.e. coagulation and sand filtration may decrease the colour intensity by 38.7%, UV absorbance at 254 nm by 23.1%, and the DOC concentration by 18.7%. Much higher degree of the organic matter removal, i.e. 74.0%, 61.5% and 41.7%, respectively for colour, UV absorbance at 245 nm and the DOC concentration was achieved when the MIEX[®] process has been applied.

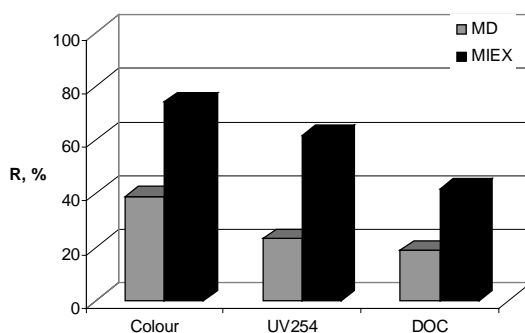


Fig. 4. The effect of raw water treatment method on the NOM efficiency removal (MD – water after coagulation and sand filtration at Mokry Dwor waterworks, MIEX – water after the MIEX[®] process)

In all cases preferential decrease of colour over the UV_{254} and the DOC was observed. This is evident, as the colour of water is related to the presence of large fractions of the NOM and coagulation is much better at removing the larger hydrophobic molecules, or acidic molecules than the smaller ones. The UV adsorption at 254 nm monitors the amount of the NOM fraction containing aromatic structures in their molecules. The smaller the molecular size of the humic fractions is, the less reliable is the quantitative estimation of the NOM concentration due to the scarcity of aromatic structures. The smallest fractions may contain compounds which have no UV absorbance. The decrease of the DOC concentration, as the most reliable method to determine the total amount of the NOM, has lower values and is the best parameter to characterize the process efficiency.

When analyzing the quality of water after membrane filtration (Table 3) it should be noted that the application of any treatment method prior to the ultrafiltration result in the increase of permeate quality. Adsorption of the organic matter on the MIEX[®] resin, followed by ultrafiltration brought about 80% reduction of water colour (retention of the organic matter was determined with reference to raw water). Also the retention factor for other measured parameters (i.e. UV absorbance at 254 nm and DOC concentration) was higher than observed for the non-membrane filtered samples (Fig.5).

Table 3. The influence of the water pretreatment method on the UF permeate quality

Sample (pretreatment method)	UF permeate quality		
	colour, g Pt/m ³	UV_{254} , m ⁻¹	DOC, g C/m ³
Raw water (no pretreatment)	10.9	9.5	4.15
Mokry Dwor waterworks (coagulation + filtration)	8.9	8.7	3.35
MIEX [®] process	2.9	3.2	1.85

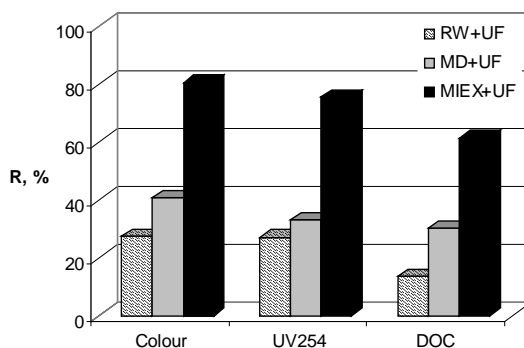


Fig. 5. The effect of the water pretreatment method on the NOM retention in ultrafiltration

3.3. THE INFLUENCE OF THE WATER PRETREATMENT METHOD ON THE UF MEMBRANE FLUX DECLINE

Fig. 6 shows the flux decline of ultrafiltration membranes when raw water, or pretreated solutions were filtered. The ratio of the initial flux (J_0) to that at i -th time (J_i) was employed to evaluate the flux decline.

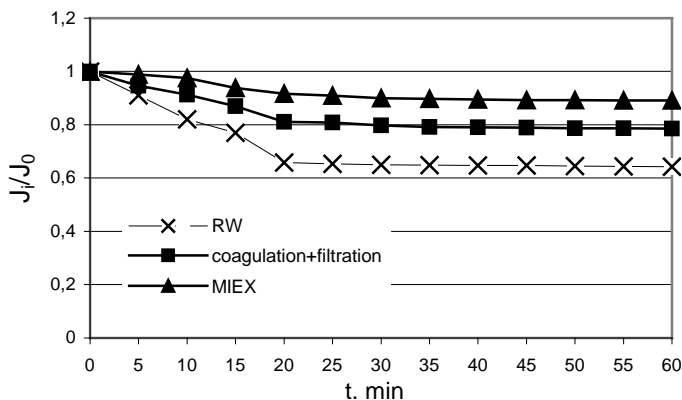


Fig. 6. The influence of the feed water pretreatment method on the permeate flux decline (J_i/J_0)

The flux of the membrane with pre-coagulation or the MIEX[®] adsorption decreased slowly compared to that of the membrane without any pretreatment. As a general observation, ultrafiltration of raw water caused flux decrease by 35%, while for the pretreated feed streams it amounted to 21% and 11%, respectively for the pre-coagulated, or MIEX[®] adsorbed samples. A rapid flux decline followed by stabilization of permeability during the initial stages of filtration was observed for all membrane treated samples.

3.3. THE EFFECTS OF THE WATER TREATMENT PROCESS ON THE HPSEC CHROMATOGRAMS

Typical chromatograms of the NOM fractions of raw water, pure water from Mokry Dwor waterworks and raw water treated with the MIEX[®] resin are presented in Fig. 7. In all analyzed samples three distinct fractions of the NOM were detected. The dominant fraction was the one of MW below 30 kDa. Conventional water treatments (i.e. coagulation and sand filtration) as well as the MIEX[®] process are quite effective in separating these organic particles. Coagulation and sand filtration eliminated about 51% of the organic fraction of MW ~25 kDa and 37% of 1 kDa fraction, while MIEX[®] was able to remove about 85% and 38%, respectively. Comparing information obtained from the HPSEC chromatograms with data presented in Fig. 6, it can be

stated that elimination of organic substances of MW < 30kDa resulted in decrease of membrane fouling and improves membrane permeability.

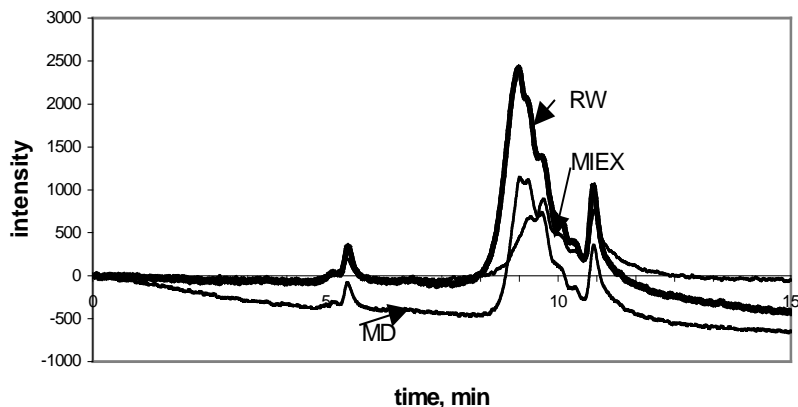


Fig.7. The HPSEC chromatogram of raw and pretreated water (RW – raw water, MD – water from Mokry Dwor waterworks, MIEX – raw water after MIEX[®] process)

Fig. 8 compares the HPSEC chromatograms of raw water and ultrafiltered samples of the raw and pretreated water. As seen in the figure, applied membrane completely eliminates the organic fraction of MW > 70 kDa, but its effectiveness in separation of small NOM particles is limited. The intensity of the profiles substantially depends on the applied pretreatment method. Integration of the MIEX[®] process with ultrafiltration resulted in the highest elimination of the organic particles. It plays a meaningful role in respect to the low MW organic fraction. In water samples pretreated with the use of conventional coagulation, the amount of the low MW organic structures was higher.

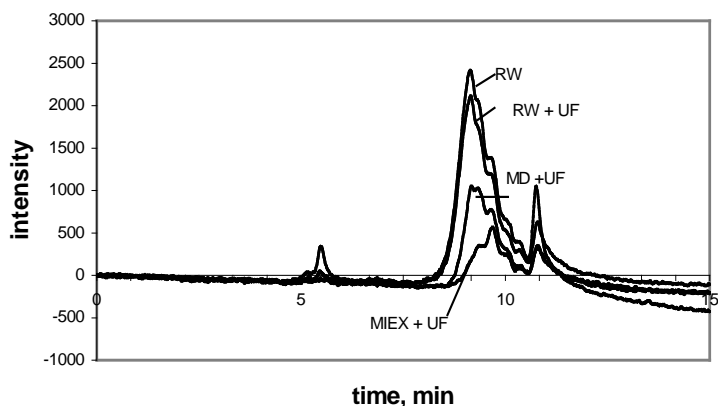


Fig. 8. The HPSEC chromatogram of permeates after the water pretreatment

However, the reliability of the HPSEC method is affected by the size calibration of the column and also by the adsorption interactions and the charge exclusion (electrostatic repulsion effects) between the humic compounds and the HPSEC gel [30]. In this study the column calibration was performed using proteins. Since the molecular structure of proteins is different from that of the NOM, protein standards tend to overestimate the molecular size of the humic substances [31]. Therefore the largest fraction might be lower than 150 kDa and the smallest fraction might be lower than 1 kDa. Thurman [32] reported that molecular size of the aquatic fulvic acids and the humic acids are in range of 0.5–2 kDa and 2–5 Da, respectively.

4. CONCLUSIONS

The objective of the reported research was to investigate the effect of water pretreatment by mean of coagulation or the MIEX[®] resin adsorption on the natural organic matter removal and on the membrane fouling during the ultrafiltration process. The conclusions of this research are as follows:

- water treatment with the MIEX[®] resin results in much higher elimination of the organic matter as compared to the coagulation,
- coagulation, or treatment with the MIEX[®] resin prior to a membrane ultrafiltration results in the increase of the permeate quality and decrease of the UF membrane fouling,
- generally, water pretreatment with the MIEX[®] seems to be a good method to increase the effectiveness of the ultrafiltration process, i.e. elimination of the organic substances and the hydraulic efficiency.

ACKNOWLEDGEMENTS

The authors would like to thank ORICA for providing the MIEX[®] resin. The work was partly supported by the Polish Ministry of Education and Science, Grant # 3 T09D 014 29 (years 2005-2007).

REFERENCES

- [1] KIMURA K., HANE Y., WATANABE Y., AMY G., OHKUMA N., *Irreversible membrane fouling during ultrafiltration of surface water*, Water Res., 38, 2004, pp. 3431–3441.
- [2] LEE N., AMY G., CROUÉ J.-P., BUISSON H., *Identification and understanding of fouling in low-pressure membrane (MF/UF) filtration by natural organic matter (NOM)*, Water Res., 38, 2004, pp. 4511–4523.
- [3] LI C.-W., CHEN Y.-S., *Fouling of UF membrane by humic substance: effect of molecular weight and power-activated carbon (PAC) pretreatment*, Desalination, 170, 2004, pp. 59–67.
- [4] AUSTIN E., SCHÄFER A.I., FANE A.G., WAITE T.D., *Ultrafiltration of natural organic matter*, Sep. Purif. Technol., 22–23, 2001, pp. 63–78.
- [5] CHOI K.Y., DEMPSEY B.A., *In-line-coagulation with low-pressure membrane filtration*, Water Res., 38, 2004, pp. 4271–4281.

- [6] LEIKNES T., ØDEGAARD H., MYKLEBUST H., *Removal of natural organic matter (NOM) in drinking water treatment by coagulation-microfiltration using metal membranes*, J. Membr. Sci., 242, 2004, pp. 47–55.
- [7] LAHOUSSE-TURCAUD V., WIESNER M.R., BOTTERO J.-Y., MALLEVIALLE J., *Coagulation pretreatment for ultrafiltration of a surface water*, JAWWA, 82, 1990, pp. 76–81.
- [8] JUDD S.J., HILLIS P., *Optimisation of combined coagulation and microfiltration for water treatment*, Water Res., 35, 2001, pp. 2895–2904.
- [9] PIKKERAINEN A.T., JUDD S.J., JOKELA J., GILLBERG L., *Pre-coagulation for microfiltration of an upland surface water*, Water Res., 38, 2004, pp. 455–465.
- [10] OH J.-I., LEE S., *Influence of streaming potential on flux decline of microfiltration with in-line rapid pre-coagulation process for drinking water production*, J. Membr. Sci., 254, 2005, pp. 39–47.
- [11] TSUJIMOTO W., KIMURA H., IZU T., IRIE T., *Membrane filtration and pretreatment by GAC*, Desalination, 119, 1998, pp. 323–326.
- [12] TOMASZEWSKA M., MOZIA S., *Removal of organic matter from water by PAC/UF system*, Water Res., 36, 2002, pp. 4137–4143.
- [13] MOZIA S., TOMASZEWSKA M., MORAWSKI A., *Studies on the effect of humic acids and phenol on adsorption-ultrafiltration process performance*, Water Res., 39, 2005, pp. 501–509.
- [14] KLONFAS G., KONIECZNY K., *Fouling phenomena in unit and hybrid processes for potable water treatment*, Desalination, 163, 2004, pp. 311–322.
- [15] CARROLL T., KING S., GRAY S.R., BOLTO B.A., BOOKER N.A., *The fouling of microfiltration membranes by NOM after coagulation treatment*, Water Res., 34, 2000, pp. 2861–2868.
- [16] BIAN R., WATANABE Y., OZAWA G., TAMBO N., *Membrane fouling of ultrafiltration: evaluation of influence of pretreatment with batch test*, J. Jpn. Water Works Assoc., 67, 1998, pp. 11–19.
- [17] ANDERSON C.T., MAIER W.J., *Trace organics removal by anion exchange resins*, JAWWA, 71, 1979, pp. 278–283.
- [18] HUMBERT H., GALLARD H., SUTY H., CROUÉ J.-P., *Performance of selected anion exchange resins for the treatment of high DOC content surface water*, Water Res., 39, 2005, pp. 1699–1708.
- [19] BOLTO B., DIXON D., ELDRIDGE R., KING S., LINGE K., *Removal of natural organic matter by ion exchange*, Water Res., 36, 2002, pp. 5057–5065.
- [20] BOLTO B., DIXON D., ELDRIDGE R., *Ion exchange for the removal of natural organic matter*, Reactive & Functional Polymers, 60, 2004, pp. 171–182.
- [21] BOLTO B., DIXON D., ELDRIDGE R., KING S., *Removal of THM precursors by coagulation or ion exchange*, Water Res., 36, 2002, pp. 5066–5073.
- [22] CROUÉ J.-P., VIOLLAEU D., BODAIRE C., LEGUBE B., *Removal of hydrophobic and hydrophilic constituents by anion exchange resin*, Water Sci. Technol., 40, 1999, pp. 207–214.
- [23] SLUNJSKI M., BOURKE M., NGUYEN H., BALLARD M., MORRAN J., BURSILL D., *MIEX[®] DOC process – a new ion exchange process*, Proc. 18th Federal Convention, Australian Water Wastewater Assoc., 11–14 April 1999, Adelaide, Australia.
- [24] SEMMENS M.J., BURCKHARDT M., SCHULER D., DAVICH P., SLUNJSKI M., BOURKE M., NGUYEN H., *An evaluation of magnetic ion exchange resin (MIEX[®]) for NOM removal*, Proc. AWWA Conference, 11–15 June 2000, Denver, USA.
- [25] SINGER P.C., BILYK K., *Enhanced coagulation using a magnetic ion exchange resin*, Water Res., 36, 2002, pp. 4009–4022.
- [26] SLUNJSKI M., BILYK A., CELER K., *Removal of organic substances from water onto macroporous anion exchange MIEX[®] resin with magnetic components*, Ochrona Środowiska, 26, 2004, pp. 11–14.
- [27] SLUNJSKI M., BOURKE M., O'LEARY B., *MIEX@DOC process for removal of humics in water treatment*, www.miexresin.com

- [28] MOŁCZAN M., BIŁYK A., SLUNJSKI M., CELER K., *Application of jar tests to estimating the efficiency of organic substances removal in MIEX®DOC water treatment process*, *Ochrona Środowiska*, 27(2), 2005, pp. 3–7.
- [29] MOŁCZAN M., BIŁYK A., SLUNJSKI M., SICIŃSKI T., STRÓŻ J., *The pilot trial for organic substances removal in MIEX®DOC water treatment process*, *Ochrona Środowiska*, 27(4), 2005, pp. 19–26.
- [30] NISSINEN T.K., MIETTINEN I.T., MARTIKAINEN P.J., VARTAINEN T., *Molecular size distribution of natural organic matter in raw and drinking waters*, *Chemosphere*, 45, 2001, pp. 865–873.
- [31] BECKETT R., JUE Z., GIDDINGS J.C., *Determination of molecular weight distributions of fulvic and humic acids using flow field-flow fractionation*, *Env. Sci. Technol.*, 21, 1987, pp. 289–295.
- [32] THURMAN E.M., *Organic geochemistry of natural waters*, Martinus Nijhoff/Dr W. Junk Publ., 1986, Dordrecht, The Netherlands.

Keywords: ultrafiltration, surfactant, polyelectrolyte, membrane

IZABELA KOWALSKA*,
KATARZYNA MAJEWSKA-NOWAK*,
MAŁGORZATA KABSCH-KORBUTOWICZ*

THE INFLUENCE OF COMPLEXING AGENTS ON ANIONIC SURFACTANT REMOVAL FROM WATER SOLUTIONS BY ULTRAFILTRATION

The paper presents the results of the removal of sodium dodecyl sulfate (SDS) from aqueous solutions by means of ultrafiltration. The transport and separations properties of polyethersulfone (PES) and polysulfone (PS) ultrafiltration membranes with different cut-off values were investigated with the addition of a complexing agent (cationic polyelectrolyte) to the SDS solution. Experiments were carried out in a laboratory ultrafiltration cell at pressure of 0.20 MPa and a pH level equal to 7. The concentration of SDS in model solutions amounted to 100, 300 and 600 mg/dm³, whereas the polyelectrolyte dose ranged from 0.2 to 5.0 mg/dm³.

As cationic polyelectrolytes were added to the SDS solution, an improvement in the retention properties of the membranes was observed. No discernible correlations between the separation efficiency of SDS and molecular weight or ionic strength of polyelectrolytes were found. The best separation effect was achieved for moderate polyelectrolyte doses (0.2–0.5 mg/dm³). The growth in polyelectrolyte dose resulted in an insignificant increase in separation properties of the membranes. The best retention coefficient of SDS was noticed for PS5 membrane and amounted to 80% for solutions containing 100 mg SDS/dm³, and over 70% for solutions containing 300 and 600 mg SDS/dm³.

1. INTRODUCTION

Surfactants are used as the basic ingredient in cleaning products and as facilitators in a wide range of industrial processes ranging from textiles and fibres through to plant production and pest control. They are used notably in cosmetics, household

* Wrocław University of Technology, Institute of Environment Protection Engineering, Wybrzeże Wyspiańskiego 27, 50-370 Wrocław, Poland. E-mail: izabela.kowalska@pwr.wroc.pl

and industrial detergents and to a lesser extent in papermaking, construction materials and plastics.

As a consequence of widespread use, surfactants can be present at relatively high concentrations in wastewaters coming from various industrial applications [1]–[3]. Their residual amounts can cause significant environment problems because of the toxicity to aquatic life and the ability to form foam.

Surface active agents are very difficult to remove from water solutions for the sake of the chemical structure and physicochemical properties. They are generally removed by biodegradation, coagulation, foaming, advanced oxidation processes and adsorption on to different types of activated carbons and polyelectrolytes. Limitations of conventional treatment method make membrane-based separation processes as an attractive alternative in wastewater treatment. The processes – because of the selectivity of the membrane – create a possibility to recover resources and process water as well as to reduce high organic load of the wastewaters.

Archer et al. [4] studied nanofiltration separation of an anionic surfactant belonging to the alkylpolyethersulfate family. Because of the high values obtained for the permeate flux and rejection ($204 \text{ dm}^3/\text{m}^2\text{h}$ and 99.5%, respectively) the authors recommend the process in environmental area, especially in the pretreatment of industrial effluents with significant amount of anionic surfactants. Also Fernandez et al. [5] reported high surfactant retention (60–70%) below critical micellar concentrations for ultrafiltration ceramic membranes with pore diameter of 20 nm.

In general, ultrafiltration has been suggested as a method of surfactant removal from aqueous solutions with critical micellar concentrations. If the surfactant concentration is as low as of monomer concentration, then nanofiltration can be applied as an effective removal process.

The objective of the experimental research was to evaluate the removal efficiency of sodium dodecyl sulfate (SDS) from water solutions by ultrafiltration in the presence of a complexing agent (cationic polyelectrolyte).

2. MATERIALS AND METHODS

In the study Intersep Nadir membranes made of polyethersulfone (PES) and polysulfone (PS) with molecular weight cut-off equal to 5, 10 and 30 kDa were used.

Experiments were performed in a laboratory set-up (Fig. 1), which was used to determine the separation and transport properties of the membranes. The main part of the system was an Amicon 8400 ultrafiltration cell with total volume of 350 cm^3 and diameter of 76 mm. In order to maintain a stable concentration of the substances in the feed solution, the permeate was recirculated. All experiments were carried out at the transmembrane pressures of 0.20 MPa.

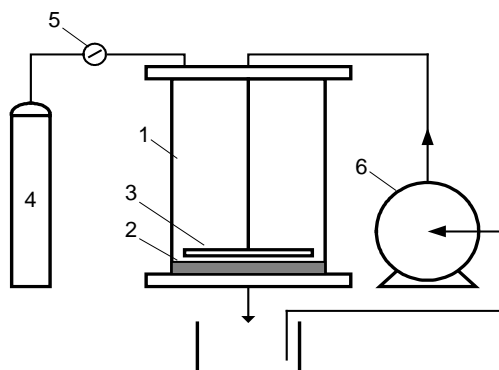


Fig. 1. Laboratory set-up: 1 – ultrafiltration cell, 2 – membrane, 3 – stirrer, 4 – gas cylinder, 5 – reducer, 6 – recirculation pump

The concentration of sodium dodecyl sulfate (SDS) in model solutions amounted to 100, 300 and 600 mg/dm³, and it was below its critical micelle concentration (CMC). For the purpose of the study nine cationic polyelectrolytes Ciba type were selected. Their characteristics are given in Table 1. In the preliminary tests the dose of polyelectrolytes amounted to 0.5 mg/dm³, whereas in the main tests the polyelectrolyte concentration was in the range between 0.2 and 5.0 mg/dm³. The pH level of the feed solutions was equal to 7.0.

Table 1. Characteristics of polyelectrolytes tested

Type of polyelectrolyte	Ionic character	Molecular weight
LT22S	moderate-/week cationic	very high
Z32	week cationic	very high
Z7651	strong cationic	very high
Z7652	moderate-/week cationic	very high
Z7653	moderate-/strong cationic	very high
Z92	moderate-/week cationic	high
Z66	moderate cationic	moderately high
Z57	strong cationic	moderately high
Z87	cationic	moderately high

The SDS concentration in the feed and the permeate was determined by means of colour reaction using the indicator Rhodamine G6 and spectrophotometric measurements of the absorbance at a wavelength 565 nm. The efficiency of the ultrafiltration process (%) was calculated by the retention coefficient R:

$$R = \frac{C_f - C_p}{C_f} \times 100\% \quad (1)$$

where C_f denotes SDS concentration in the feed and C_p denotes SDS concentration in the permeate.

Permeate volume flux was calculated as follows:

$$J = \frac{V}{t \cdot A} \quad (2)$$

where J is permeate volume flux ($\text{m}^3/\text{m}^2 \cdot \text{day}$), V denotes volume of permeate sample collected within time t (day), and A is effective membrane surface area (m^2).

3. RESULTS AND DISCUSSION

The objective of the experimental research was to evaluate the removal efficiency of sodium dodecyl sulfate (SDS) in the presence of cationic polyelectrolyte as a complexing agent from water solutions by ultrafiltration. In the preliminary investigation the polyelectrolyte dose in model solutions amounted to $0.5 \text{ mg}/\text{dm}^3$ and SDS concentration to 100, 300 and $600 \text{ mg}/\text{dm}^3$. As can be seen from the Fig. 2 no discernible correlations between the separation efficiency of SDS (as a consequence of the agglomeration process) and molecular weight or ionic strength of polyelectrolytes were found. Generally, the highest retention coefficient of anionic surfactant from the feed solutions was achieved in the presence of the LT22S polyelectrolyte, whereas for the other polyelectrolytes retention was a little bit lower. Exemplary, for the $300 \text{ mg}/\text{dm}^3$ SDS solution and in the presence of the LT22S polyelectrolyte, the increase in retention coefficient of SDS amounted to 15%, 15%, 17%, 16%, 12% and 10% for PES5, PS5, PES10, PS10, PES30 and PS30 membranes, respectively. For $600 \text{ mg}/\text{dm}^3$ SDS solution the rise in separation coefficient of SDS was lower (especially in case of membranes with lower cut-off values) and was equal to 12%, 12%, 9%, 10%, 5% and 4% for PES5, PS5, PES10, PS10, PES30 and PS30 membranes, respectively. For PES5 membrane the best separation properties was noticed for Z66, Z57 and Z87 polyelectrolytes.

The second part of the experiments was focused on examination how polyelectrolyte dose influence the transport and separation properties of ultrafiltration membranes. The exemplary relationships for three polyelectrolytes (LT22S, Z87 and Z92) are given in Fig. 3.

As can be seen, the best separation effect was achieved for moderate polyelectrolyte doses (0.2 or $0.5 \text{ mg}/\text{dm}^3$). Higher polyelectrolyte doses resulted in an insignificant increase in separation properties of the membranes. For PS10 membrane the rise in retention coefficient of SDS was following: for the LT22S polyelectrolyte from

53% to 64% (0.2 g LT22S/m³), 69% (0.5 g LT22S/m³) and 72% (5.0 g LT22S/m³); for the Z87 polyelectrolyte from 53% to 60% (0.2 g Z87/m³), 61% (0.5 g Z87/m³) and 70% (5.0 g Z87/m³), for the Z92 polyelectrolyte from 53% to 60% (0.2 g Z92/m³), 59% (0.5 g Z92/m³) and 59% (5.0 g Z92/m³). From among membranes tested the PS5 membrane was characterized by the best separation properties. The retention coefficient rose from 67% to 81%, 78% and to 77% in the presence of LT22S, Z87 and Z92 polyelectrolytes with concentration of 0.5 mg/dm³, respectively.

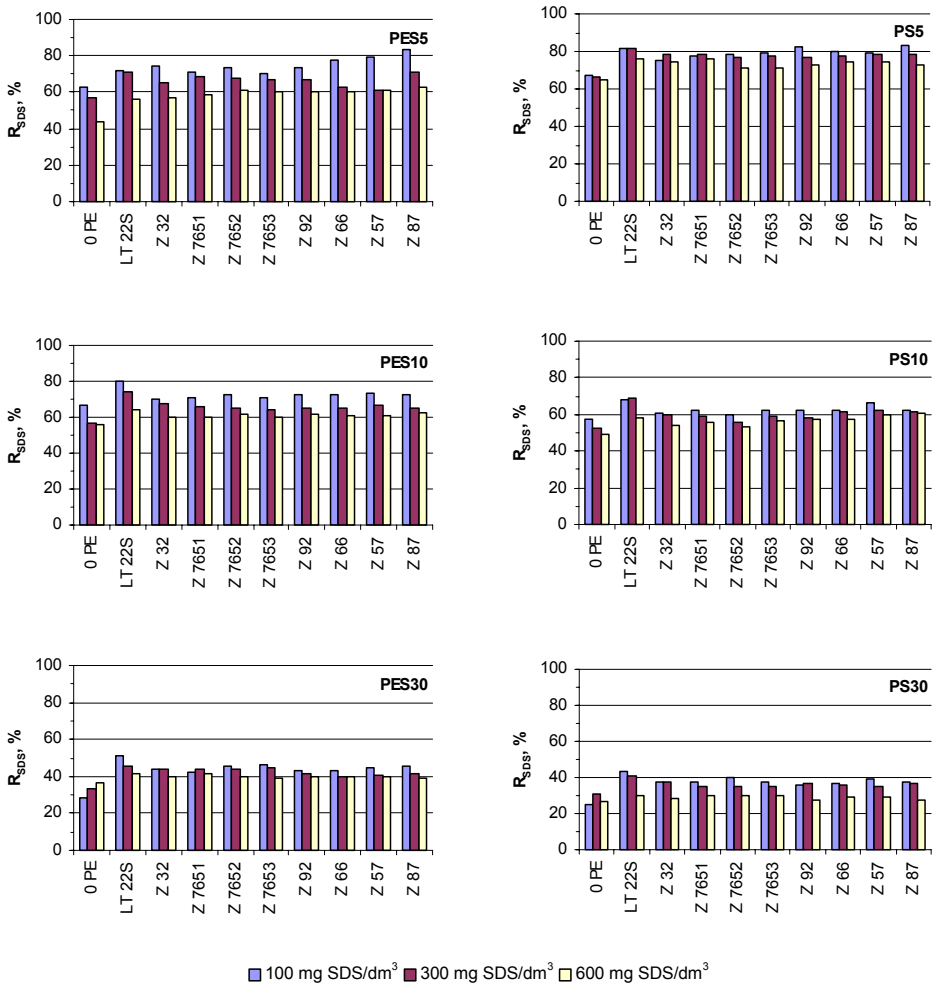


Fig. 2. Separation properties of Intersep Nadir membranes (cut-off 5, 10, 30 kDa) in the presence of cationic polyelectrolytes (0.5 mg/dm³)

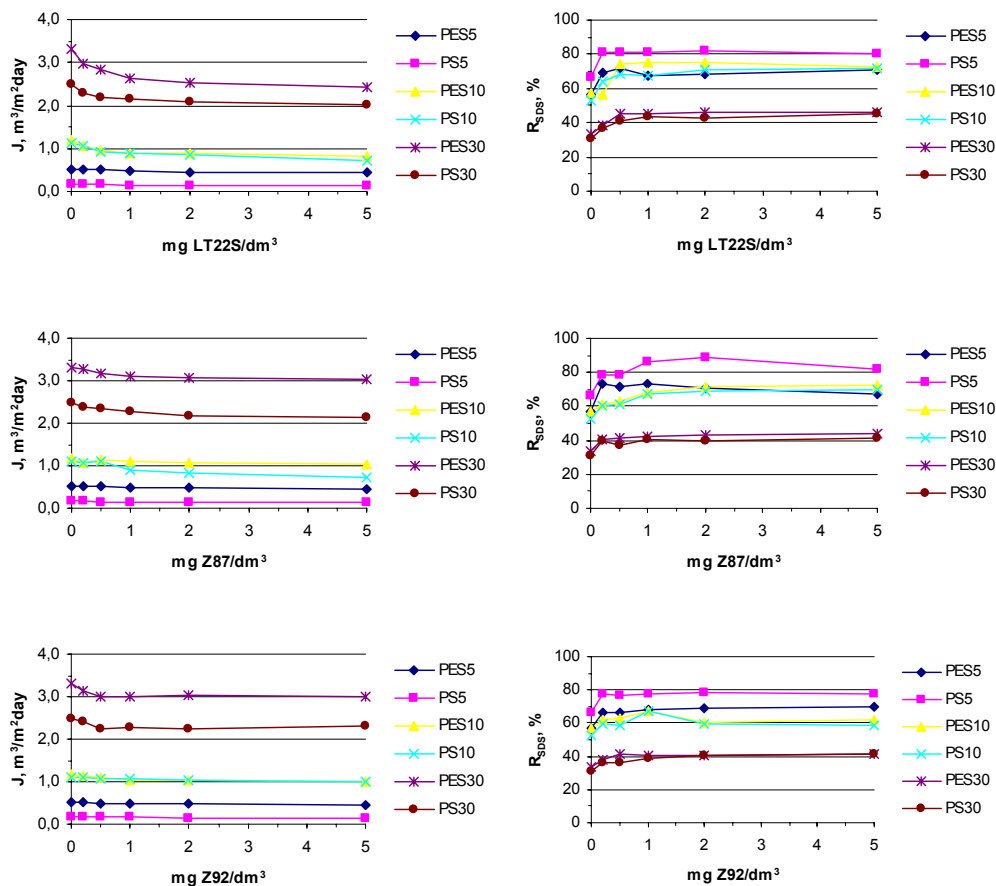


Fig. 3. The effect of concentration of cationic polyelectrolytes on transport and separation properties of Intersep Nadir membranes ($300 \text{ mg SDS}/\text{dm}^3$)

It was also found that ultrafiltration of surfactant and polyelectrolyte containing solutions brought an insignificant drop in permeate volume flux in relation to membrane permeability for SDS solutions. This effect was more pronounced for membranes of higher cut-off values.

The phenomenon of decreasing in membrane permeability for SDS solutions can be attributed to the concentration polarisation at the membrane surface. The SDS monomers accumulate at the membrane surface and in the membrane pores. It can be anticipated that the greater the molecular weight cut-off of the membrane, the membrane clogging is more intensive. In case of polyelectrolytes, which are characterized by very high molecular weight, the clogging process of the membrane is limited.

The improvement in SDS separation in the presence of polyelectrolyte is connected with forming specific agglomerates, which are retained by the membrane. According to Bremmel et al. [6] in the presence of polyelectrolyte the anionic surfactant in the first phase is attracted to the cationic polyelectrolyte through the electrostatic forces, and after neutralization the surfactant molecules are adsorbed as a result of hydrophobic interaction between the hydrocarbon chains. At low surfactant concentration a small number of surfactant molecules aggregate at the interface. At higher surfactant concentration, sufficient surfactant is available to form thermodynamically complete aggregates at the interface (Fig. 4).

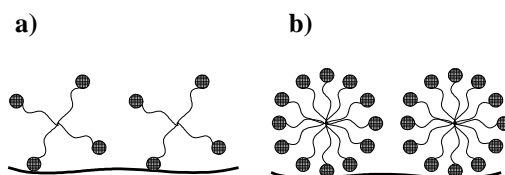


Fig. 4. Adsorption scheme of a possible conformation of anionic surfactant and cationic polyelectrolyte
(a – low surfactant concentration, b – high surfactant concentration)

According to Biekturov [7] the polyelectrolyte chain changes its conformation as a result of electrostatic interactions with surfactant and it leads to a compact (spherical) form of the polymer chain. It is supposed that the separation efficiency of SDS in the presence of polyelectrolyte is connected with a limited access of surfactant to active centres of the polyelectrolyte structure.

4. CONCLUSIONS

1. The improvement in the separation properties of the membranes in the presence of polyelectrolyte was observed.

2. No discernible correlations between the separation efficiency of SDS (as a consequence of the agglomeration process) and molecular weight or ionic strength of polyelectrolytes were found.

3. The best separation effect was achieved for moderate polyelectrolyte doses (0.2 or 0.5 mg/dm³). The growth in polyelectrolyte dose resulted in insignificant increase in separation properties of the membranes.

4. The best retention coefficient of SDS was noticed for PS5 membrane and amounted to 80% for solutions containing 100 mg SDS/dm³, and over 70% for solutions containing 300 and 600 mg SDS/dm³.

ACKNOWLEDGEMENTS

The financial support of Polish Committee of Science, Grant #3 T09D 025 26, is greatly appreciated.

REFERENCES

- [1] DIRILGEN N., INCE N., *Inhibition effect of the anionic surfactant SDS on duckweed, Lemna minor with considerations of growth and accumulation*, Chemosphere, 31(9), 1995, pp. 4185–4196.
- [2] PETERSSON A., ADAMSSON M., DAVE G., *Toxicity and detoxification of Swedish detergents and softer products*, Chemosphere, 41, 2000, pp. 1611–1620.
- [3] WAGNER S., SCHINK B., *Anaerobic of nonionic and anionic surfactants in enrichment cultures and fixed-bed reactors*, Water Research, 21(5), 1987, pp. 615–622.
- [4] ARCHER A.C., MENDES A.M., BOAVENTURA R.A.R., *Separation of an anionic surfactant by nanofiltration*, Environmental Science and Technology, 33, 1999, pp. 2758–2764.
- [5] FERNANDEZ E., CAMBIELLA A., BENITO J.M., PAZOS C., COCA J., *Ultrafiltration of surfactant solutions using ceramic membranes*, Proceedings of Engineering with Membranes, Granada, Spain, 3–6 June 2001, Vol. 2, pp. 68–73.
- [6] BREMMELL K.E., JAMESON G.J., BIGGS S., *Forces between surfaces in the presence of cationic polyelectrolyte and an anionic surfactant*, Colloids and Surfaces A: Physicochemical and Engineering Aspects, 155, 1999, pp. 1–10.
- [7] BIEKTUROW J.A., KUDAJBERGIENOW S., CHAMZAMULINA R.E., *Polimery kationowe*, PWN, Warszawa 1991 (in Polish).

ISBN 83-7085-922-4